Brandteknik
Lunds tekniska högskola
Lunds universitet

Department of Fire Safety Engineering
Lund Institute of Technology
Lund University

Report 5008

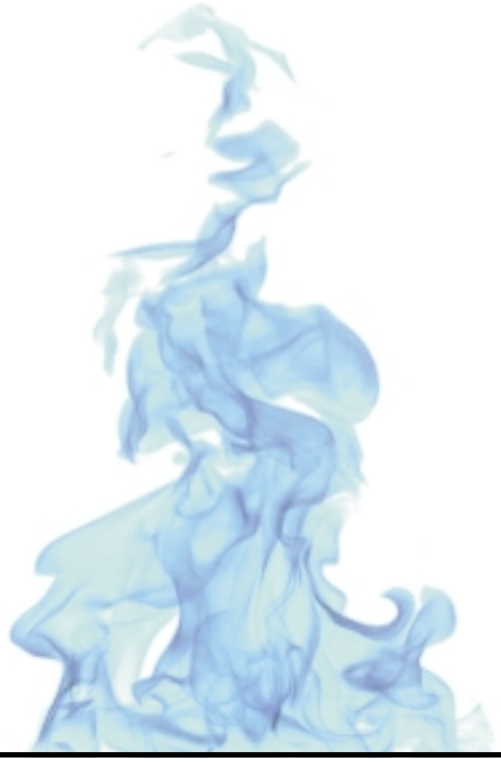

HIGH PERFORMANCE CONCRETE

DESIGN GUIDE LINES

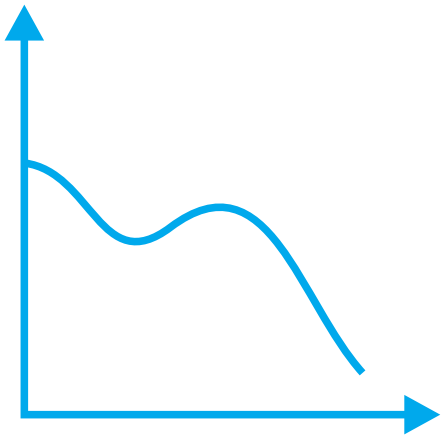

Böðvar Tómasson

LUND, FEBRUARY 1998

ISSN 1102-8246
ISRN LUTVDG/TVBB--5008--SE

Author:
Bödvar Tomasson

Keywords:
High performance concrete, material properties, structural fire design, concrete beams, slabs, columns, test simulation, interaction diagrams.

Abstract:
In this master thesis a basis for design rules, for High Performance Concrete (HPC) under fire attack, has been assessed and preliminary design guide lines have been suggested. The report encompasses detailed discussions on mechanical as well as thermal properties of HPC.

The report also gives a methodology for the development of simplified design methods. The methodology differs somewhat for beams and slabs, and for columns, where structural factors have to be taken into consideration.

The calculation method presented is based on a simplification of the relative strength at elevated temperatures, derived from specimen furnace tests. The simplification consists in the employment of single isotherm strength curves (the 400 and 500 °C isotherms) for calculation of load bearing capacity.

Tests, carried out in Japan and Germany, were compared to computerised predictions of the structural behaviour of columns. The comparison gave acceptable and conservative results.

Cover/Layout/Figures: Bödvar Tomasson

Department of Fire Safety Engineering · Lund Institute of Technology · Lund University

Postadress/Postal Adress:	Gatuadress/Office address:	Telefon/Telephone:	Telefax:
Box 118	John Ericssons väg 1	+46 46 - 222 73 60 (vx)	046 - 222 46 12
S-221 00 LUND	LUND	INT + 46 46 222 73 60	INT + 46 46 222 46 12
e-post/e-mail: brand@brand.lth.se	Sweden		

I SUMMARY

As part of the Swedish research project on High Performance Concrete (HPC) structures, the properties, and the structural behaviour, at high temperatures had to be determined. In 1992 this task was assigned to Fire Safety Design AB.

The overall objective of the project was to develop design guide lines for practical use in a broad range of HPC applications. A handbook is in preparation and will be published in 1998 by the assemblance of contributions from the numerous sub-projects, thus covering all relevant aspects of HPC as a material and as a structural component.

In this master thesis a basis for design rules, for HPC under fire attack, have been obtained and preliminary design guide lines have been suggested. The report encompasses detailed discussions on mechanical as well as thermal properties, as these have previously not been determined and published.

The calculation method presented is based on a simplification of the relative strength at elevated temperatures, derived from specimen furnace tests. The simplification consists in the employment of single isotherm strength curves (the 400 and 500 °C isotherms) for calculation of load bearing capacity. The overall approach is, with some adjustments to account for the properties of HPC, in accordance with the design method for ordinary performance concrete (OPC), presented by Anderberg and Pettersson 1992.

A large amount of elements have been analysed with respect to load bearing capacity in fire. These consist of two types:

- Beams and slabs
- Columns

Beams and slabs were calculated on a cross-sectional level, where moment capacity as a function of temperature was compared for various design alternatives, in the process of determining the most appropriate design guide lines. The parameters varied were: cross-sectional geometry, type of reinforcement and degree of fire exposure.

Columns were analysed on a structural level, comparing the fire resistance time, for various design guide line alternatives. The parameters varied were: cross-sectional geometry, buckling length and loading.

Generally, the strength in the concrete for beams and slabs has to be reduced according to the 500 isotherm curve. Additional reduction of the moment capacity is necessary for cross-sections exposed to fire on the compression zone.

For columns, the concrete can be assumed to have a full ambient strength up to 400 °C and zero thereafter (reduction according to the 400 isotherm curve).

For verification of the adopted approach for columns, the computer program CONFIRE has been used to simulate tests performed in Japan and Germany, with acceptable conformity as a result.

II ACKNOWLEDGEMENT

This master thesis is the final chapter in the long book of High Performance Concrete research, for which FSD has had the responsibility for the part concerning properties at high temperatures. It has been very interesting to deal with problems connected to such a practical reality as design guide lines.

I would like to extend my thanks to the staff at Fire Safety Design AB for many interesting and giving discussion, especially Jens Oredsson and Ulf Göransson for their guidance throughout the project, Sebastian Jeansson for his valuable technical support and, furthermore, I would like to thank Dr. Yngve Anderberg for initiating the work.

Office space, computer and software as well as most of the literature was supplied by Fire Safety Design AB.

Special thanks to Dr Björn Karlsson at the Department of Fire Safety Engineering, Lund University, for his quick response and patience at different stages of the work and for valuable comments on the report.

Thanks are also due to everybody who assisted me in any way during the course of the work.

Finally, I would like to thank my parents for their support and love through the years.

Lund, February 1998.

Böðvar Tómasson

III NOMENCLATURE

Units

In general the SI-system has been employed in this report adopting the following units:

- Length [mm]
- Time [s]
- Mass [kg]
- Force [N]
- Stress [Pa]
- Temperature [°C]

Definitions

The superscript ”c” indicates compression and ”t” indicates tension.

Tensile forces, tensile stresses and tensile strains are defined as positive in accordance with the conventional definition. And similarly, compression is denoted with a negative sign.

Notations

All symbols used in the report are defined under the headline: Symbols. However, in order to simplify the reading, some symbols are explained repeatedly in the text with no consistent strategy to lean upon.

Symbols

symbols	definition	dimension
$A_{s,i}$	area of steel *i*	mm^2
E	modulus of elasticity	MPa
E_c^*	slope of the descending branch in compression zone	MPa
EI	flextural rigidity, which should allow for the effects of cracking, creep and non-linearity of the stress-strain curve	N m^2
$M_{d,fi}$	design moment capacity in the fire situation	N m
M_{500}	calculated moment capacity based on the effective cross-section, defined by the 500 ºC isotherm	N m
N_{cr}	critical load	N
N	axial load	N
T	temperature	°C
T_g	gas temperature	°C
T_y	boundary temperature	°C
T_y	ordinary room temperature	°C
DT	temperature interval where the steam is generated	°C

Q	generated heat	W m^{-3}
a	actual reduction of the cross-section	mm
a_{500}	reduction of the cross-section according to the 500 isotherm.	mm
b	cross section width	mm
$c_{c,q}$	specific heat determined at the temperature q	J kg^{-1} K^{-1}
$c_{c,peak}$	value of specific heat at the peak	J kg^{-1} K^{-1}
c_c	specific heat	J kg^{-1} K^{-1}
d	effective depth	mm
e	eccentricity	mm
e_0	initial out of straightness	mm
f_c	cylinder compression strength of concrete	MPa
f_{cc}	cube compression strength of concrete	MPa
h_c	heat transfer coefficients of convection	W m^{-2} $^oC^{-1}$
h	height of cross section	mm
i	radius of inertia	mm
k_2	material related factor equal to 2.35	-
k_1	material related factor equal to 0.1	-
$k_{x,y}$	thermal conductivity	W m^{-1} $°C^{-1}$
l_c	critical length	m
(l_c/h)	slenderness ratios	-
q_n	heat flow at the boundary	W m^{-2}
r	reduction factor for effective cross section	-
t	time	min
x	depth of the compression zone	mm
y	y axis	mm
z	z axis	mm
a_k	convection heat transfer coefficient	W $m^{-2}°C^{-1}$
α_s	thermal expansion	-
β	effective length factor	-
c	empirical correction factor for the buckling phenomenon	-
DT	temperature difference	^oC
d	water content by weight	-
e	strain	-
$\bar{\varepsilon}$	pre-history of stress equal to zero	-
e_{cr}	creep strain	-
ε_{cu}	strain in the concrete	-
ε_{crack}	strain at which cracking starts	
e_{crush}	strain at which cracking starts	-
e_{pl}	plastic strain	-
ε_r	heat transfer coefficient of emissivity	
ε_s	strain in the steel	-
ε_{th}	thermal strain	-
e_{tot}	total strain	-
ε_{tr}	transient strain	-
ε_u^t	stain at which maximum tensile stress is reached	-
e_y	yield strain	-
e_s	stress related strain	-

ε_1	pre-history of stress considered	-
e_1	ultimate strain at ultimate stress	-
ε_{1o}	ultimate strain at room temperature	-
e_2	strain at the transition between parabolic branch and the linear second branch	-
e_r	resulting emissivity	-
ε_σ	stress-related strain	-
l	slenderness ratio	-
l	thermal conductivity	W m^{-1} K^{-1}
n	Poisson´s ratio	-
q_c	temperature	ºC
q	temperature where the peak is situated	°C
r	density	kg m^{-3}
s	Stefan-Boltzman constant	W $m^{-2}K^{-4}$
s	stress	Pa
$\tilde{\sigma}$	stress history	Pa
σ_u^t	tensile strength of concrete	Pa
σ_{uo}^c	is cylinder compression strength at normal temperatures	Pa
σ_u	compressive strength	Pa

IV CONTENTS

1. INTRODUCTION

1.1 BACKGROUND

High performance concrete (HPC) is concrete with improved mechanical behaviour in comparison to ordinary performance concrete (OPC). The improvement is accomplished by moderation of the concrete mixture. The division or characterisation is done by measuring the cube compression strength for which HPC has to exceed 80 MPa. By intensive research the properties of HPC have been measured and mapped and form as basis for the design methods derived in this report. Up till now it has not been possible to take advantage of the HPC to a full extent as accepted design rules have not been developed. In 1992 a Swedish national research project was started with the aim towards development of design rules for HPC at every design field. The project is sponsored by Cementa, Euroc Beton, NCC Bygg, SKANSKA, Strängbetong and Elkem Materials as well as BFR and NUTEK. Fire Safety Design (FSD) in Lund, Sweden, was engaged in the part concerning the properties at high temperatures, part M7. The work involved sub- and full scale furnace tests as well as computer modelling. In the last year or so the main focus has been on derivation of the design rules.

The aspects concerning concrete subjected to fire are several. For a ”new” material like HPC one aspect is the basic work of measuring the mechanical, and thermal properties which are necessary for any practical use where the design rules play a vital role. New problematic areas also appeared in the course of the research work, a consequence of a microscopic property of HPC, namely the spalling phenomenon.

Considerable research on concrete’s fire resistance was carried out in the late sixties and in the seventies where models describing the overall behaviour of concrete under fire attack were developed. These models are also used for HPC with some modifications to account for new properties. This has made it possible to use existing computer codes for design method development and it will also result in a better understanding of the design rules.

1.2 OBJECTIVES

The purpose of the investigation presented, is to obtain design rules for HPC at elevated temperatures. The assessed design guidelines should be applicable on member analysis for beams and slabs as well as on structural level for columns. These design rules are based upon mechanical and thermal properties of HPC obtained in an earlier part of the project.

It is preferable that as many cross-sections and structures as possible are covered by the design rules so these will have a wide range of application.

The design rules should be easy to use since they are meant for simplified calculations. Hence it would be preferred to use a similar approach for HPC as for OPC, as the latter rules are widely accepted and used in practice.

1.3 LIMITATIONS AND ASSUMPTIONS

Only the ISO-834 standard fire /1975/ has been used for simulations so the methods will only be applicable to that fire or other time heat regimes that will cause similar temperature fields in the concrete. Special analysis must take place for other time heat regimes which do not comply with this criteria.

For beams and slabs it is assumed that member analysis is a sufficient way to describe the overall behaviour and that no restraint forces will be present. External forces causing shear deformations are excluded in the analysis.

Only rectangular columns have been analysed. No temperature gradient along the length of the column has been accounted for.

Reinforcing steel is assumed to have a tension strength of 500 MPa and pre-stressing steel a tension strength of 1860 MPa. The design method is assumed to be valid for all regular types of steel.

The design methods can only be applied to structures similar to the ones used in the following calculations. Other types of structures have to be analysed separately.

The effect of spalling has not been accounted for and hence it is assumed that a sufficient amount of polypropylene fibres are used in the concrete blending process to account for this phenomenon.

1.4 REPORT DISPOSITION

The design rules are obtained by individually looking at member and structural sections. These two parts are covered in Chapters 6 and 7. Earlier chapters provide a background for the calculations. Figure 1.1 describes the internal involvement of the different chapters.

In Chapter 6 a member analysis is performed for cross-sections of beams and slabs. The required information for performing computer calculations are provided in sections 6.1 and 6.2 for the mechanical behaviour and parameter configuration respectively. In Section 6.3 the main calculation procedure is explained (see Figure 6.1) and the results are represented in Section 6.4.

In Chapter 7 where columns are investigated, the procedure is similar to that for beams and slabs with the extension that structural factors are added. Section 7.5 includes a verification of the structural program used for the computer calculation by simulation of full scale tests performed in Japan and Germany. The interaction diagram shown in Section 7.6 gives a better understanding of the structural behaviour of columns under fire attack.

For the computer calculations the mechanical and thermal properties of HPC and steel are required and these are provided in Chapters 3 and 4 respectively.

For each cross-section the temperature field is calculated and the general heat flow factors governing in the section are described in Chapter 5.

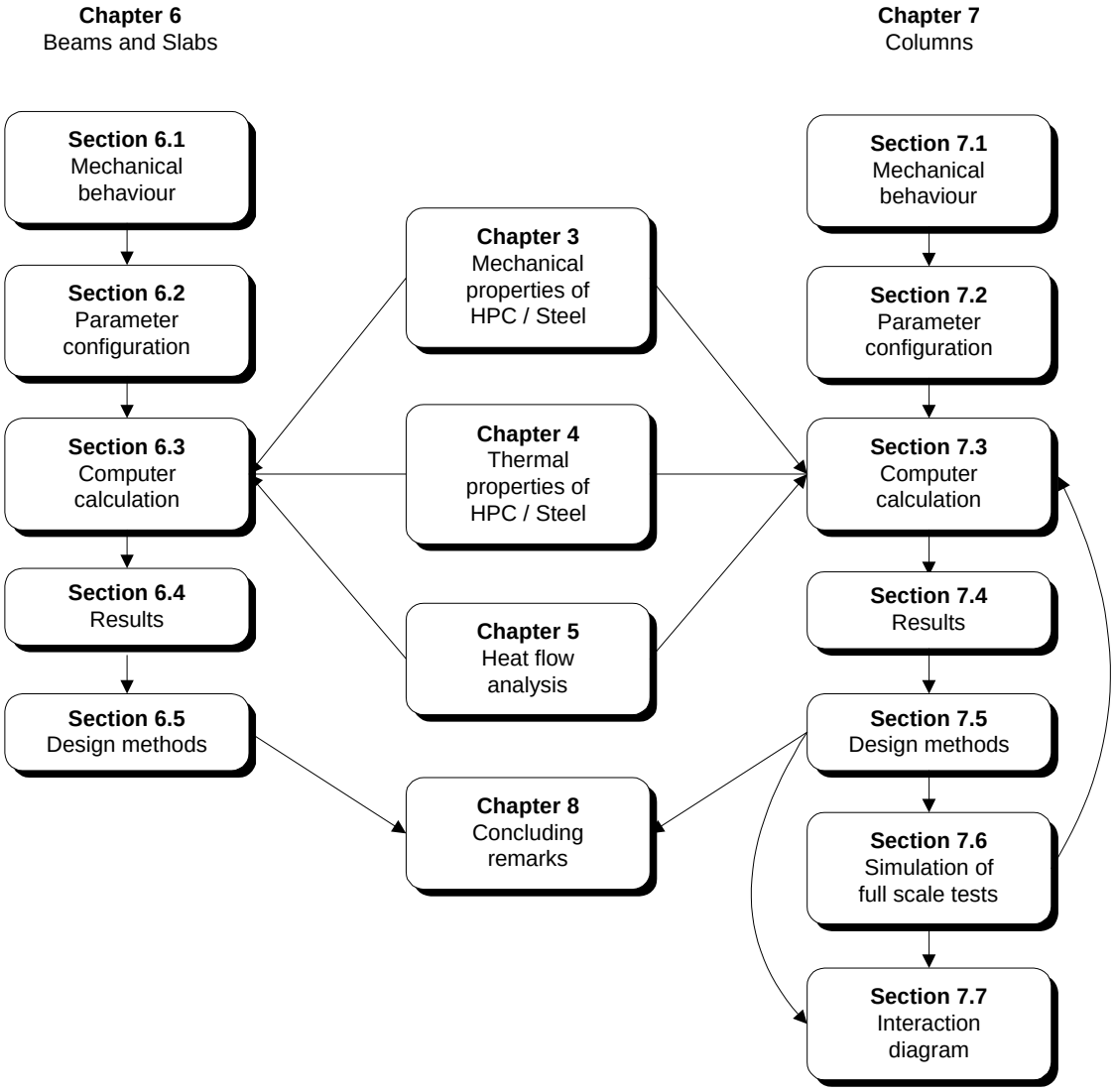

Figure 1.1 *Relation between chapters and sections.*

2. WORK METHODOLOGY

The overall work methodology denotes an introduction to the methods applied in developing the design rules.

The structures included when developing the design rules were of several kinds to account for most practical types available. The structures were divided into beams and slabs, where a cross sectional analysis was assumed to be sufficient, and columns were structural calculation was performed. All of the actual structures are listed in Appendix A. Steel types and fire exposures were also varied.

The mechanical properties for HPC including the relative strength curve were adapted into existing computer programs to simulate the actual behaviour of HPC at elevated temperatures. For each analysis the temperature field of the structure had to be calculated for which an ISO-834 time-temperature relationship was applied. Computer calculation procedures for beams and slabs and columns can be viewed in Figures 6.9 and 7.4 respectively.

The mechanical behaviour was then compared to several kinds of simplified mechanical behavioural approaches until an acceptable result was obtained. The resulting simplification proved to be the curve for relative strength of concrete at high temperatures compared to the strength at normal temperatures. This is due to the already accepted method for OPC where this curve is assigned a full strength up to 500 ºC and zero strength after that (single isotherm curve). The simplified approach can be viewed in Figure 1.1.

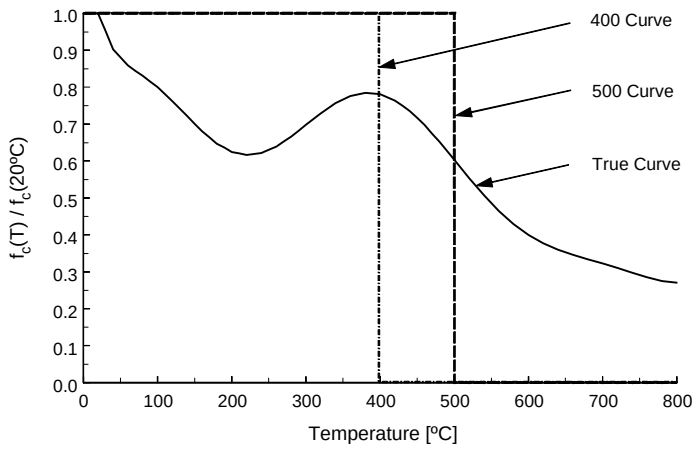

Figure 2.1
Relative strength measured for HPC, the True curve according to Holst /1994a/ and simplified single isotherm curves, the 400 and 500 curves.

The ”True” curve stands for the actual HPC relative strength curve as measured in tests (*Holst /1994a/*) whereas the single isotherm curves have a sudden descending strength at 400 and 500 ºC respectively.

The temperature field in the cross-sections was calculated with aid of the finite element code Super-Tempcalc, with the exposure in accordance with ISO-834 /1975/ standard fire. For a verification of the computer program the reader is referred to Anderberg /1991/.

The analysis on member level has been performed using the program CBEAM where the moment reduction in the cross-section is calculated as a function of time given a temperature variation in the cross-section. The same is done for columns but a finite element program CONFIRE is used for structural analysis. For a verification the reader is referred to Forsén /1982/.

3. MECHANICAL PROPERTIES

Chapter 3 summarises test results obtained for HPC concerning mechanical properties. These properties will to some extent be compared to those for OPC and a theoretical model, developed for OPC, will be modified to account for HPC properties. The last section will list the mechanical properties of the steel adopted in the model.

Fire is a transient process where temperature changes with time. It is thus important that transient tests are used when material properties at elevated temperatures are measured. Steady state tests (constant temperature under varying stress or strain) cannot by used solely to determine the properties in all cases. The different test regimes are shown in Figure 3.1 (Anderberg /1983/).

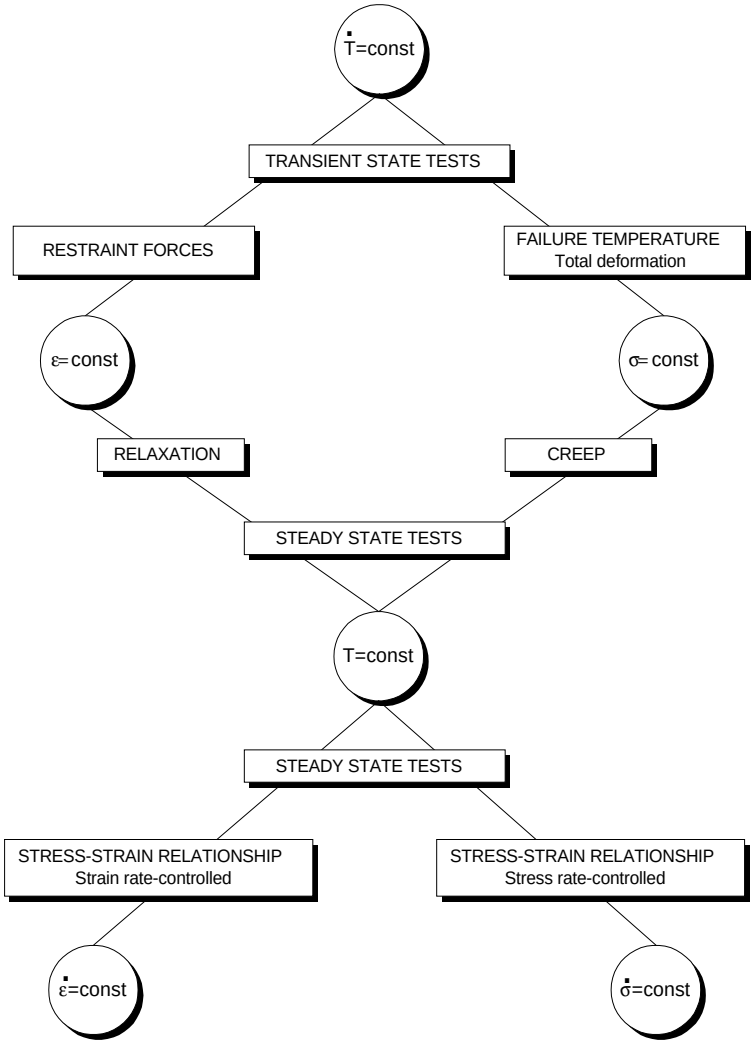

Figure 3.1
Different testing regimes for determining mechanical properties (Anderberg, /1983/).

Where

T is temperature.
ε is strain.
σ is stress.

3.1 HIGH PERFORMANCE CONCRETE (HPC)

A knowledge of the mechanical properties of the modeled material is essential for structural calculations. The mechanical properties discussed are, essentially, ultimate strength, modulus of elasticity and stress-strain relationship (constitutive model), all of which vary with increasing temperature.

In modelling mechanical properties of HPC the properties of OPC can be adapted. The properties of HPC have been obtained at transient as well as steady state conditions within the M7 project. For further information see Göransson /1996/ and Holst /1994a/.

3.1.1 Ultimate strength

The curve for relative ultimate strength versus temperature of HPC, shown is Figure 3.2, is different from corresponding observations for OPC (Anderberg, /1976/). The strength of HPC decreases at much higher rate than for OPC for temperatures in the range of 20 - 100 ºC. At about 200 ºC it reaches a local minimum of approximately 60 % of the initial strength at room temperature.

The temporary decrease is probably due to high steam pressure which builds up in the interval 150 - 200 ºC as the vaporising water is trapped within the concrete. In the interval from 200 - 400ºC the strength increases again, when the water has vaporised. This basic phenomenon is observed by many researches (Jumppanen, /1989/) and is illustrated in Figure 3.2.

The proposed relation (continuous line) is a best fit to the test results obtained in the M7 project.

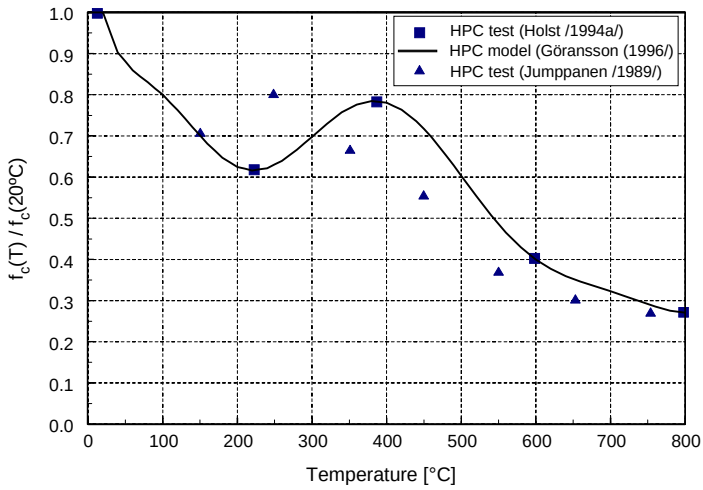

Figure 3.2
Strength of HPC as a function of temperature. Test values and proposed model.
(■ : HPC f_c=103 MPa, ▲:HPC f_c=92 MPa (at 20 °C))

3.1.2 Modulus of Elasticity

HPC is stiffer than OPC and therefore has a higher modulus of elasticity. However, the relative increase the in modulus of elasticity is not as large as the increase in strength.

The modulus of elasticity is calculated from steady state tests (see Figure 3.1) at various temperatures and the results are seen in Figure 3.3 below.

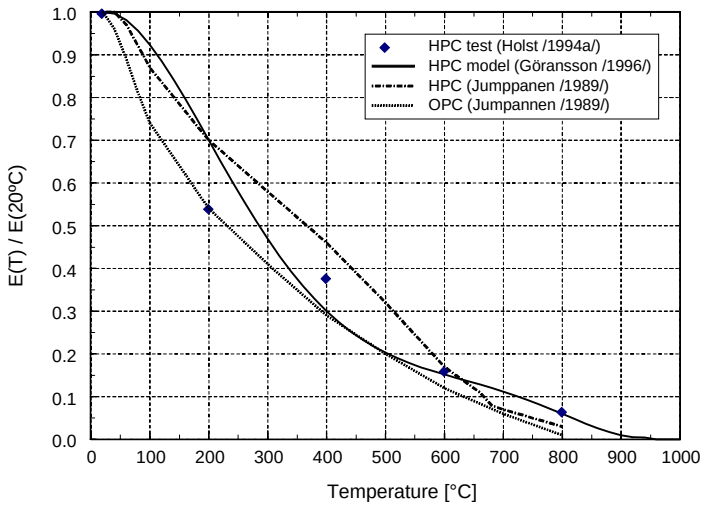

Figure 3.3
Relative modulus of elasticity as a function of temperature. The data is based on stationary σ-ε tests, with no load applied during the warm-up. (HPC test: f_c=103 MPa, E(20 °C)= 48 GPa)

The continuous line is a 5th degree polynomial (see Equation 3.1) which describes the modulus of elasticity for temperatures between 20 and 940ºC.

$$E(T) = E(20^{o}C)\cdot(0.99 + 0.0888\cdot(T/100) - 0.20232\cdot(T/100)^{2} + 0.05279\cdot(T/100)^{3} - 0.00543\cdot(T/100)^{4} + 0.000199\cdot(T/100)^{5}) \quad (3.1)$$

where

E is modulus of elasticity [MPa]
T is temperature [ºC]

Restraint forces at different loads and restricted deformation (limited thermal expansion) are relatively lower in HPC than in OSC. Typically the restraint stresses amount to 15-20 % of f_c at 20 ºC for HPC, whilst they are approximately 40 % for OSC. The temperature range during which the restraint force develops is smaller for HPC since the restraint forces start decreasing at lower temperatures than for OPC (Göransson /1996/).

3.1.3 Constitutive model

The constitutive model is a stress-strain model used to describe the mechanical properties of concrete at high temperatures. Here the constitutive model proposed by Anderberg and Thelandersson /1976/ will be used as a basis for the HPC model.

The expression of the total strain can be separated in to four different components as indicated in Equation 3.2.

$$\varepsilon_{tot} = \varepsilon_{th}(T) + \varepsilon_{\sigma}(\tilde{\sigma},\sigma,T) + \varepsilon_{cr}(\sigma,T,t) + \varepsilon_{tr}(\sigma,T) \quad (3.2)$$

where

ε_{tot}	is total strain [-]
ε_{th}	is thermal strain [-]
ε_{σ}	in stress-related strain [-]
ε_{cr}	is creep strain [-]
ε_{tr}	is transient strain [-]
T	is temperature [ºC]
t	is time [s]
σ	is stress [MPa]
σ^{*}	is stress history [MPa]

In Figure 3.4 (Göransson, /1996/) the four components are compared. The loading is 20% of the initial 28 days cylinder compression strength. The creep deformation is included in the transient deformation since it is difficult to assign a separate value to this component.

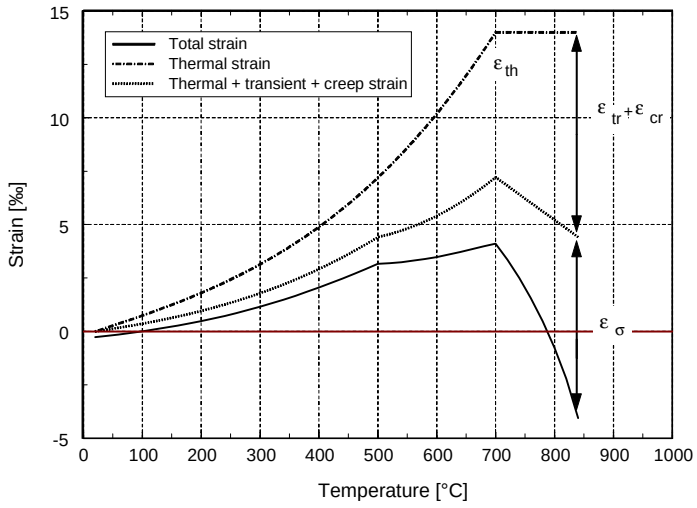

Figure 3.4
Total deformation divided into the four deformation components. Concrete made of standard portland cement and siliceous concrete (Göransson /1996/).

In the next sections the individual components included in the constitutive model are separately treated.

3.1.3.1 Thermal Strain

The thermal strain was measured on unstressed specimens under elevating temperature. The creep strain was included in the thermal strain and no other considerations are made for the shrinkage. This approximation is justified as the model is used at rapid heating only, for time temperature regimes equal or similar to the ISO 834 /1975/ standard fire exposure.

The difference in thermal strain between HPC and OPC is relatively small and the thermal strain model is given in ENV 1992-1-2 /1995/ can be used for HPC as measured in the M7 project. Equation 3.3 and 3.4 employs the thermal strain as a function of temperature for HPC as given in ENV 1992-1-2 /1995/.

$$\varepsilon_{th}(T) = -1{,}8 \cdot 10^{-4} + 9 \cdot 10^{-6}\, T + 2{,}3 \cdot 10^{-11}\, T^{3} \qquad 20\ °C < T < 700\ °C \qquad (3.3)$$

$$\varepsilon_{th}(T) = 14 \cdot 10^{-3} \qquad 700\ °C \le T < 1400\ °C \qquad (3.4)$$

where

$\varepsilon_{th}(T)$ is thermal strain [-]
T is temperature [ºC]

Figure 3.5 showns the difference between the HPC model and OPC according to Anderberg & Pettersson /1992/.

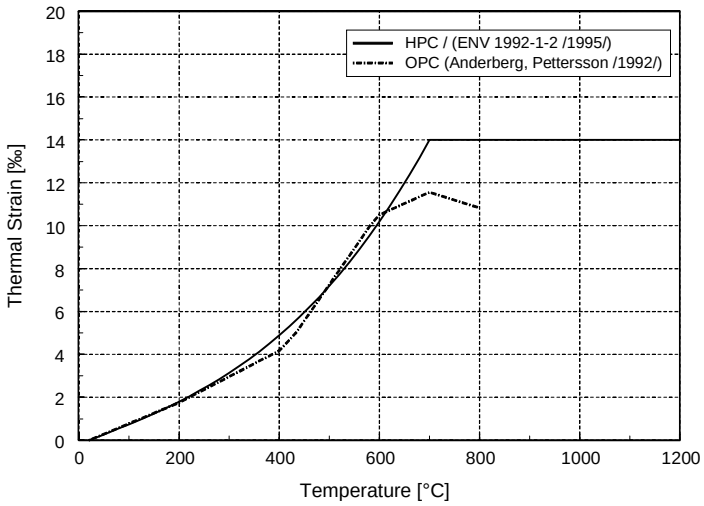

Figure 3.5 *Thermal strain for siliceous concrete, OPC and HPC according to Anderberg and Pettersson /1992/and ENV 1992-1-2 /1995/.*

3.1.3.2 Stress-related Strain

The stress strain relationship is obtained from stationary tests and is shown in Figure 3.6 (Göransson, /1996/). Any descending branch has not been measured in these tests, nor the influence of stress history.

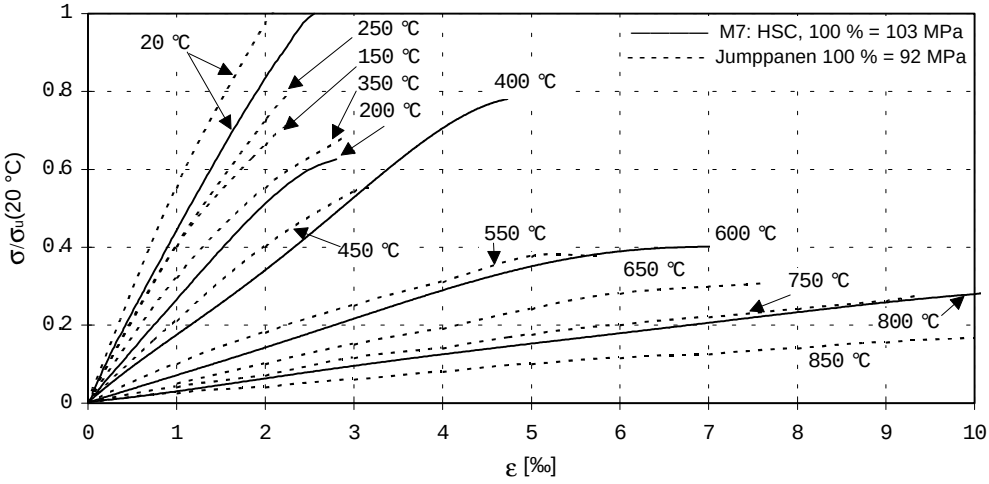

Figure 3.6 *Stress-strain relation of HPC obtained in M7 on stationary tests (Göransson, /1996/) and results from similar tests by Jumppanen /1989/.*

The theoretical stress-strain model according to Anderberg /1976/ is described in Figure 3.7 below. On the compression side the curve consists of a parabolic branch followed by a linear descending branch until crushing occurs.

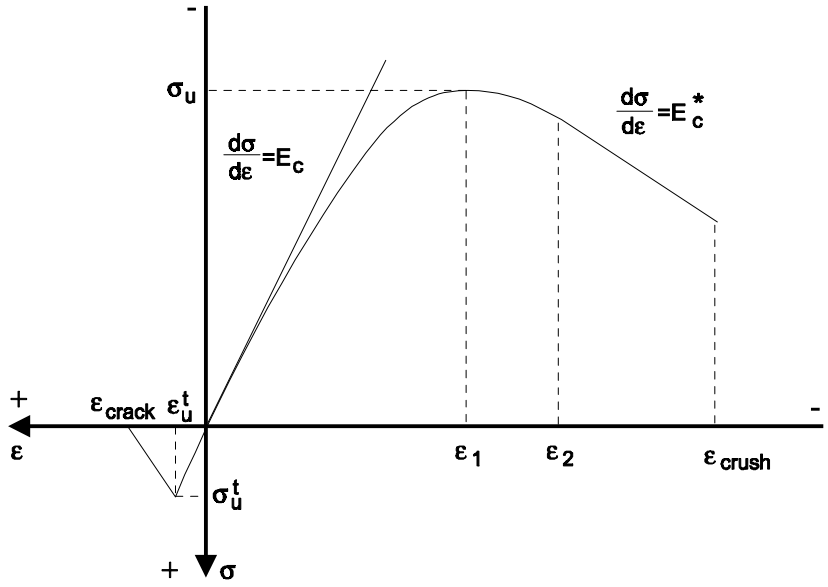

Figure 3.7
Theoretical model of the strain-stress relationship for concrete (Anderberg, /1976/).

where

$\sigma_u(T)$ is ultimate compressive stress [MPa]

$\varepsilon_1(T)$ is ultimate compressive strain at which $\sigma = \sigma_u(T)$ [-]

$\varepsilon_2(T)$ is the strain at the transition between parabolic and the linear descending branch [-]

$E_c^*(T)$ is slope of the descending branch in the compression zone [-]

$\sigma_u^t(T)$ is tensile strength of concrete [MPa]

ε_{crack} is strain at which cracking starts [-]

ε_{crush} is crushing strain [-]

The boundary conditions of the parabolic curve in Figure 3.7 are

$$\sigma = \sigma_u \quad \text{when } \varepsilon_\sigma = \varepsilon_u \tag{3.5a}$$

$$\frac{\partial \sigma}{\partial \varepsilon_\sigma} = 0 \quad \text{when } \varepsilon_\sigma = \varepsilon_1 \tag{3.5b}$$

$$\frac{\partial \sigma}{\partial \varepsilon_\sigma} = E_c^* \quad \text{when } \varepsilon_\sigma = \varepsilon_2 \tag{3.5b}$$

where

ε_σ is stress related strain.

The curve in Figure 3.7 can be described by four equations.
For the parabolic branch the curve can then be described with the following equation:

1. $$\sigma = \sigma_u \cdot \frac{\varepsilon_\sigma}{\varepsilon_1}\left(2 - \frac{\varepsilon_\sigma}{\varepsilon_1}\right) \qquad 0 \geq \varepsilon_\sigma > \varepsilon_2 \tag{3.6}$$

The initial fictitious modulus of elasticity E_c (when $\varepsilon \to 0$) can then be obtained as:

$$E_c(T) = \alpha \frac{\sigma_u(T)}{\varepsilon_1(T)} \quad \text{or} \quad \varepsilon_1(T) = \alpha \frac{\sigma_u(T)}{E_c(T)} \tag{3.7}$$

The non-dimensional coefficient α has been found out to be **1.2** for HPC (2.0 for OPC). This means that for the same stress, HPC will have 40% less strain.

The linear descending branch is given by:

$$2. \qquad \sigma = E^* \cdot \varepsilon_\sigma + \sigma^* \qquad \varepsilon_1 \geq \varepsilon_\sigma > \varepsilon_{crush} \tag{3.8}$$

where

E^* is the stain at which maximum tensile stress is reached [MPa]

$$\sigma^* = \sigma_u \left(1 - \frac{E^*}{E_c}\right)^2 \tag{3.9}$$

On the tension side the elasto-plastic behaviour is defined as:

$$3. \qquad \sigma = E_c \cdot \varepsilon_\sigma \qquad 0 \leq \varepsilon_\sigma < \varepsilon_u^t \tag{3.10}$$

where

ε_u^t is the strain when the maximum tensile stress is reached and $\varepsilon_u^t = \frac{\sigma_u^t}{E_c}$ [-]

The superscript 't' indicates tension.

$$4. \qquad \sigma = E_c \cdot \varepsilon_u^t \frac{\varepsilon_{crack} - \varepsilon_\sigma}{\varepsilon_{crack} - \varepsilon_u^t} \qquad \varepsilon_u^t \leq \varepsilon_\sigma < \varepsilon_{crack} \tag{3.11}$$

$$\sigma = 0 \qquad \varepsilon_{crack} \leq \varepsilon_\sigma$$

Ultimate stress $\sigma_u(T)$

Ultimate stress is higher for HPC than for OPC. It is a function of the temperature and the load history to some extent and also dependent on some concrete mixture parameters. The temperature dependence can be seen in Figure 3.2.

Ultimate strain $\varepsilon_1(T)$

The ultimate strain is history and temperature dependent. The temperature dependence is shown theoretically in Figure 3.8.

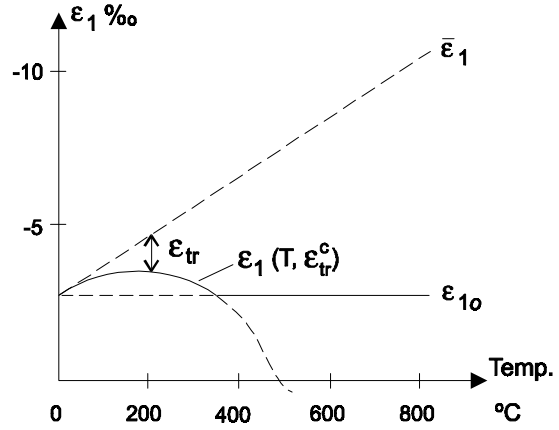

Figure 3.8
Theoretical model of ultimate strain (Anderberg, /1976/).

where

$\bar{\varepsilon}$ is pre-history of stress equal to zero [-]
ε_{1o} is ultimate strain at room temperature [-]
ε_1 is pre-history of stress considered [-]

The ultimate strain at elevated temperatures is always lower than the ultimate strain at room temperature but always higher than the strain when pre-history stress ($\bar{\varepsilon}$) is set to zero.

The ultimate strain as a function of the relative strength (σ_c) is shown in table 3.1. The value for the ultimate strain at room temperature (ε_{uo}) at 110 MPa is extrapolated to be 3.02 ‰.

Table 3.1 *Ultimate strain at room temperature as a function of relative strength (Design Handbook, /1996/).*

σ_c [MPa]	80 *	90 *	100 *	110
ε_u [‰]	2.72	2.82	2.92	3.02

* Applies to the reference in the table text.

The slope of ε_u for elevated temperatures can be determined by two methods:

1) Using Figure 3.6 to find a straight line between the ultimate strain at different temperatures (stationary tests). The line for the temperatures 20 and 800 °C has the slope 0.0083.
2) Using Equation 3.6 with $\sigma_u(T)$ from Figure 3.2 and $E_c(T)$ from Figure 3.3. Using a straight line fit the slope is 0.010.

As a result of 1) and 2) the slope of ε_u is chosen as **0.09**.

Modulus of descending branch

As mentioned earlier the descending slope, E^* (see Figure 3.7), is very difficult to measure and has not been considered for HPC at elevated temperatures. For room temperatures, the slope for HPC is much steeper than for OPC. For OPC this slope is assumed -880 MPa according to Anderberg /1976/ whilst slopes between -7 000 to -50 000 MPa have been observed for HPC (Glavind, Stang /1991/). As the descending slopes have not been measured in the M7 project it can not be accounted for in design calculation at elevated temperatures.

For using programs at structural level (CONFIRE, see Appendix D) a descending slope still has to be assigned. Here the slope was chosen to be -10,000. A line of this steep slope will not have any crucial influence on the strength and behaviour of the concrete but has to be included as an input variable in the computer simulation.

Tensile strength σ_u^t

The knowledge about tensile strength at elevated temperatures is very poor. For ambient temperatures the tensile strength is assumed to be higher for HPC than for OSC due to denser concrete. It would therefore be on the safe side to assume that the strength of HPC is the same as for OSC as has been done in present calculations.

Cracking strain ε_{crack}

The cracking strain is a measure of the deformability of the concrete in tension. The stiffness of the HPC makes it deform less than OPC but as it is denser, with higher tensile strength, cracking strain can be assumed to be the same as for OPC. The influence of rising temperature on the cracking strain is not clarified, and is therefore assumed to be invariant with temperature.

3.1.3.3 Creep Strain Model

Constant temperature creep of concrete is measured under constant compressive stress at a stabilized temperature level. Creep tests have not been carried out for HPC in the M7 project but as the tests have been carried out on a time length similar to that in a real fire, there is reason to believe that the measured test results includes the influence of creep. The creep is therefore included in the transient strain model (see below) (Göransson, /1996/).

3.1.3.4 Transient Strain Model

Transient strain develops under stress when the concrete is heated. This strain is not reversible and thus occurs only during the first heating. The transient strain is calculated form the measured total strain from which the calculated thermal and stress-induced strains are subtracted.

Linear equations on two intervals can be used to describe the transient strain in relation to compressive stress level. These equations apply to OPC (Anderberg, /1976/) but have shown good agreement with HPC as well (Göransson, /1996/).

$$\varepsilon_{tr}^c = -k_2 \frac{\sigma}{\sigma_{uo}^c} \varepsilon_{th}^c \qquad T \le 500^o C \tag{3.12}$$

where

k_2 is material constant equal to *2.35*
σ is stress [Pa]
σ_{uo}^c is cylinder compression strength at normal temperatures [Pa]
ε_{tr}^c is transient compression strain [-]
ε_{th}^c is thermal compression strain [-]

and

$$\varepsilon_{tr}^c = k_1 \cdot 10^{-3} T \frac{\sigma}{\sigma_{uo}^c} \qquad 500 < T \le 800^o C \tag{3.14}$$

where

k_1 is material constant equal to *0.1*

The measured transient strain for HPC as well as the transient strain according to Equations 3.13 and 3.14 is plotted in Figure 3.9 (Göransson, /1996/). Note how well these two agree.

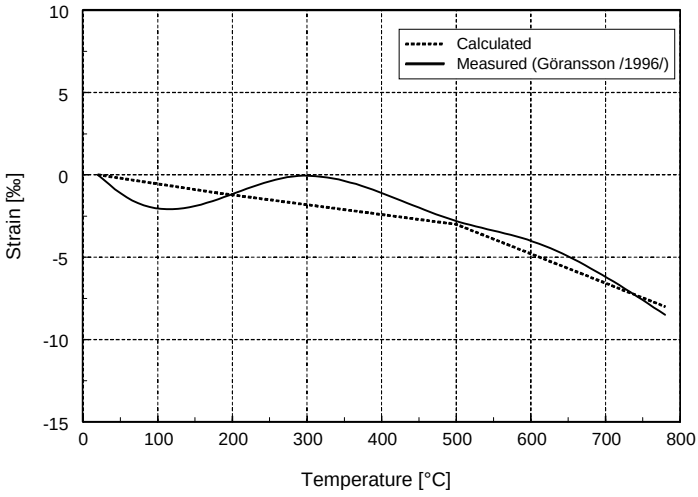

Figure 3.9
Transient strain for 20 % load, measured according to Göransson, /1996/, compared with original transient strain model according to Equations 3.13 to 3.14 with k2=2.35 and k1=0.1

3.1.3.5 Total Strain

A total strain model is then put together as the sum of the parts from thermal, stress-related and transient strains as seen in Figure 3.4. Measurements of total strain have been carried out in the M7 project for different loading as shown in Figure 3.10 (Göransson, /1996/).

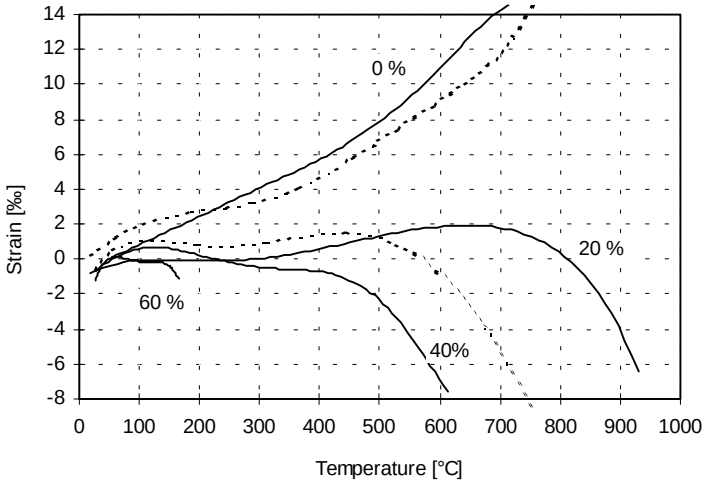

Figure 3.10
Total strain at different loading levels for HPC and OPC.
(— HPC, f_c=103 MPa (Göransson, /1996/),
- - OPC, f_c=54 MPa (Jumppanen, /1989/))

3.2 STEEL

Mechanical properties of reinforcement steel are of great importance when structural elements are subjected to fire especially when the reinforcement has a primary load bearing function as in beams and slabs. It's location close to the surface, to gain a maximum moment capacity at ordinary temperature, makes it vulnerable as the temperature rises due to fire.

The same type of reinforcing steel is used in HPC as in OPC. This means that the amount of reinforcement to account for the extra strength of HPC has to be increased. This furthermore implies that the mechanical properties of the reinforcement will play an increasing role in the behaviour of reinforced HPC in comparison with OPC.

The reinforcement type used in this project is Ks500. The model for mechanical properties is however based on a reinforcement type Ks400 (Anderberg, /1976/) but the difference is assumed to be very small (Anderberg, Pettersson, /1992/) .

3.2.1 Relative Strength

The strength reduction with temperature depends on the magnitude of residual strain considered. For beams and slabs in the fire situation the criteria provided by EUROCODE (ENV 1991-2-2, /1994/) will be used. For tension reinforcement the stress reduction at 2 % proof strain curve have been used. The reduction is shown in Figure 3.11 as well as the values for pre-stressing steel. The stress reduction at 0.2 % proof strain curve have been used for reinforcement in the compression zone.

For columns sensitive to buckling, the deformations must be kept low. Therefore, it is suitable to permit a low residual strain. For the design method presented in this report, the 0.5 % proof strain curve have been chosen as recommended in Sweden (BBK 94, /1995/) and the strength-temperature curve according to this strain criteria is shown in Figure 3.11.

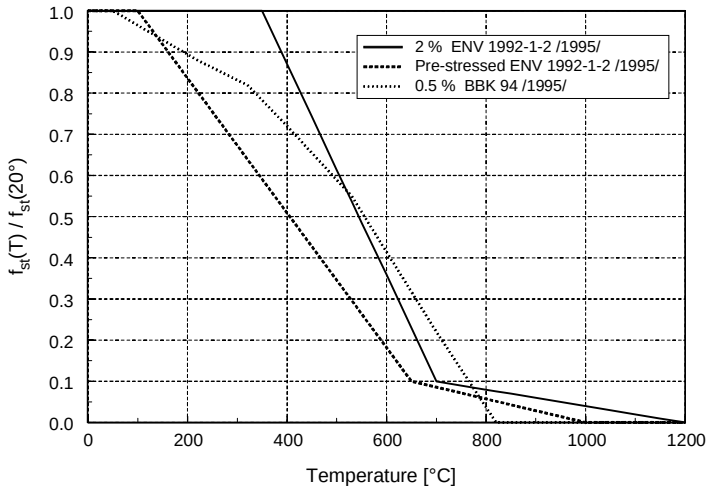

Figure 3.11
Relative strength of steel for 0.5 % proof strain, according to BBK 94 /1995/ and for 2 % proof strain and pre-stressed steel according to ENV 1992-1-2, /1995/.

3.2.2 Constitutive Model

For both reinforcing and pre-stressing steel, the transient strain is assumed to be insignificant, and furthermore no consideration to the load history needs to be taken. The total strain can, therefore be described as follows:

$$\varepsilon_T(T) = \varepsilon_\sigma(\sigma,T) + \varepsilon_{th}(T) + \varepsilon_{\sigma r}(\sigma,T,t) \tag{3.15}$$

where

$\varepsilon_T(T)$	is total strain [-]
$\varepsilon_\sigma(\sigma,T)$	is (effective) instantaneous stress-related strain [-]
$\varepsilon_{th}(T)$	is thermal strain [-]
$\varepsilon_{\sigma r}(\sigma,T,t)$	is creep strain [-]

The stress-strain model for steel includes no transient state strain component and is thus simpler than the constitutive model of concrete. The thermal strain is normally the largest of the three components.

3.2.2.1 Stress-Strain Relationship

A model for the stress-strain curve of reinforcement has been proposed by Anderberg /1976/ in which a bi-linear approximation is used. This is shown schematically in Figure 3.12 (Anderberg, /1976/). The slope of the first branch, E_S coincides with the elastic modulus and continues until it coincides with the strain, $\varepsilon_y(T)$, i.e. the break point of the two lines.

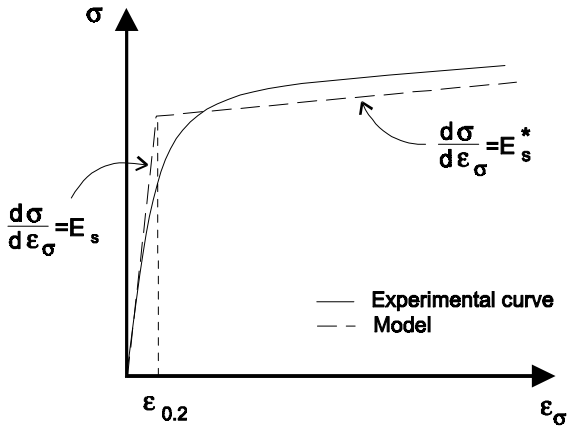

Figure 3.12
Model for stress-strain curve in principal, as presented in Anderberg /1976/.

The slope of the second branch $E_s^*(T)$ is temperature dependent and it's variation with temperature is shown in Figure 3.13 (Anderberg, /1976/). For practical purposes the values for E_S and $E_s^*(T)$ must be derived from experiments.

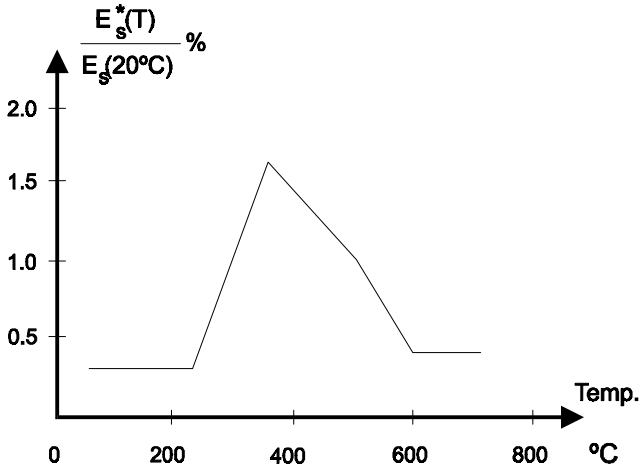

Figure 3.13
Variations of the slope of the second branch of the modulus of elasticity $E_s^*(T)$ as a function of temperature (Anderberg, /1976/).

The modulus of elasticity is different for reinforcing steel and pre-stressing steel. This is due to different manufacturing processes of the respective kinds of steel. It is important to point out that the test procedures are of great importance when assessing the curve for the modulus of elasticity of a certain material.

The relative modulus of elasticity as function of temperature is displayed in Figure 3.14 for reinforced and pre-stressing steels respectively (ENV 1992-1-2 /1995/).

.

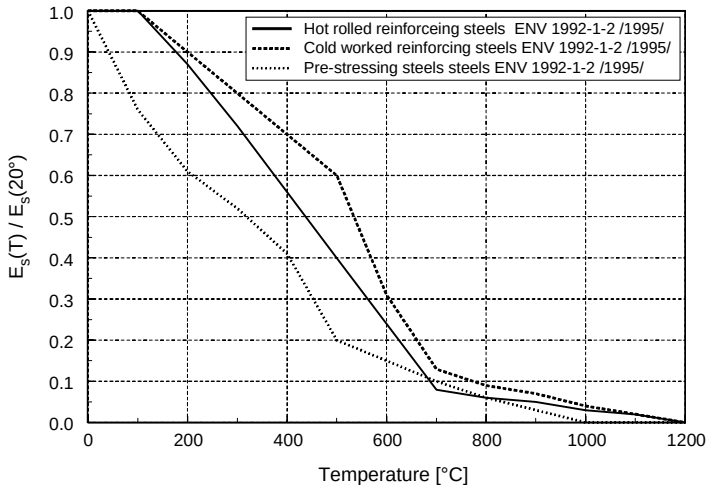

Figure 3.14
The variation of the modulus of elasticity with temperature for hot rolled and cold worked reinforcing steel and pre-stressing steel (ENV 1992-1-2 /1995/).

3.2.2.2 Thermal Strain

The thermal strain of steel is an important factor in calculation of the total deformation of a structural member subjected to fire exposure. Thermal strain is given by $\varepsilon_{sth}=\alpha_s \cdot T$, where as is the coefficient of thermal expansion [$°C^{-1}$]. In ENV 1992-1-2 /1995/ thermal elongation, $\Delta l/l$, is used to express the length changes in the steel at high temperatures. It differs for reinforcing steel and pre-stressing steel according to Equations 3.16 and 3.17 ENV 1992-1-2 /1995/.

Reinforcing steel:

$$(\Delta l/l)_s = -2.416\cdot10^{-4} + 1.2\cdot10^{-5}\,T + 0.4\cdot10^{-8}\,T^2 \qquad 20ºC < T \le 750ºC \qquad (3.16a)$$

$$(\Delta l/l)_s = 11.0\cdot10^{-3} \qquad 750ºC < T < 860ºC \qquad (3.16b)$$

$$(\Delta l/l)_s = -6.2\cdot10^{-3} + 2.0\cdot10^{-5}\,T \qquad 860ºC < T \qquad (3.16c)$$

Pre-stressed steel:

$$(\Delta l/l)_p = -2.016E^{-4} + 1.0E^{-5}\,T + 0.4E^{-8}\,T^2 \qquad 20ºC < T \le 1200ºC \qquad (3.17)$$

where

l_s, l_p is the length at room temperature for reinforced and pre-stressed steel [mm]
Δl_s, Δl_p is the temperature induced elongation for reinforced and pre-stressed steel [mm]
T is temperature in the steel [°C]

3.2.2.3 Creep Strain

The creep in steel becomes significant at elevated temperatures and therefore it is important to include its influence in the structural analysis. The creep does not have any significance at temperatures below approximately 400ºC, but after that it increases rapidly (Anderberg, Pettersson, /1992/). It is thus possible to separate the creep into two phases, viz. a primary creep phase having a parabolic curve and a secondary phase which is linear (Anderberg, /1976/).

4. THERMAL PROPERTIES

Chapter 4 lists the thermal properties of HPC and steel. The HPC properties, obtained in recent tests, will be compared to the thermal properties of OPC and a basis will be formed for how the practical assignment of thermal properties should be made.

4.1 HIGH PERFORMANCE CONCRETE (HPC)

Concrete is considered an isotropic material in temperature calculations, i.e. invariant thermal conductivity with respect to direction of heat flow.

The thermal properties of concrete can be described by three different material properties: thermal conductivity, specific heat and density.

4.1.1 Thermal Conductivity

The values for the thermal conductivity of HPC according to Holst, /1994b/, have shown an acceptable agreement with values for OPC according to ENV-1992-1-2 /1995/, where a 2nd degree polynomial has be adapted. The Equation (4.1) only considers temperature as a variable although λ_c is known to vary with moisture content as well. This is assumed to be of sufficient accuracy but gives a somewhat high temperature.

$$\lambda_c = 2 - 0.24\frac{T}{120} + 0.012\left(\frac{T}{120}\right)^2 \qquad (4.1)$$

where

λ_c is thermal conductivity [W/(m K)]
T is temperature [°C],

Thermal conductivity as a function of temperature is shown in Figure 4.1. For comparison the thermal conductivity for OPC (Anderberg, Pettersson, /1992/) is plotted in the same graph.

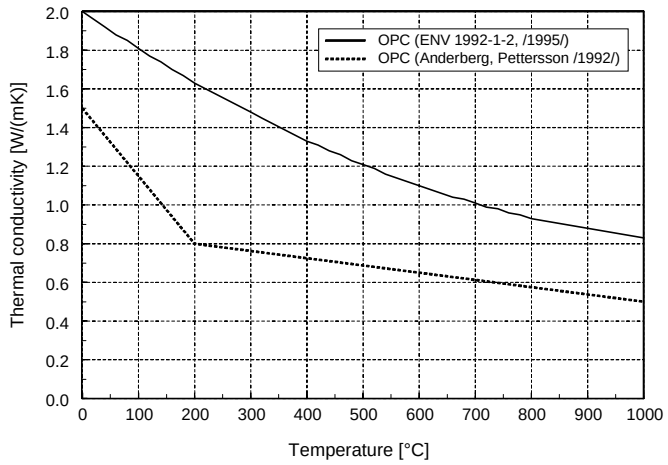

Figure 4.1
Thermal conductivity as a function of temperature for OPC with siliceous aggregate according to ENV-1992-1-2, /1995/, which is assumed to apply to HPC as well (Holst, /1994b/), and OPC according to Anderberg and Pettersson, /1992/.

4.1.2 Specific Heat and Thermal Capacitivity

Measurements of specific heat are difficult to perform and the results are often associated with a relatively high level of uncertainty. The specific heat of each test specimen is determined based on the moisture content measured for each specimen.

In ENV 1992-1-2, /1995/ an equation for determination of the specific heat as function of temperature is given for siliceous and calcareous concrete:

$$c_c = 900 + 80\frac{T}{120} - 4\left(\frac{T}{120}\right)^2 \tag{4.2}$$

where

c_c is specific heat [J/(kg K)],
T is temperature where the peak is situated [°C]

Due to steam generation the curve describing the specific heat will have to be modified. As the thermal properties of water are known and the amount of water needed to account for the moisture in the concrete is known, the area under the c_c curve can be calculated. Exactly how the curve looks like is not known but here the curve has been completed by a peak situated between 100 °C and 200 °C. The value of the specific heat peak in ENV 1992-1-2, /1995/ is declared for the water content 2 and 4 % by weight as 1875 and 2750 $^{J}/_{kgK}$ respectively.

The following Equation (4.3) is adopted to determine the peak of the specific heat curve for an arbitrary water content in HPC (Holst, /1994b/):

$$c_{c,peak} = 2\frac{2500 \cdot 10^3 (1 - 0.001\theta) \cdot \delta}{\Delta T} + c_{c,q} \tag{4.3}$$

where

$c_{c,peak}$ is value of specific heat at the peak [J/(kg K)],
T is temperature where the peak is situated [°C],

δ is water content by weight [-]
ΔT is temperature interval where the steam is generated [K]
$c_{c,q}$ is specific heat determined according to Equation 4.2 at the temperature T [J/(kg K)]

The temperature calculations presented in this report are based on a nominal specific heat, determined according to Equation 4.2. To this nominal specific heat curve an addition of the energy consumption associated with a steam generation is made in the temperature interval 100 - 200 °C, and the peak is located at 120 °C. The value of this addition is a function of moisture content in the current specimen and is determined in agreement with Equation 4.3. Since the peak of the specific heat curve depends on the moisture content, different curves can be derived for concrete with different moisture content. For concrete characterised by a water cement ratio of 0.3, a silica fume cement ratio of 0.1 and a relative humidity of 40 % the weight of vapourable moisture per cement weight is approximately 0.105 (desorption) according to Atlassi, /1994/. The corresponding value for 60 % RH is 0.155 (Holst, /1994b/).

The specific heat at elevated temperatures for high strength concrete has been determined for concrete characterised by a water cement ratio of 0.3, a cement weight of 465 kg/m^3, 10 % silica fume of cement, concrete density of 2450 kg/m^3 and the relative humidities of 40 and 60 %. The specific heat curves are illustrated in Figure 4.2. In Figure 4.2 is also listed values of specific heat for OPC according to Anderberg and Pettersson, /1992/ and OPC according to ENV 1992-1-2, /1995/.

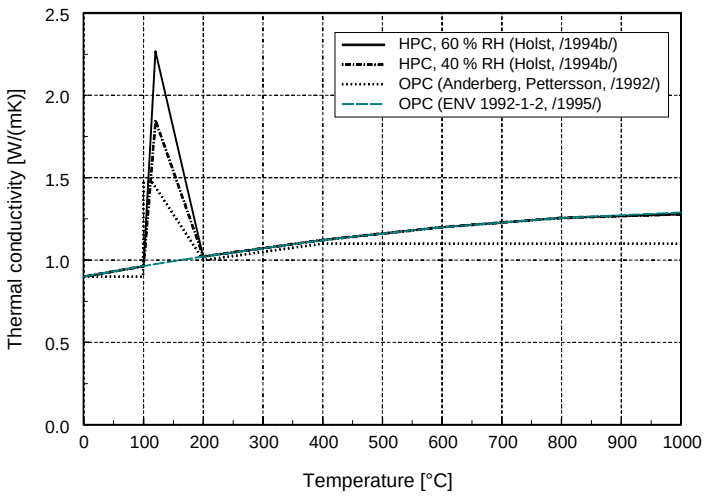

Figure 4.2
Specific heat at elevated temperatures for HPC measured in the M7 project for 40 and 60 % relative humidities (Holst, /1994b/) and OPC according to Anderberg and Pettersson, /1992/ and ENV 1992-1-2, /1995/.

4.1.3 HPC versus OPC

HPC is denser than OPC which means that the thermal conductivity λ_c as well as the specific heat c_p is higher per cubic meter. Still it is important to notice that c_c per kilogram is the same for HPC and OPC, as these materials consists of the same ingredients. The OPC parameters used here are obtained from Anderberg and Pettersson, /1992/.

A higher thermal conductivity of HPC means that the heat conducts faster in the concrete than for OPC, resulting in a higher temperature. The higher specific heat on the other hand works in the

opposite direction providing an enhanced heat storage potential. The product of the specific heat and density is called capacitivity and is often used to indicate this potential.

The factors mentioned above can cancel out each other to some extent but how much is difficult to say. To be able to judge the difference in the temperature field between HPC and OPC comparison of important parameters have been carried out. This will be done in Chapter 5.

As the thermal properties have been assumed similar for HPC to the ones given in ENV 1992-1-2 /1995/ the temperature fields can be determined from annex B in ENV 1992-1-2 /1995/.

4.2 STEEL

The thermal properties of steel are shown in Figures 4.3 and 4.4. Thermal capacitivity is the product of specific heat and density. The values are obtained from ENV 1993-1-2 /1995/.

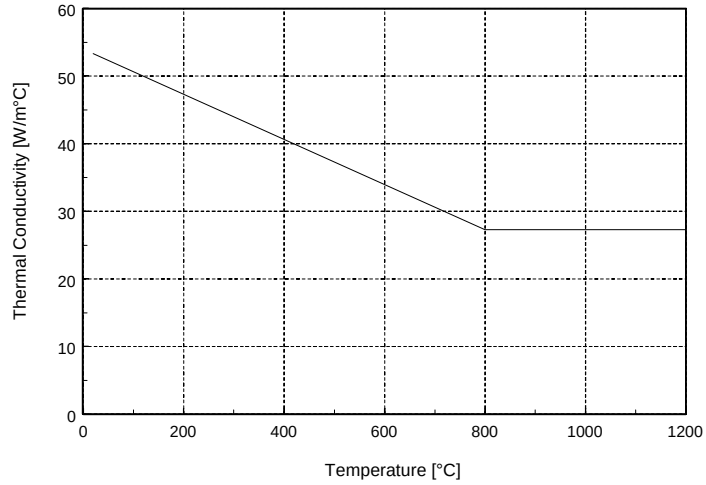

Figure 4.3
Thermal conductivity of steel as a function of temperature (ENV 1993-1-2 /1995/).

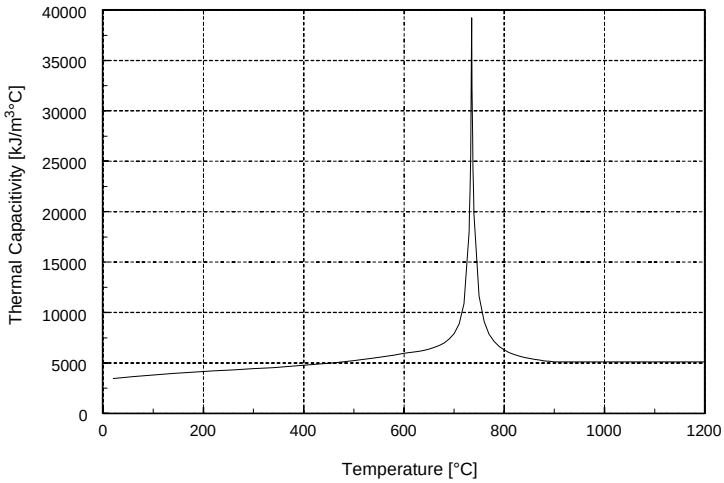

Figure 4.4
Thermalcapacitivity of steel as a function of temperature (ENV 1993-1-2 /1995/).

5. HEAT FLOW ANALYSIS

Chapter 5 takes up basic theories and assumptions for the heat flow calculation in the concrete given the HPC thermal properties (Chapter 4). Fire exposure will be assigned and the way numerical calculations are performed is discussed. Furthermore an analysis will be carried out to differentiate thermal fields of HPC in comparison to OPC.

For structural fire engineering the thermal response of a structure is of fundamental importance and therefore the transient heat flow analysis has to be modelled to apply in the structural analysis. The mechanism governing the heat flow in a structure exposed to fire is a combination of the geometry, material and the mechanism of heat flow. The heat flow mechanisms are highly influenced by the state of the concrete and are controlled by factors like moisture content and mix proportions. Factors, e.g. thermal properties of materials, changing with increasing temperature must be accounted for when thermal flow is calculated.

5.1 THEORY AND CALCULATION

5.1.1 The Fourier Equation

The temperature field in a construction is controlled by Fourier's differential equation for heat balance and for the two dimensional case it is as follows:

$$\rho c_c \frac{\partial T}{\partial t} - \frac{\partial}{\partial x}\left(\lambda_c \frac{\partial T}{\partial x}\right) - \frac{\partial}{\partial y}\left(\lambda_c \frac{\partial T}{\partial y}\right) - \dot{Q} = 0 \qquad (5.1)$$

where

T	is temperature [ºC]
t	is time [s]
x,y	is cartesian coordinates
ρ	is denisty [kg/m^3]
λ	is thermal conductivity [W/mK]
c_p	is thermal capacity [J/(kg*K)]
Q	is generated heat in unit volume [J/(s*m^3)]

Equation 5.1 on the other hand gives only an approximation for the temperature distribution as the moisture and vapour movement also affect. This is accounted for by varying the thermal factors like thermal capacity according to experiments.

The boundary conditions can be set as either prescribed boundary conditions or prescribed boundary heat flux. Considering the first option, the heat flow at the boundary is based on convection and radiation according to Equation 5.2.

$$\dot{q}''_n = \alpha_k (T_g - T_b) + \varepsilon_r \sigma (T_g^4 - T_b^4) \quad (5.2)$$

where

$\dot{q}''_n$ is heat flow at the boundary [W/m^2]
T_g is gas temperature [°C]
T_b is boundary temperature [°C]
α_k is convection heat transfer coefficient [W/m^2°C]
ε_r is resulting emissivity
σ is Stefan-Boltzman constant [W/m^{2}K^4]

As for prescribed heat flow at the boundary, the magnitude of the heat flow is simply given by the current time dependent value, thus the flow, $\dot{q}''_b = \dot{q}''(T)$.

5.1.2 Heat Transfer Coefficients at Boundaries

In a fire, the heat transfer at the structure surfaces is dependent on conditions like:

- Distance from burning objects and gases to the actual surface.
- Properties and direction of the actual surface.
- Surrounding gas turbulence (Forsén, /1982/).

The heat exchange at the boundaries of the fire exposed member depend on the heat transfer coefficients of both emissivity and convection. Resultant emissivity and convection factors were adopted in accordance with Table 5.1.

Table 5.1: *Resultant emissivity and convection factor for exposed and unexposed surfaces.*

Emissivity / Convection	ε_r [-]	h_c [Wm^{-2}°C^{-1}]
Unexposed surface	0.8 (Thelandersson, /1974/)	9 (ENV 1992-2-2, /1994/)
Exposed surface	0.56 (ENV 1992-2-2, /1994/)	25 (ENV 1992-2-2, /1994/)

5.1.3 Numerical Calculation

The temperature calculation is based on the finite element method (FEM), where the cross sections are divided into small (finite) elements.

The computer program SUPER-TEMPCALC (see Appendix D) used for the calculations has been developed at Fire Safety Design, Sweden. For further reference see Anderberg /1991/. With it's aid, it is possible to use the non-linear heat conduction equation mentioned earlier (see Equation 5.1) to calculate the temperature distribution in the cross section as a function of time given the boundary conditions, in this case the ISO-834 curve and the material properties.

Symmetry in cross section and boundary conditions often make it possible to reduce the cross-section to the half or one-fourth of the original size, simplifying input as well as shortening the calculation time. This is only interesting when these reductions can also be made when calculating

the moment capacity for e.g. beams and slabs or structural fire resistance time in the case of columns.

5.2 FIRE EXPOSURE

In representing fire resistance classes in national codes the Standard Fire is used, defined by the heat exposure given by ISO-834. This temperature-time relationship on the boundary of the member is defined in equation 5.3 and shown graphically in figure 5.3.

$$T_b = 345*\log_{10}(8t + 1) + T_0 \qquad t > 0 \tag{5.3}$$

where

T_b is boundary temperature [°C]
T_0 is ambient temperature [°C]
t is time [min]

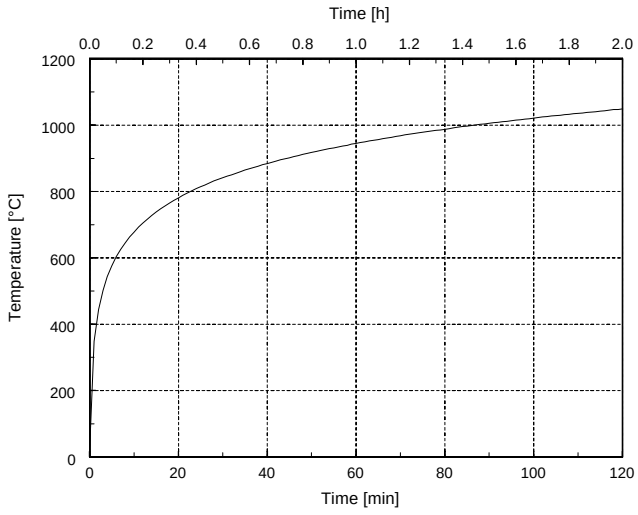

Figure 5.3
ISO-834 Standard fire time temperature curve /1975/.

5.3 TEMPERATURE FIELD OF MEMBERS

5.3.1 General

In the temperature calculation presented in this rapport only a two-dimensional case has been analysed since at the time being, three dimensional temperature calculation programs are not available. The temperature field in the cross section is therefore assumed to be constant along the length of the structure.

It has been shown that with a good approximation the temperature distribution in a cross-section can be calculated without taking into account the reinforcement (Ehm, /1967/) as the temperature in the homogenous concrete approximately equals the temperature at the central point of the reinforcement. This is due to a lower thermal conductivity of the reinforcement as well as variations in heat transfer coefficients at the surface of the reinforcement. The phenomenon is visually explained in Figure 5.1

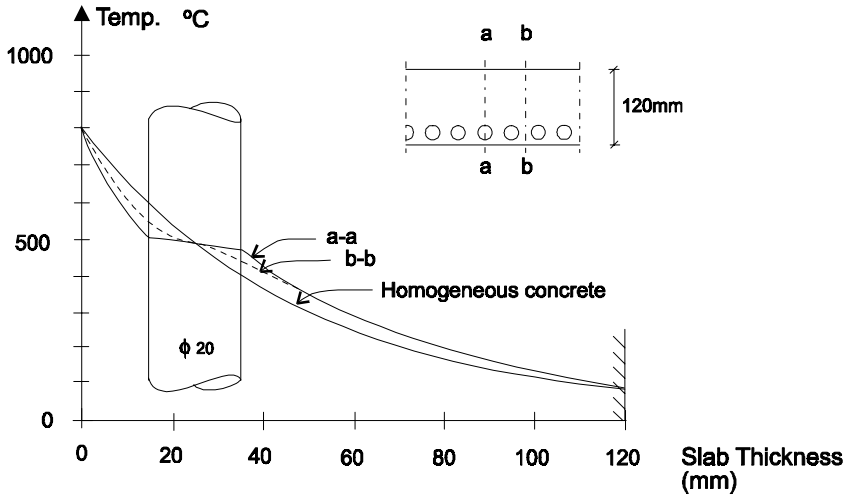

Figure 5.1
Influence of reinforcement on temperature distribution in a slab (Anderberg, Pettersson, /1992/).

The effect seen in Figure 5.1 is usually only to account in the case when reinforcement is placed in the compression zone as increase in the concrete at tension is of minor importance. The concrete tension strength is usually not accounted for in design.

The temperature distribution in a cross section is highly affected by the geometry. This is automatically taken into account in a computer calculations but when calculation have to be done by hand these two-dimensional effects can be discarded to a certain amount. The two dimensional effects are demonstrated in Figure 5.2.

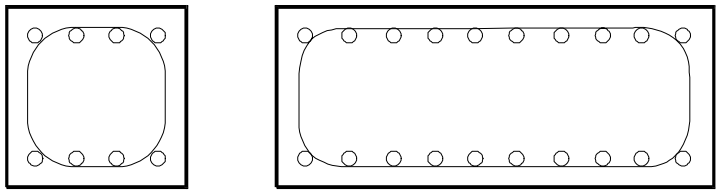

Figure 5.2
Penetration of a heat isotherm at a certain time for different types of cross sections.

Two dimensional effects arise in corners and other curvatures when one-dimensional heat flow can't be applied, and becomes very important when calculating beams or columns with small cross-sections (see Chapter 6 and 7).

5.3.2 HPC versus OPC

As mentioned in Section 4.1 there are thermal properties of HPC according to Holst /1994b/ differ from those for OPC according to Anderberg and Pettersson /1992/. HPC has both higher thermal conductivity (Figure 4.1) and higher specific heat (Figure 4.2).

For thermal calculation, use have been made of the capacitivity, defined as specific heat multiplied with density. For OPC the density is known to decrease with increase in temperature but this variation is low for ordinary aggregate. For HPC the density has been considered constant in the calculations.

It is interesting to see how the differences in thermal capacity and specific heat between HPC and OPC influence the temperature field of the concrete. For OPC, temperature fields have been calculated for numerous cross-sections (Anderberg /1992/) and it is of interest to be able to use these graphs even for HPC. Calculations have been carried out to analyse the difference between temperatures in a HPC and OPC.

The first analysis is done on the depth of the 500 °C isotherm in a 300 mm thick slab. The result is shown in Table 5.2.

Table 5.2 *Differences in penetration of the 500 °C isotherm for a 300 mm slab, between HPC and OPC thermal properties.*

Time [min]	Penetration [mm]		Proportion [-]
	HPC	OPC	HPC/OPC
30	8.9	9.1	0.99
60	21.7	19.0	1.14
90	31.4	26.8	1.17
120	39.8	33.4	1.19

Table 5.2 reveals that the penetration of the 500 °C isotherm is greater when thermal properties for HPC are used than when using thermal properties for OPC. The proportion difference is at most 1.19. Similarly when the criteria is the 400 °C isotherm, the result of the HPC/OPC proportion is as shown in Table 5.3.

Table 5.3 *Differences in penetration of the 400 °C isotherm for a 300 mm slab, between HPC and OPC thermal properties*

Time [min]	Penetration [mm]		Proportion [-]
	HPC	OPC	HPC/OPC
30	15.3	14.5	1.06
60	32.0	27.0	1.19
90	44.7	36.7	1.22
120	55.2	44.8	1.23

The results from temperature calculation given in Tables 5.2 and 5.3 indicate that it is non-conservative to apply the thermal properties of OPC to HPC. The cross-section heats up faster in HPC and the proportion difference is up to 1.23, greatest at 120 minutes.

Reinforcement temperature is also important in the for the calculation of load bearing capacity. Therefore is it important to see what temperature results at a constant distance from the exposed boundary, where the reinforcement could be supposed to be placed. For reasons discussed above the reinforcement bar is absent in the calculation.

Table 5.4 *Differences in temperature at a 25 mm distance from the exposed boundary for a 300 mm slab, using HPC ands OPC thermal properties*

Time [min]	Temperature at 25 mm [°C]		Proportion [-]
	HPC	OPC	HPC/OPC
30	281	223	1.26
60	461	411	1.12
90	568	524	1.08
120	645	602	1.07

As before the thermal properties of HPC result in higher temperatures than obtained for OPC. The proportion difference is greatest 1.26 at 30 minutes but decreases to 1.07 at 120 minutes.

The difference between OPC and HPC can be taken into account by using some multiplication factors for adjustment. This is necessary so that similar penetration is obtained (for HPC) when OPC properties are used as for using the real HPC thermal properties. The same applies to temperatures in the reinforcement when OPC thermal properties are used. In both cases a factor of 1.20 might be suitable.

Note that in Table 5.4 the proportion difference decreases with time (with increased temperature). This is opposite to what is observed for the penetration in Table 5.2 and 5.3 where the difference increases with time. For members exerted to bending, the moment capacity is dependent on both the penetration of the single isotherm that make up the concrete compression zone and the temperature in the reinforcement which make up the tension strength of the reinforcement. Reduction of both the concrete compression zone and the reinforcement strength might become too conservative as the proportion difference is not 1.20 for both cases at the same time.

6. BEAMS AND SLABS

In Chapter 6 the general mechanical properties of beams and slabs at elevated temperatures are discussed. Varying parameters of the analysis are described as well as the calculation procedure. Results from the calculations are analysed in detail and the different phenomena arising explained. These lead to the recommended design rules.

6.1 MECHANICAL BEHAVIOUR

6.1.1 Bending Capacity

Beams are structural elements carrying transverse external loads that cause bending moments and shear forces along their length.

The flexural (bending) strength of sections and beams is counteracted by the concrete compression force and the tension in the reinforcement. The principal forces are shown in Figure 6.1.

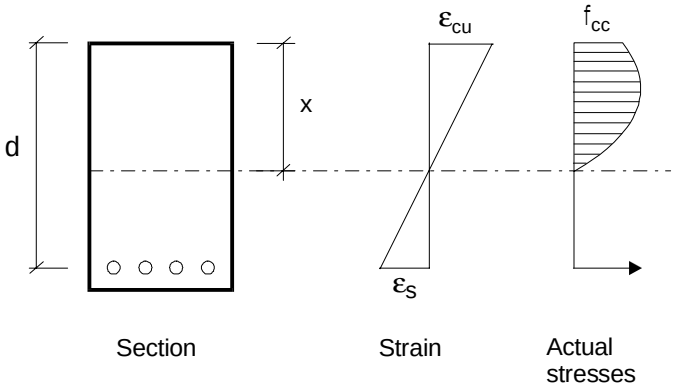

Figure 6.1
Strain and stresses in a reinforced concrete beam element (Park, /1975/).

where

d	is effective depth [mm]
x	is the depth of the compression zone [mm]
ε_{cu}	is strain in the concrete
ε_s	is strain in the steel
f_c	is concrete compression strength [MPa]

The neutral axis is at depth x from the top of the compression zone. The stress is however not uniformly distributed on the area but has the form shown in Figure 6.1. For simplification the compression zone is often set as a rectangle having depth less than x (0.85*x in BBK /1995/). However, it is not necessary to make this simplification when calculations are performed with the aid of computers as discussed in Section 6.3.

Beams at ordinary temperatures can have three kinds of failures; tension-, compression- and balanced failure. In tension failure the yielding of the reinforcement occurs before the concrete reaches it's maximum capacity. With increase in loading the reinforcement strength will still be the same as the steel has yielded but the strain increases. This will eventually lead to reduction in

the resistance of the concrete and crushing commences. Still the failure is initiated by the tension in the steel and therefore named tension failure.

Yielding in the primary reinforcement, i.e. tension failure, is normally the reason for failure in a beam or slab. The grade of fire exposure is of great importance as it controls the temperature in the reinforcement and the concrete compression zone.

When a concrete compression failure occurs the concrete has reached it's maximum capacity before the steel has yielded. This happens if the steel content or strength of the section is large. Before failure occurs the neutral axis depth increases considerably, causing an increase in the compression force which however is reduced by a simultaneous reduction in the lever arm. The reinforcement has still not yielded.

Compression failure can be very dangerous as this failure form happens in a brittle manner. The visual warning is much less than for tension failure where flexural cracks in the concrete are formed sooner because of larger strain in the steel.

In a fire, the risk for brittle failure of a concrete element because of over-reinforcement is decreased as the ultimate stresses in the reinforcement are lowered with increasing temperature. When the element cools down the reinforcement strength is gained partly or fully (for pre-stressed and reinforcing steel respectively) while the compressive strength of the concrete is subject to a further decrease. As long as the load percentage is sufficient and the structure will not fail, it may become over-reinforced (Herz, /1985/).

Balanced failure is when the steel yields and the concrete reaches it's maximum compression strength at the same time. This is of course very unlikely to happen in practice.

There is little research done on shear forces in HPC beams under fire attack. Some phenomena are however possible to explain from today's knowledge of OPC.

Following assumptions have been made:

- The tensile strength of the concrete is assumed to be zero.
- As the steel area in the above discussion is quite small it is assumed that the stress is uniformly distributed over the cross section.
- The temperature in the concrete is not affected by the steel temperature and the steel temperature may be calculated as the temperature in the concrete at the centre of the steel (see Chapter 5).
- Shear has not been taking into account.

6.1.2 General Behaviour of HPC Beams and Slabs at Elevated Temperatures

The difference in the relative strength curve for HPC compared to OPC is considerable (see Figure 3.2). This difference is well visible in strength behaviour of a HPC element. The OPC relative strength curve has a very steep descending branch from about 450 to 600 ºC. It has therefore been easy to judge the decrease in the strength within the element based on the temperature. For HPC the relation is not as simple as demonstrated in Figure 3.2 and reviewed in Figure 6.2.

For a slab with thickness 80 mm the temperature field due to a ISO-834 fire exposure from underneath is after 60 minutes as shown in Figure 6.3. The factors governing the heat flow in the concrete are explained in Chapters 4 and 5.

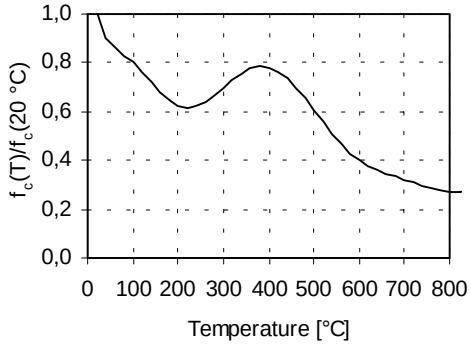

Figure 6.2 *(Figure 3.1) Relative strength versus temperature for HPC (see Figure 3.1)*

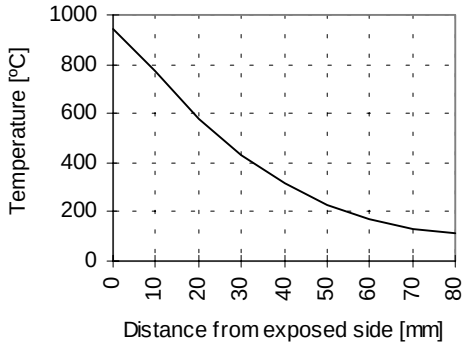

Figure 6.3 *Temperature field in a 80 mm slab after 60 minutes (ISO-834 /1975/)*

If Figure 6.2 and 6.3 are combined so that the concrete slab is assigned a relative strength according to the temperature field in Figure 6.3, the result will be as shown in Figure 6.4.

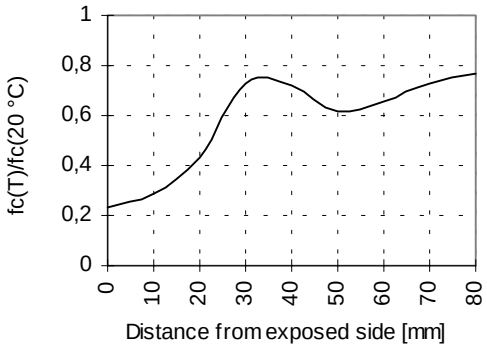

Figure 6.4
The relative strength in the concrete at 60 minutes as a function of the distance from the exposed side

The relative strength in the concrete as a function of the distance from the exposed side (Figure 6.2) will obtain similar form as the relative strength curve as a function of temperature (Figure 6.2). Note the drop in the relative strength that occurs at temperatures 100 to 350 ºC. Note also that the general form in Figure 6.4 is mirrored from the one in Figure 6.3 as the temperature is greatest at the exposed side.

Only simply supported elements have been analysed in this report. Hyperstatic elements have different moment distribution than observed in single supported beams, i.e. negative moments over intermediate supports. A redistribution of the moment occurs when the element is heated from beneath as the stiff supports restrain the effects of the heating. This causes additional moments over the supports, increasing the stresses there but lowering the stresses in the midspan sections. Normally this redistribution will continue until the yield stress of the upper, cooler reinforcement over the intermediate supports are reached. Final failure will occur when plastic hinges have been created over the supports and the reinforcement in the midspan region reaches it's critical temperature (CEB, /1991/).

6.1.3 Beams

The relationship between relative strength and temperature (see Figure 3.2) will affect every type of structure, and not only one dimensional slabs as in the example above. The effect will as a matter of fact have a greater influence on structures with three or four sided exposure. In Figure 6.5 a beam with three sided exposure (vertical sides and lower horizontal side) is shown. The forces in the reinforcement and concrete compression zone are being reduced by increase in temperature. In the compression zone the relative strength might be similar to that experienced by a one dimensional slab in Figure 6.4 but here the temperature is increasing from both vertical sides. The form of the relative strength also varies with time within the cross-section as the temperature increases.

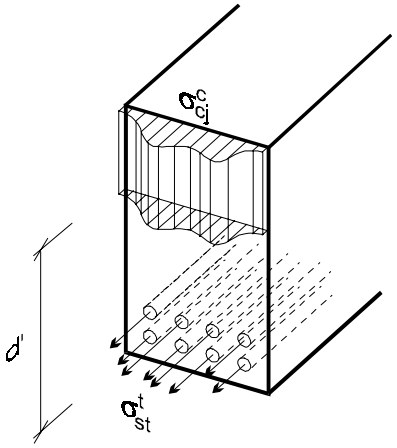

Figure 6.5
Strength distribution in HPC and reinforcement when exposed to fire on three sides. Note the compression zone strength has a similar form as shown in Figure 6.2.

where

d' is reduced effective depth [mm]

σ^c_{cj} is concrete stress in each element j of the compression zone [MPa]

σ^t_{sti} is stress in steel i at temperature T_i [MPa]

The reduction of the strength of the reinforcement is dependent on the temperature as shown in Figure 3.11. The reduction of concrete strength follows a more complicated correlation with the temperature according to Figure 3.2 or Figure 6.2.
In practice this complicated reduction will be assumed to be uniform and equal to f_c over a reduced area. This will be studied in detail in Section 6.5.

6.1.4 Slabs

The forces in a slab are the same as in a horizontally exposed beam Moreover, the temperature can be calculated as one-dimensional for simple slabs if the influence of reinforcement is not included (see Chapter 5). In this sense it is worth reviewing Figures 6.3 and 6.4.

The temperature can theoretically be on two sides at the most but in practice the fire is almost always considered on one side only. The ceiling always becomes warmer than the floor in a fire in a compartment but when the compartment has reached a flashover these differences diminish.

Different from beams, where the temperature in the compression zone usually decreases from the vertical sides, the temperature gradient in the compression zone is now from the top of the plate. This means that the isotherms are now parallel to the neutral axis instead of perpendicular for

beams. For practical purposes this can result in a simplification as both the strain and the temperature varies from horizontal sides and the stresses at different strain levels can be estimated using different stress-strain curves.

6.1.5 Pre-stressed Structures

For beams with pre-stressed steel the failure mode will vary somewhat from what is observed for beams with ordinary reinforcement. As mentioned in Chapter 3.3 the pre-stressing steel is more affected by increase in temperatures.

Pre-stressing steel is stronger and therefore normally has less area than ordinary reinforcement. This means that the total area of pre-stressed steel is less than for ordinary steel giving the same force. Pre-stressing steels are also placed denser and with less concrete cover as a result of the smaller diameter. That means that this kind of steel will be heated up faster than ordinary reinforcement.

The faster heating combined with the lower resistance to temperatures make pre-stressing steel structures more vulnerable to fire than ordinary reinforcement structures.

Full original strengths of pre-stressed steel are not regained when cooling.

6.1.6 TT- and I-Structures

In I- and TT- structures the pre-pressed steel is situated in the compact lower part of the element. The dominating two dimensional heat transfer will make the thin structure heat up quickly decreasing the load capacity of the structure rapidly. These types of structures are therefore very critical to fire.

The most sensitive parts of a pre-stressed concrete structure are the end anchorage points (Anderberg, Pettersson, /1992/). This specially applies for thin I- and TT- structures which are always pre-stressed nowadays.

6.1.7 Hollow slabs

For hollow slabs it is necessary to take into account the void within the slab. SUPER-TEMPCALC is able to calculate temperature on different sides of the void and take into consideration radiation and conduction. As air is good isolating material the voids reduce the heat transported in the slab and thus work towards preserving the moment capacity. The flange element increases the lever arm of the slab (this is observed for ordinary slabs) and therefore the moment capacity of the slab.

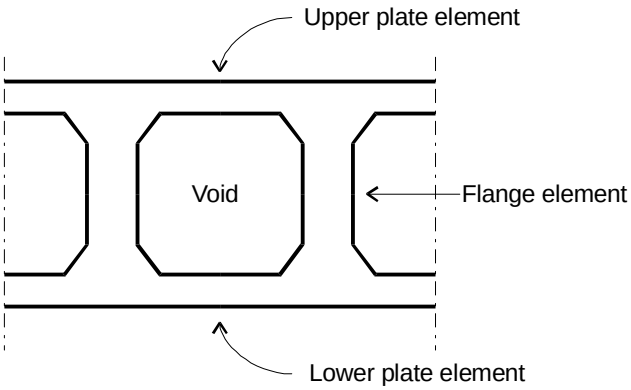

Figure 6.6
Principal figure of a hollow plate element showing different cross-sectional parts.

The steel, which is always pre-stressed, is located in the lower part of the slab. For a fire on the underside of the slab the decrease in the strength of the steel will probably be critical for the strength of the plate.

It is necessary that the horizontal plate elements are resistant to spalling as the slab would break if these parts are subject to spalling. The risk is however not as great as for TT and I- beams where the flanges are directly affected by the fire.

The hollow slabs analysed in this report are of three different sizes. These are viewed in Section 6.2.

6.2 PARAMETER CONFIGURATION

The main objective by performing the calculation of beams and plates is to gain an understanding of how it is possible to use different methods to simplify calculations when the element is attacked by fire.

By simple comparison of moment capacity at different times, given geometrical factors and fire exposure percentage, the different methods can be compared. In the case of beams and slabs it is considered sufficient to look at factors on cross-sectional level as mentioned in Chapter 6.1.

6.2.1 Parameter Study

In the analysis of a beams and slabs the following factors need to be defined:

- Cross-sectional geometry
- Reinforcing cross-sections
- Pre-stressed cross-sections
- Fire engulfment

Note that the external factors like the boundary conditions do not have to be defined as the calculations are carried out on a cross-sectional level.

Eight cross sections have been analysed: rectangular beams (2 cases), flanged beams (2 cases), TT-cassett (2 cases), I-beams (3 cases), slabs (2 cases) and hollow slabs (3 cases). The actual cross-sections are shown in Table 6.1 as well as in Appendix A.

6.2.2 Cross-sectional Geometry

The cross sections can be divided into two groups depending on what type of design is used in the tension zone, i.e. reinforcing steel and pre-stressed steel. Simplified figures showing the different kinds of cross-sections are shown in Table 6.1.

Table 6.1 *Cross-sections and type of design method (r = reinforcing steel, p = pre-stessing steel)*

Name	Steel type	Cross-section
A 1, 2	r, p	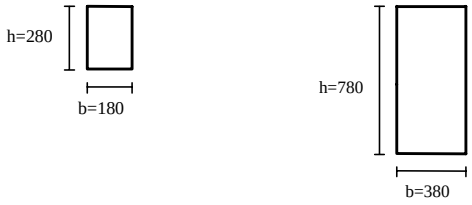
B 1, 2	p	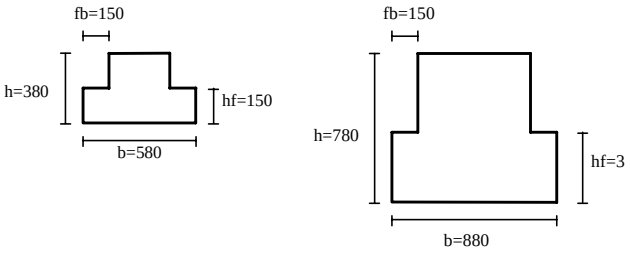
C 1, 2, 3	p	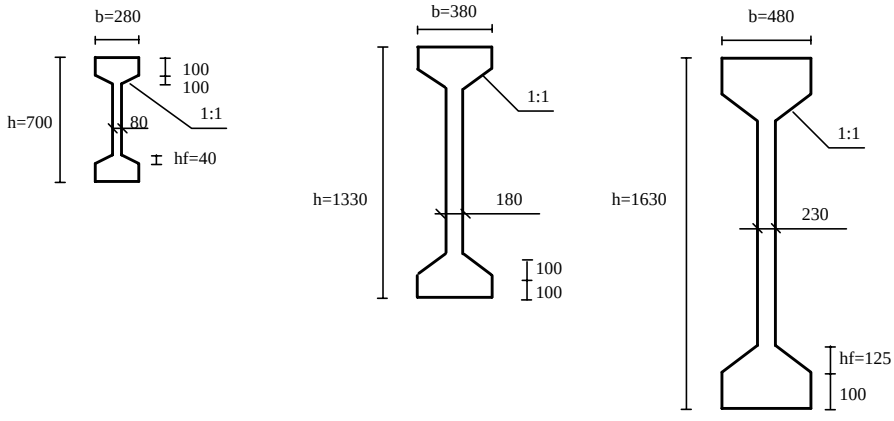
D 1, 2	p	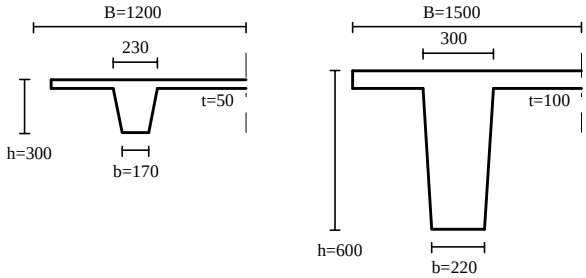

E 1, 2	r, p	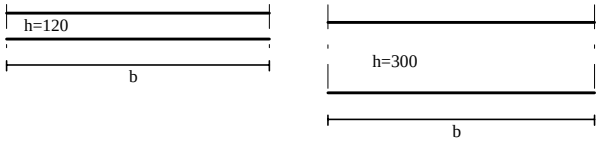
F 1, 2, 3	p	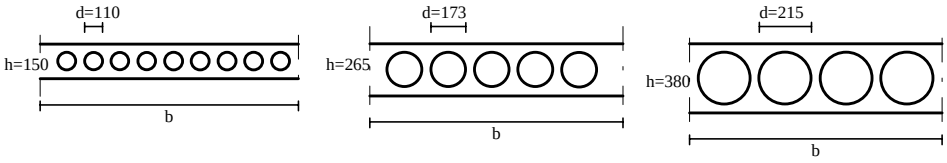

6.2.3 Reinforcing Cross-sections

The cross-sections with reinforcing steel are, as indicated in Table 6.1, rectangular beams and slabs.

The amount of reinforcement in respective cross-sections were calculated by assuming a balanced reinforcement (see Section 6.1) which means that a large amount of reinforcement is necessary to account for the high strength of HPC.

The characteristics of the reinforcement type used are listed in Table 6.2.

Table 6.2 *Characteristics of reinforcing steel*

	Value	Unit
Tensile strength	500	MPa
Modulus of elasticity	200	GPa
Diameter tensile steel	16, 20, 25	mm

Other steel characteristics are as discussed in section 3.3 (Mechanical Properties) and Section 4.2 (Thermal Properties).

The topology of the reinforcement is obtained by using the Swedish rules for necessary concrete cover and distance between the reinforcement bars (BBK, /1994/) see Figure 6.7.

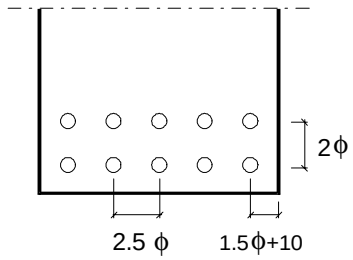

Figure 6.7
Topology of reinforcing steel according to BBK /1994/

The number of reinforcement bars are therefore as indicated in Table 6.3.

Table 6.3 *Reinforcement of cross-sections given in Table 6.1.*

Geometry number	Diameter [mm]	Total number of reinforcing steel bars	Number of rows
A1	16	12	3
A2	25	30	5
E1	12	32 *	1
E2	12	32 *	1
E2	12	64	2

* [per m]

6.2.4 Pre-stressed Cross-sections

Pre-stressed cross-sections are marked in Table 6.1. These are rectangular beams, flange beams, I-beams, TT-slabs, slabs and hollow slabs.

For the calculation of the amount of pre-stressed steel to use it was assumed that the steel should be able to counteract a 20 MPa stress in the concrete. The necessary number of steel bars was then calculated simply by dividing the tensile stress of the steel by the total stress (se Table 6.4) in the concrete.

Reinforcing steel is also provided to account for tension in the pre-stressed cross-section at unloaded stage.

Table 6.4 *Characteristics of pre-stressing steel*

	Value	Unit
Tensile strength	1860	MPa
Diameter steel in tension zone	12.9	mm
Diameter reinforcing steel in compression zone	12, 16, 20, 25	mm

As before is the topology of pre-stressed steel bars obtained by using the Swedish rules for necessary concrete cover and distance between the reinforcement (BBK, /1994/) see Figure 6.8. The reinforcing steel

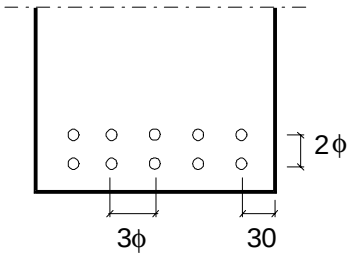

Figure 6.8
Placement of pre-stressing steel according to BBK /1994/

Topology information on pre-stressed steel in respective cross-sections are listed in Table 6.5. The diameter of pre-stressed steel is 12.9 mm (1 cm^2) in all cases.

Table 6.5 *Pre-stressing and reinforcing steel in pre-stressed sections.*

	Pre-stressing steel		Reinforcing steel (compression)		
Geometry number	Total number of bars	Number in each rows	Diameter	Total number bars	Number is each row
A1	5	4+1	16	3	3
A2	26	9+9+8	16	20	8+8+4
B1	10	10	16	4	4
B2	40	25+15	16	29	13+13+3
C1	15	6+6+3	20	4	4
C2	30	10+10+10	20	4	4
C3	39	13+13+13	25	4	4
D1	7	4+3	16	3	3
D2	17	5+5+5+2	16	12	12
E1	7	7 *	12	2	2 *
E2	13	13 *	12	13	13 *
F1	1	1 **	12	1	1 **
F2	2	2 **	12	1	1 **
F3	3	3 **	12	2	2 **

* [per meter], **[between each void]

6.2.5 Fire Engulfment

As mentioned earlier the goal is to obtain design rules to use in practical situations. Hence, the fire exposure in each cross-section will have to be practically assigned e.g. it is judged highly unlikely that a slab is exposed on more than one side at a time. A beam is also seldom exposed on only one side.

For both the reinforcing structures as well as the pre-stressed ones the fire exposure varies. The beams have been analysed with 3-sides and 4-sides exposure, flange-beams with exposure from above as well as the 3-sides (on the tension zone) and I-beams only exposure on 3-sides.

Slabs (slabs, TT-slabs and hollow slabs) have only been analysed with 1-side exposure with fire from above or from underneath. Table 6.6 provides a visualisation of the different fire exposures.

Table 6.6 *Fire exposure on actual cross-sections*

Geometry number and fire exposure number	Fire exposure
A i, ii	

B i, ii	
C i, ii	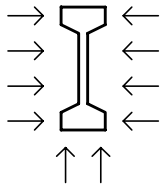
D i, ii	
E i, ii	
F i, ii	

The fire exposure is very important for the mechanical behaviour of the cross-section when the reduction in moment capacity is calculated.

The limitations are that the design rules can therefore only be applied to structures similar to the ones considered here with similar fire exposure and separate calculations have to be carried out for other cases.

6.3 COMPUTER CALCULATION

Sections 6.1 and 6.2 provide a background for the computer calculation. For each of the cross-sections listed in Table 6.1 (both reinforcing and pre-stressing steel) and for every fire exposure (Table 6.6) a calculation is carried out. This is done for fire endurance of 30, 60, 90 and 120 minutes. Totally 132 simulations were carried out.

6.3.1 Calculation Procedures

A simplified approach for describing the simulation process can be seen in Figure 6.9. The way the temperature file is generated is described in more detail in Section 5.4 and in Appendix D.

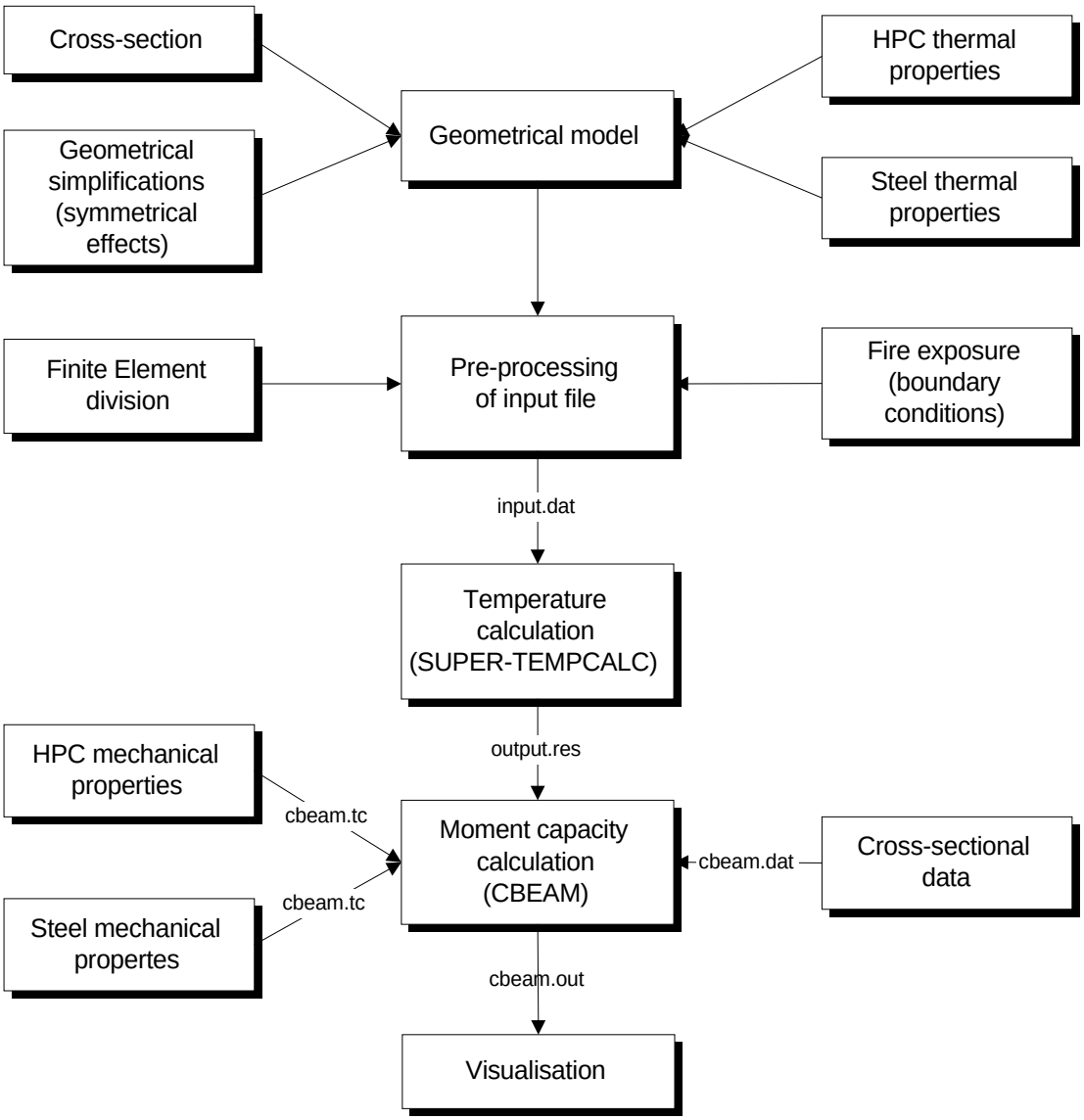

Figure 6.9 *The calculation process for moment capacity reduction in a cross-section.*

For each of the cross-sections listed in Table 6.1 a temperature file has to be generated. The input is the thermal properties for HPC and steel as well as the cross-sectional data. The general boundary condition properties for exposed and unexposed surfaces are listed in Chapter 5.

CBEAM (see Appendix D) calculates the reduction in moment capacity on a cross-sectional level from the original capacity given the increase in the temperature within the cross-section. Mechanical properties are updated for each time step (increase in temperature).

The moment capacity is calculated both for the actual HPC relative strength curve as and then compared to the moment capacity calculated by a simplified curve where the relative strength is assigned a value of one to a certain temperature and zero after that. These curves are viewed in Figure 6.10.

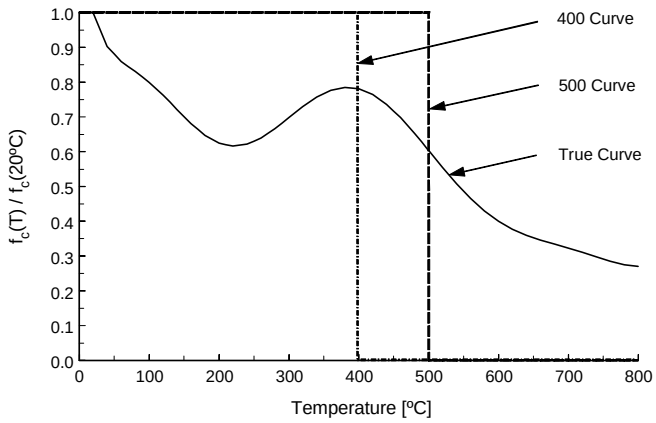

Figure 6.10
Relative strength for HPC from project M7(Holst /1995a/) and a simplified design approach.

The reduction in strength from 100 % to zero can of course take place at any temperature level, but the concentration in this report has been on the single isotherm's strength curves of 400 and 500 ºC, hereafter referred to as the 400 and 500 curves.

6.3.2 Computer Model

As mentioned in section 5.1 SUPER-TEMPCALC uses a finite element division of the cross-section or a "meshed" cross-section. Each node in the mesh contains information about the temperature for each time step.

A meshed cross-section can be seen in Figure 6.11.

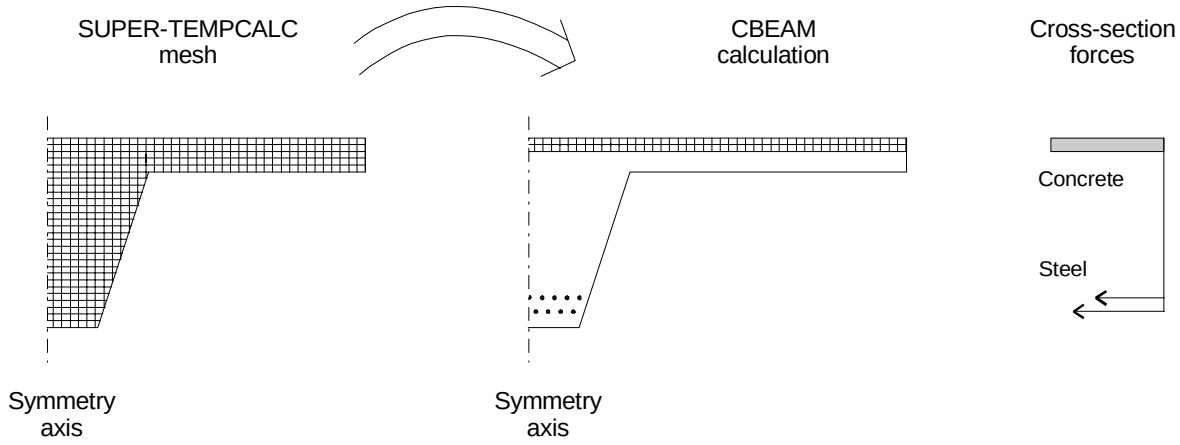

Figure 6.11: *CBEAM modelling from SUPER-TEMPCALC temperature mesh and forces in the cross-section.*

The information from SUPER-TEMPCALC is read by CBEAM for each time step and the moment capacity of the cross-section is calculated according to Figure 6.10. The forces in each section of the concrete are summarised in CBEAM to be compared with the forces in the steel. This comparison makes up for the moment capacity of the cross section. Each node of the cross-section will obtain a force according initial forces and reduction due to the temperature in the node. The nodes are then summarised and compared to the force in the steel which also is temperature dependent.

6.4 RESULTS

A total of 132 calculations where carried out varying cross-sections, steel types and fire exposures. The calculated times where 30, 60, 90 and 120 minutes. In this Section a few cases will be analysed to explain the phenomenon governing the behaviour of the cross-sections where others can be viewed in Appendix B.

Each of the figures below illustrates a moment capacity reduction with time. The figures contain two parts, where part a) shows the actual strength reduction and part b) the percentage reduction of the 400 and 500 curves in comparison to the True curve.

The concrete will gain a maximum temperature of about 1200 ºC in the 120 minutes calculated, applying the ISO-834 /1975/ standard fire. By assigning full strength to the concrete up to 1500 °C reduction in the moment capacity calculated will only be due to the loss of strength in the steel. This curve will be drawn in the above mentioned figures as well as the 400 and 500 isotherm curves where it is assigned the name ”Steel”.

The Steel curve should always have greater moment capacity than the other curves as the concrete has full original strength the whole time. The most interesting comparison is on the other hand the difference between the True and the single isotherm curves (400 and 500 curves).

A moment calculation giving ”conservative result” for the single isotherm curves results in lower moment capacity than the True curve. The difference is best viewed in part b) of the diagrams below where negative percentage difference stands for conservative moment capacity.

To be able to judge the importance of different factors on the behaviour of the moment reduction curves, it is necessary to compare them when other things remain equal. The factors to be varied are fire exposure, geometry, steel type and steel amount.

All cross-section types and reinforcement types can be viewed in Table 6.1 and the fire exposure type in Table 6.11.

Influence of fire exposure

The role of fire exposure will best be illustrated by varying the fire exposure for the same cross-section, other factors being unchanged. Figure 6.12 shows the A1 cross-section with reinforcing steel (r) (see Table 6.1). The fire exposure are of type *i* in Figure 6.12 and *ii* in Figure 6.13 (see Table 6.6).

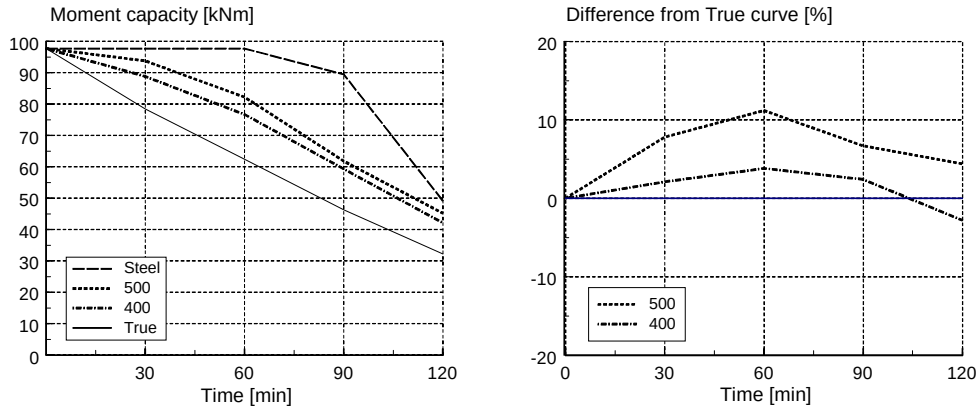

Figure 6.12 *Cross-section A1r with fire exposure i. (280x180 mm rectangular cross-section with three side fire exposure).*

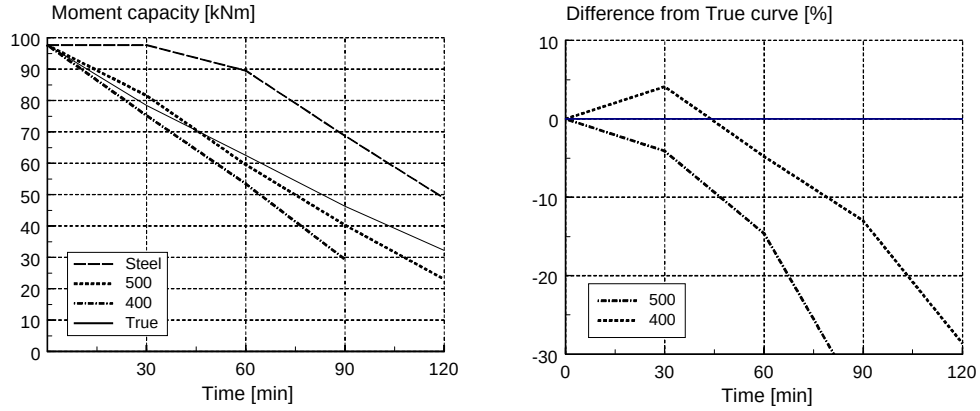

Figure 6.13 *Cross-section A1r with fire exposure ii. (280x180 mm rectangular cross-section with four side fire exposure).*

The difference between Figure 6.12 and 6.13 is quite large as can be seen by looking at the percentage difference (part b). To fully understand the behaviour it is necessary to review how the strength reduces as a function of temperature for HPC in an exposed cross-section as seen Figure 6.4.

The behaviour is explained by how the temperature in the cross-section and hence the relative strength changes with the distance from the exposed boundary but also by how the effective depth is affected by the varying reduction in strength. The phenomena is illustrated in Figure 6.14. Remember that the compression zone is the interesting part in this discussion as the fire exposure is the same on the lower part of the structure.

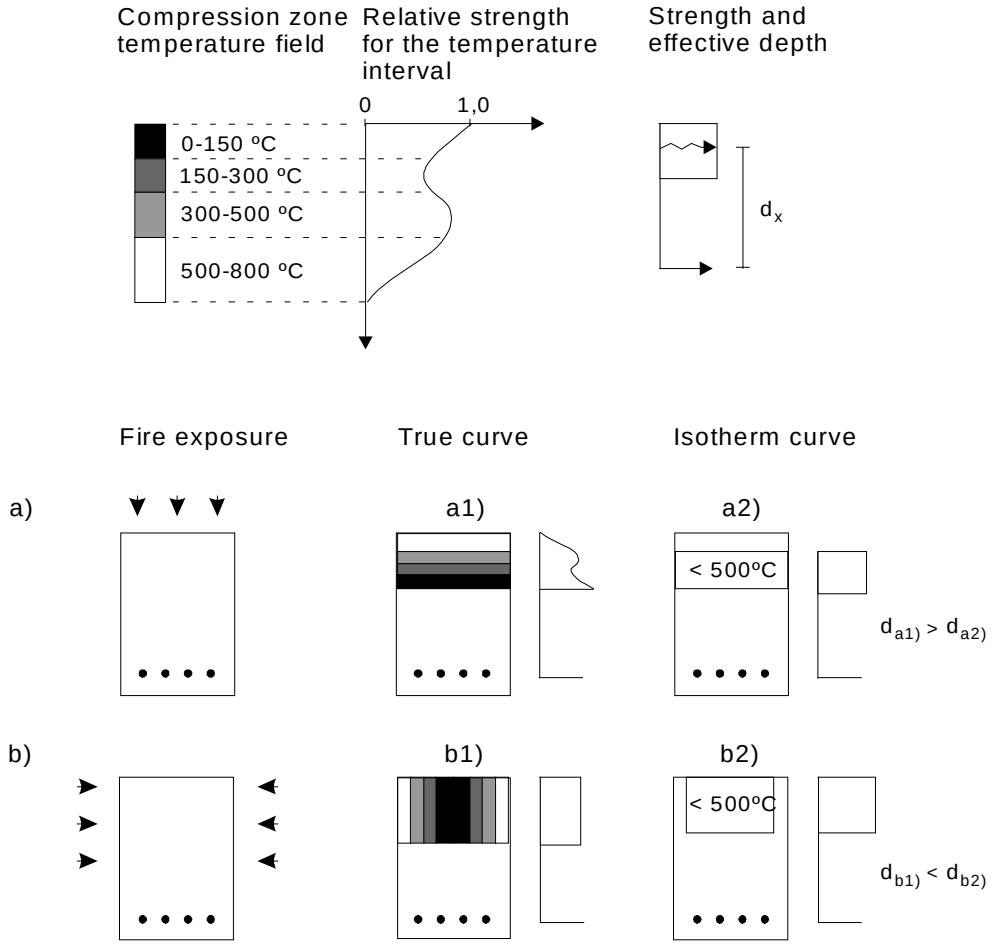

Figure 6.14 *Temperature / relative strength interaction in the cross-section of a beam element.*

Here

d_x is effective length of the cross-section for actual time period.

Note that the 500 isotherm reduction curve is used for explanation in Figure 6.14 but it could as well be the 400 curve which in comparison to the 500 curve would give more conservative results.

For a given steel strength the moment capacity is a function of the effective depth and the compression zone necessary for balancing the forces. This compression zone changes as a function of temperature (or time) for the transient fire phenomena.

The area of the compression zone times the strength times the effective length gives the moment capacity for the cross section. For the True curve, the compression zone forces behave in much more complex manner than when the reduction is according to a single isotherm curve. The temperature interval 150 to 300 ºC is very critical as in this interval the reduction in strength for the true curve is large in comparison to the single isotherm curves.

Now let's look at part a) in Figure 6.14. The single isotherm does possibly have larger effective length than the single isotherm curves in the beginning when the area with temperature in the

interval 500 to 800 ºC is small. When this temperature zone is increased the effective length of the single isotherm curves are lowered much faster than for the true curve. This effect is clearly seen in Figure 6.12 where the 500 curve gives greater moment capacity than the true curve up to about 42 minutes and lower after that and the 400 curve gives lower moment capacity the whole time interval.

For part b) in Figure 6.14 the fire exposure is on the sides which means that the critical interval with temperatures between 150 and 300 ºC will have a larger area in the cross-section. This results in faster reduction of the effective length than for case a).

For A1ri the fire exposure is on the lower part of the cross-section which is similar to part b) in Figure 6.14 but A1rii is exposed on the whole boundary. The effect for Arii will therefore be combined effects from part a) and b).

Note that in Figure 6.14 the temperature in the steel is not assumed to affect the total capacity to ease the comparison. In the actual case the steel strength will be reduced in accordance to the steel curve in Figure 6.12 and 6.13 which in turn will reduce the necessary compression zone necessary to counteract for the forces in the steel.

The trivial case where the compression zone is not exposed at all results in reduction in moment capacity independent of the concrete reduction curves and only equal to the steel reduction curves. This is the case for B1 and B2 with fire exposure *i* (see Appendix B).

Influence of cross-section size.

The geometry plays an interesting role in the moment capacity development. Figure 6.15 illustrates the role of the size of the cross-section on the moment capacity over the time period for the case A2ri. A2 is as seen in Table 6.1 a rectangular cross-section like A1 but a larger one. The amount of steel in the A2r cross-section should be comparable to A1r as both are designed to have balanced forces (see Section 6.1) at ordinary temperatures. The moment reduction for A1r is shown in Figure 6.12. The comparison is carried out for cross-sections with fire exposed on three sides.

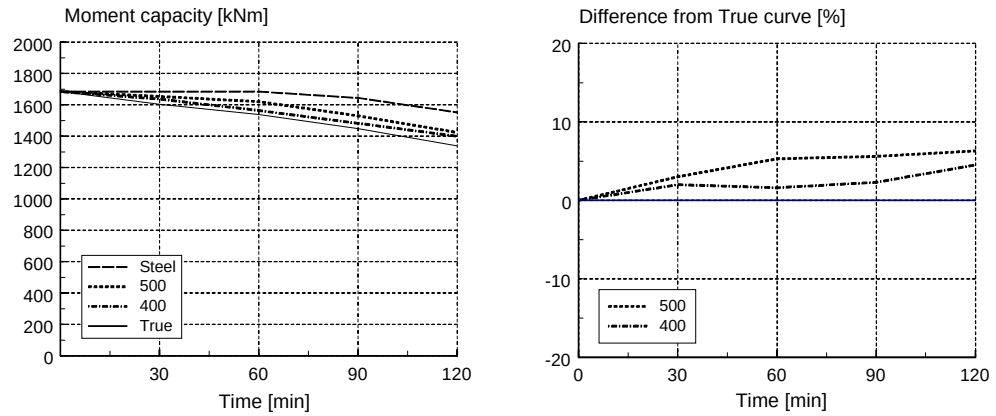

Figure 6.15 *Cross-section A2r with fire exposure i. (780x380 mm rectangular cross-section with three side fire exposure).*

As experienced for A1r, the difference in the moment capacity between the True and the single isotherm curves is positive which means that these curves are non conservative. The difference is however not as great as for A1r (see Figure 6.12). The upswing of the 400 curve at 120 minutes is

quite unique for A2r but a similar phenomena is also observed for simple slabs with reinforcing steel (E1r and E2r). This will not be discussed further in this report.

Influence of steel type

The steel type is of great importance when it comes to fire behaviour as mentioned in Sections 6.1.2.4 and 3.3. Pre-stressed steel is much more sensitive to high temperatures than reinforcing steel and that is clearly observed in Figure 6.16 where the A1 cross-section with fire exposure *i* is provided with pre-stressed steel. This difference is clear by comparing Figure 6.16 with Figure 6.12 where ordinary reinforcement is used for the same structure.

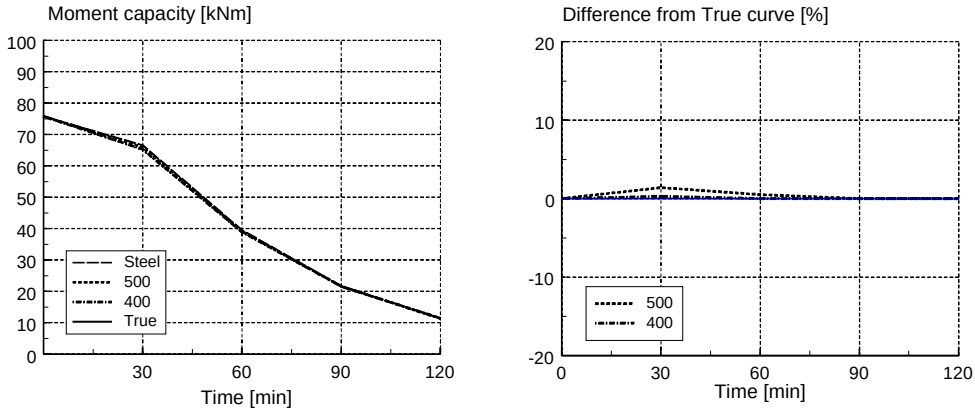

Figure 6.16 *Cross-section A1 with fire exposure i and steel type p. (280x180 mm rectangular cross-section with three side fire exposure) and pre-stressed steel.)*

The reduction in strength for the cross-section in Figure 6.16 is similar for all the concrete moment reduction curves calculated as well as for the Steel curve. This implies that the reduction is pretty much independent of the reduction of strength in the concrete and almost only dependent on the reduction in the steel strength.

The difference between the pre-stressed and reinforced sections is not only because of the difference in relative strength reduction at high temperatures but also because of the amount of steel in the cross sections. To obtain a balanced cross-section a larger area of reinforcing steel is required and the pre-stressed steel is also more compact which means that it is closer to the sections boundary. The total steel area therefore warms up quicker than if reinforcing steel where to be used. This has been discussed in Section 6.1.5.

The behaviour is quite extreme for the A1p cross-section compared to other pre-stressed cross-sections although the trend is similar for all pre-stressed sections. This can partly be explained by the small cross-section of A1 where the steel gains high temperatures quicker than in larger sections.

Influence of reinforcing steel amount

All the structures above have been designed with the criteria of balanced forces in the cross-section.. In Figure 6.17 the total steel area of the A1 cross-section, with reinforcing steel, have been lowered to one third of the original amount.

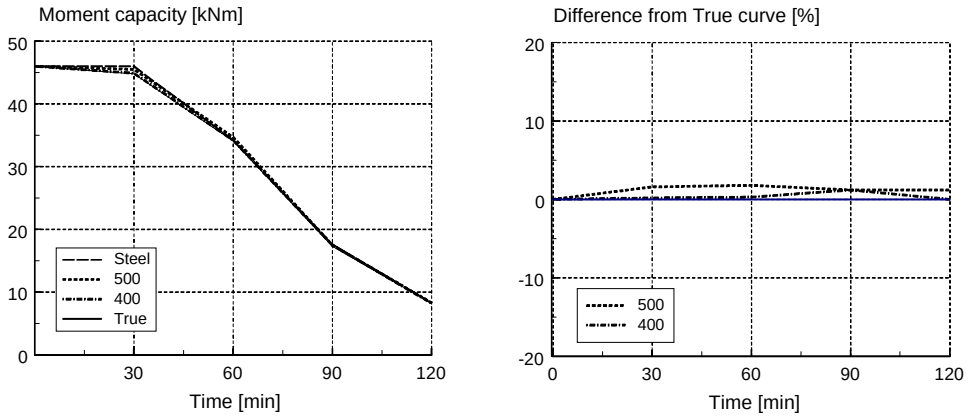

Figure 6.17 *Cross-section A1ri with one third of steel area. (280x180 mm rectangular cross-section with three side fire exposure.)*

The 400 and 500 curves are non-conservative when compared to the True curve but the difference is much less than when larger amount of steel is used. This has a rather simple explanation.

Greater amount of steel means that the moment capacity is greater in the cross-section. This in turn requires that the concrete has to balance the steel strength for a longer time period. Hence the reduction characteristics for the concrete plays a greater part in the overall moment reduction behaviour than otherwise.

Figures for all calculated cases can be viewed in Appendix B.

6.5 DESIGN METHOD

6.5.1 General Results from Calculation

There are several solutions possible for a derivation of a design method based on the calculations presented in Section 6.3. The method does have to be applicable as a simple design method which means that the complexity has to be minimised.

The 400 curve gives a more conservative results in all cases than the 500 curve but it does not give sufficiently secure result for all cases. Other methods have to be considered in this sense.

The 500 isotherm strength reduction curve will be used for beams and slabs with some modifications to cover all cases calculated. The solution is to reduce the final moment capacity for the entire cross-section by some percentage after it has been reduced according to the 500 curve.

The difference in the moment capacity for different cases, using the True curve and the 500 curve, is given below. As mentioned in Section 6.4 positive percentage difference stands for non-conservative moment capacity.

Reinforced beams

Maximum positive difference observed is 11.2 %, obtained for the smallest rectangular section, and sinks to 6.3 % for the larger rectangular section. In these cases the compression zone is exposed to the fire. Otherwise the moment capacity is controlled by the reduction in strength of the steel.

As mentioned in Section 6.4, reinforcing sections have been designed with balanced forces of the concrete and the steel. For a design in practice, less steel would be used to avoid brittle failure as reasoned in Section 6.1.1. Lower steel amount result in a less difference of the concrete reduction curves as explained in Section 6.4. Positive differences of 11.2 % as observed above would therefore hardly happen in practice.

Reinforced slabs
For the thinner slab (120 mm) the maximum positive difference is only 0.3 % for reinforcement in one layer but if the layers are doubled (almost the double strength) the difference will increase to 2.4 %.

Pre-stressed cross-sections
The moment capacity is often somewhat higher for the 500 ºC isotherm curve in comparison to the True curve for pre-stressed cross-sections or about 1.0 %. The maximum difference of a pre-stressed cross-section is 1.6 % for flange beams.

6.5.2 Minimum Plate Thickness

For slabs exposed on the tension side only, the reduction in the slab's moment capacity will be governed by the steel strength reduction. This only applies to the minimum thickness of 120 mm as thinner slabs have not been analysed in this report. The compression zone of thinner slabs might start to gain temperatures high enough to cause a strength reduction after having been exposed on the tension side for a time period less than 120 minutes. Hence, special calculation is necessary for thinner slabs than 120 mm.

6.5.3 Thermal Calculation

The thermal properties follow to great extend ENV 1992-1-2 /1995/ but with some modifications. The thermal conductivity should be applied by using Equation (4.1) or Figure 4.1 and the specific heat by using Equation (4.2) or Figure (4.3), both according to ENV 1992-1-2 /1995/. To count for arbitrary water content in the concrete Equation (4.3) should be applied (Holst /1994b/).

OPC properties can be used for HPC with some modifications. The penetration in the concrete compression zone does have to be increased as well as the temperature in the reinforcement, both by 20%. This is discussed in section 4.1.3 and 5.3.2.

6.5.4 Design Method

Design methods applicable for hand calculation must be simple enough to allow a quick calculation. This of course means that for some structures the rules will be quite conservative.

The simple approach is illustrated in Figure 6.18

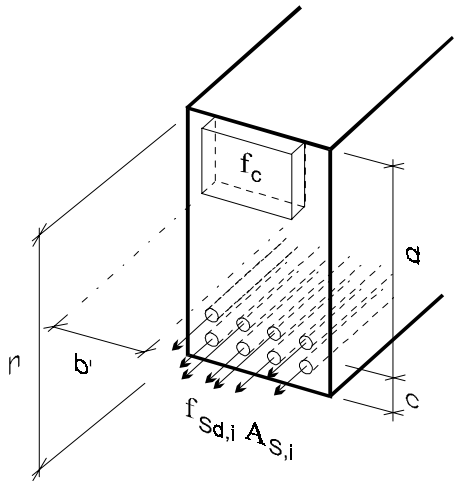

Figure 6.18
Simplified design of HPC concrete beam exposed to fire. The concrete compression zone is assigned a width (b') according to the 500 isotherm curve.

Here

h	is initial cross-sectional height [mm]
d	is effective depth [mm]
b'	is width of the effective compression zone [mm]
c	is distance from effective cross-section to centre of the steel bar group [mm]
f_c	is compression strength of concrete [MPa]
$f_{sd,i}$	is tension strength of steel bar i [MPa]
$A_{s,i}$	is area of steel bar i [mm^2]

For calculating moment capacity, both the concrete and the steel strength have to be reduced. The following methods should be applied:

Concrete
Moment capacity in HPC beams and slabs shall be reduced according to Equation 6.1.

$$M_{d,fi} = M_{500} \cdot r \qquad (6.1)$$

where

$M_{d,fi}$	is design moment capacity in the fire situation
M_{500}	is calculated moment capacity based on the effective cross-section, defined by the 500 ºC isotherm
r	is a reduction factor in accordance with Table 6.7

Table 6.7 *Moment capacity reduction factors for beams and slabs.*

Item	Reinforcement type	r
beams	Reinforced	0.90
beams	Pre-stressed	0.95
slabs	Reinforced	0.95
slabs	Pre-stressed	0.95

The compression strength in the reduced cross-section will be the same as at 20 °C while the concrete with temperatures higher than 500 °C will be assigned zero strength. This is according to the 500 curve in Figure 6.10.

Reinforcement

The steel bar core temperature is assigned according to cross-sectional temperature field graphs of ENV 1992-1-2 /1995/ or by using temperature fields of OPC in accordance with Section 6.5.3. Temperature calculation programs can also be used.

The reduction of strength of reinforcing and pre-stressing steel as well as the modulus of elasticity may be chosen in accordance with Figure 3.11 and Figure 3.14 respectively. For compression reinforcement in beams and slabs and for tension reinforcement with calculated tension strain less than 2 %, the 0.2 % proof strain curve should be adopted. For tension reinforcement with calculated tension equal or greater than 2 %, the 2 % proof strain curve applies. The 0.5 % proof strain curve should be applied to columns.

The average steel strength of a group of steel may then be calculated according to Equation 6.2.

$$f_{sd}(T) = \frac{\sum_i \left(f_{sd,i}(T) A_{s,i} \right)}{\sum_i A_{s,i}} \tag{6.2}$$

where

$f_{sd,i}$ is design strength of steel bar *i*
$A_{s,i}$ is area of steel bar *i*

The distance, c (see Figure 6.18), from the effective cross-section to the centre of the steel bar group is calculated in accordance with Equation (6.3).

$$c = \frac{\sum_i \left(c_i f_{sd,i}(T) A_{s,i} \right)}{\sum_i \left(f_{sd,i}(T) A_{s,i} \right)} \tag{6.2}$$

where

c_i is axis distance from effective cross-section of steel bar *i*

7. COLUMNS

Chapter 7 is introduced by going into mechanical behaviour of columns both generally and at high temperatures followed by sections describing the varied parameters and calculation procedures. Detailed analysis is performed on every column simulated and the resulting phenomena are discussed. Tests on columns are simulated to verify a calculation program. In the last Section an interaction diagram for a column under fire attack is introduced.

7.1 MECHANICAL BEHAVIOUR

The primary function of columns is to carry axial loads. Two general kinds of columns can be identified, short columns where the load bearing capacity is governed only by the strength of the material and the dimension of the cross section, and slender columns for which the ultimate load is also influenced by slenderness. This report only deals with slender columns which is the more critical of the two kinds; at ordinary as well as elevated temperatures.

7.1.1 Slenderness

The slenderness of a column, or other compressed members, is a parameter that gives information about it's sensitivity to buckling phenomena. It takes into account the critical load at which the structure will become instable, the length, the stiffness and the cross-section dimensions. The equations are obtained from Johannesson /1993/. The buckling length of a compressed member is defined as:

$$l_c = \pi \sqrt{\frac{EI}{N_{cr}}} \tag{7.1}$$

where

EI is the flextural rigidity, which should allow for the effects of cracking, creep and non-linearity of the stress-strain curve.

N_{cr} is the critical load.

Another way to express the buckling length is to give it as a function of the design length of the column. The critical length is then simply expressed as:

$$l_c = \beta \cdot l \tag{7.2}$$

where

β is the buckling length factor.

l is the geometrical length of column.

The buckling length factor β must take into account the degree of lateral and rotational restraint at the ends of the column. Columns in frames, braced against end displacement have values of β

ranging between 0.5 and 1.0. For columns with end displacement permitted, the values may range from 1 to ∞, typical values being between 1 and 2. The values of β must often be assessed by the judgement of the designer. For frame structures, general alignment charts can be used for an approximation.

The slenderness ratio gives information about the columns resistance to withstand deformations because of buckling.

The slenderness ratio is defined as follows:

$$\lambda = \frac{l_c}{i} \tag{7.3}$$

where

i is the radius of inertia.

For the rectangular columns analysed in this chapter a slenderness ratio defined by Equation (7.4) will be used:

$$\lambda = \frac{l_c}{h} \tag{7.4}$$

where

h is the height of the cross-section.

7.1.2 Instability

For columns in practise there is always some bending present. This is evident by the slight initial out of straightness of columns, the manner in which load is applied and the moments introduced by continuous construction (Park, /1975/).

When an initially straight column is subjected to an axial force *N* with eccentricity *e*, a moment *N·e* is introduced which will cause bending. The bending deformation of the column causes the eccentricity of the critical section to become $e+\Delta$, where Δ is the additional eccentricity due to lateral deflection at this section. Hence the maximum bending moment increases to $N\cdot(e+\Delta)$. This is commonly referred to as the secondary effect which is the result of the initial moment.

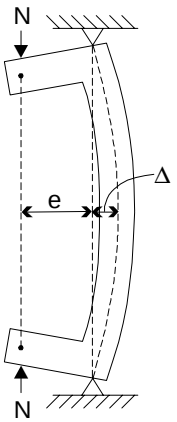

Figure 7.1
Loading and deflection of an eccentrically loaded slender column (Park, /1975/).

Where

N is axial force [N].
e is eccentricity [mm].
Δ is additional eccentricity caused by the bending [mm].

For short columns, reduction of the ultimate load with respect to buckling does not apply, but additional bending moment is still usually created in practice.

7.1.3 Interaction Diagram

Interaction diagrams show the possible combination, of axial loading and the moment. The moment may be a result of the eccentricity for the applied load. Such a diagram is shown in Figure 7.2 for the column in Figure 7.1.

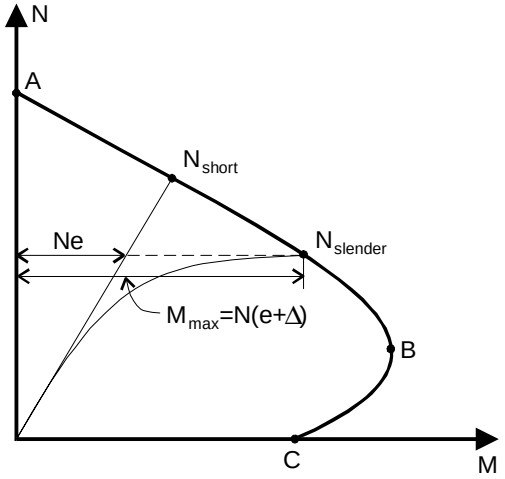

Figure 7.2
Interaction diagram for eccentrically loaded slender reinforced concrete column section indicating the combinations of load and eccentricity that cause failure (Park, /1975/).

where
N is axial force.
e is eccentricity of the column.
Δ is additional eccentricity caused by the bending.
M is moment.

In Figure 7.2, any combination of load and eccentricity on the curve from A to B will cause a compression failure, while a combination on the curve from B to C will cause a tension failure. At point A there is only compression and zero eccentricity, a case which do not appear in practice. At point C pure bending is causing the failure of the column. At point B there is a balanced failure where the compression strength of the concrete and the yield strength of the reinforcement are reached at the same time. Any combination of load and eccentricity that can be plotted within the interaction line is supportable but a point in the graph outside the line is not acceptable with respect to structural safety.

Short columns are independent of the additional eccentricity Δ and therefore a material failure which occurs when the interaction line is reached, will determine the load bearing capacity of the column. Failures for slender columns can be of two kinds. Either a column is stable at lateral deflection Δ_1 but material failure occurs when the interaction line is reached, or it may, prior to the material failure, become unstable and therefore fail. This theory is also applied to HPC.

7.1.4 Behaviour at High Temperatures

Fire exposed columns are often subject to variations in forces and moments during the exposure. These variations can be caused by direct changes in the mechanical behaviour of the column caused by the fire or by interaction between the column and the frame of which it forms part. Forsén /1982/ mentions a few factors which influences the structural behaviour at high temperatures. These are:

- Additional shear forces and moments may occur due to dilation of adjacent horizontal members. This may be the case even for columns which are not directly fire exposed.
- Additional axial forces may occur due to restrained thermal elongation of the column.
- Restraint moments and forces from adjacent members may be transferred at stiff connections.
- Second order moment may prove to be significant due to increased transversal displacement.

In this rapport it has not be possible to take into account the influence of restrained thermal elongation or other factors introduced by the columns being a part of a structural system. In design of a concrete frame system it is necessary to take these factors into account as they can seriously influence on the behaviour of the system in question.

The longitudinal compression reinforcement in a column is often placed near the surface of the column as it increases the moment of inertia of the cross section. However, for columns exposed to fire, the strength reduction will occur faster in comparison to a column with the reinforcement further in the cross-section.

The reinforcement near the fire exposed surface will heat up faster than if it is placed further into the concrete as the concrete cover layer works as a thermal protection for the reinforcement. The yield point of mild steel and hot rolled bars disappears at rather low temperatures, and cold worked bars do not have any yield point at all. Furthermore the modulus of elasticity of the reinforcement decreases as the compression strength is applied (see Figure 3.14) and that’s the case with concrete as well (see Figure 3.3).

The strength in the concrete is reduced with increasing temperature (see Figure 3.2) as is the modulus of elasticity for which the reduction however happens faster. This means that the risk of buckling failure increases in comparison to the risk of compression failure when a concrete column is exposed to fire (Hertz, /1985/).

7.2 PARAMETER CONFIGURATION

Five different columns have been analysed, based on three rectangular cross-sections.

7.2.1 Parameter Study

When analysing the fire resistance of a concrete column many factors have to be considered which can influence the simulation. The varying factors for the simulation can be divided into the following:

- Cross-sectional geometry
- Structural factors
- Loading
- Fire engulfment

Geometrical factors concern the height and width of the cross-section as well as the reinforcement topology etc. This includes also the structural part like the length of the column and boundary conditions. Fire related factors are those concerning the fire exposure (here ISO-834), the engulfment percentage of the cross section etc. Load factors include the applied axial load and initial eccentricity (or moment).

The parameters of importance from the three categories mentioned above are listed in Table 7.1. How these factors were obtained will be explained later in this chapter.

Table 7.1 *Parameters for column calculation*

	Cross-section number				
Geometry number	**1**	**2**	**3**	**4**	**5**
Cross-section (mm)	150x150		300x300		400x400
Reinforcement (mm)	4ϕ16		8ϕ25		16ϕ25
Concrete cover (mm)	34		47.5		47.5
Column Length (mm)	1000	2000	2000	6000	8000
Slenderness	13	27	13	40	40
Initial out of straightness (mm), e_a	1/200	1/282.8	1/282.8	1/489.9	1/565.7
”Ultimate load” * (kN)	1141	330	4690	490	835
Tested degree of loading (%)	100 80 60 40 20	100 80 60 40 20	100 80 60 40	140 120 100 80 60	100 60 40 20
Fire exposure	ISO-834				
Boundary conditions for temperature analysis	4-sides (100%)				

* Calculation according to extrapolated values for OPC concrete (see section 7.2.4 for further explanation).

7.2.2 Cross-sectional Geometry

Three cross-sections where used for the column calculations and these are shown in Figure 7.3.

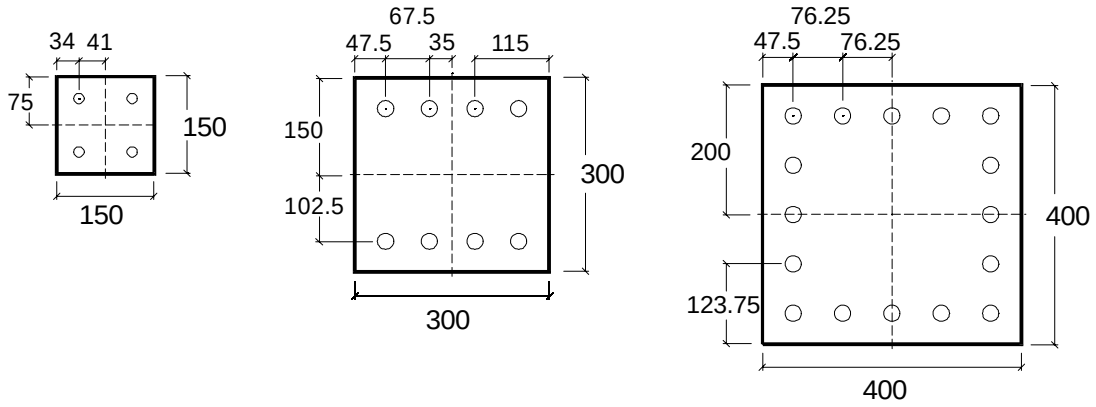

Figure 7.3 Cross-sections used for analyses of columns.

Geometry

The three rectangular cross-sections that where analysed in the column calculations are shown in Figure 7.3. The variations in width are assumed to have a broad number of cross-sections to cover the influence of the geometry.

Circular columns were not included for two main reasons. Firstly, these were not expected to provide any different phenomena compared what can be observed from rectangular columns. This because of the location of the reinforcement where all the bars are placed equally from the surface and differences in reinforcing steel temperatures do therefore not have influence on the strength at a fixed time. The phenomena that could occur because of this should be accounted for by the 150x150 mm rectangle, which has four reinforcing bars, one in each corner and which therefore have the same temperatures. Secondly, the methods for calculating load bearing capacity for circular columns are more complicated than for rectangular columns and as circular columns are not as common, computer programs have not been developed for calculation of circular columns.

Reinforcement

In contradiction to the moment calculations of the cross-section for beams, slabs, etc. total reinforcement areas for the columns were simply decided after consulting experts within the field of concrete engineering. The reinforcement steel topology may be seen in Figure 7.3.

The reinforcement topology is calculated according to Swedish regulations (BBK 94, /1994/) which require that the concrete cover is no less than $1.5 \cdot \phi + 10$ mm and the distance between reinforcement bars at least $2.5 \cdot \phi$ mm.

Calculating reinforcement topology according to ENV 1991-1-2 /1995/ would have resulted in increasing complexity of the calculations, as the minimum concrete cover depends on the fire resistance time for which the structure is designed (ENV 1991-1-2, /1995/). To include the total time period of fire exposure (0 - 120 minutes) in the same computer calculation, several concrete covers would have to be used in stead of one according to BBK 94 /1994/ for this time period. This would result in an increasing number of calculations.

7.2.3 Structural Factors

Slenderness

Slenderness ratios (see Equation 7.4) were chosen early in the project to be 13, 27 and 40. The ratios 4 and 67 were also possible candidates but were judged to be to extreme and thus were excluded after some discussion. For a visualisation, a column of 400x400 mm with a slenderness ratio 4 and β=2 (one fixed end), would give the actual length *l* as 0.8 m. This length can not be considered as practical and is also hard to simulate in the computer programs available.

Boundary conditions

The boundary conditions are of importance when the slenderness ratio has to be calculated, as it determines the critical length formulated in Equation. 7.2, i.e. the β factor. Figure 7.4 shows different boundary conditions and the resulting deflection when an axial force N is applied.

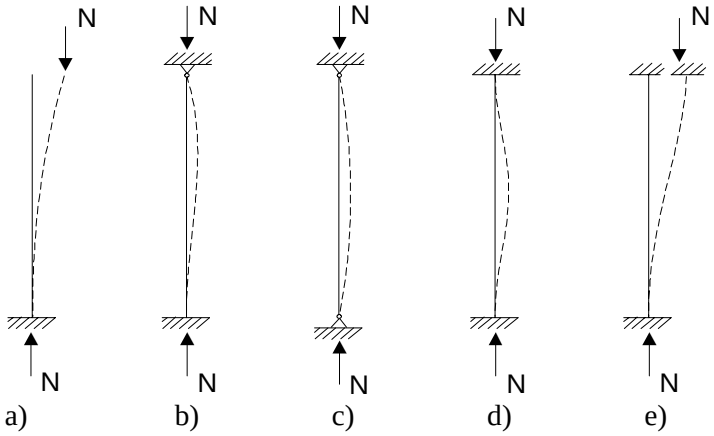

Figure 7.4
Different boundary conditions for columns. Whole line shows the initial conditions and the dashed line the deflection after applying the axial force N.

It is possible to simulate three of these boundary conditions in CONFIRE (see Appendix D) and these are shown in Figure 7.4 part a), b) and c).

Note that it is possible to simulated part c) as in part a) by only using half the length. It is therefore enough to simulate the conditions in Figure 7.4 a) only, where the effective length factor (β) is determined as 2.

Simulation length

For determining what actual length, l, to use in the simulation the following procedure was adopted: As mentioned above slenderness ratios (l_c/h) were chosen as 13, 27 and 40. With the given cross section and the critical length l_c calculated according to Equation 7.3 and with the given effective length factor, β=2, the actual length was calculated according to Equation 7.2.

Initial out of straightness

The only modelled eccentricity incorporated in the simulations was the normative initial out of straightness. It was set according to ENV 1992-1-1 /1993/ as a function of the actual length and is shown in Equation 7.5.

$$e_a = l_c/(200 \cdot l \text{ ^0.5}) \quad \text{when } \beta = 2 \tag{7.5}$$

where

e_a is modelled eccentricity [m].
L_c is critical length [m].
l is the actual length [m].
β is effective length factor [m].

The initial out of straightness is set to account for imperfections in the manufacturing of the column and decreases with increased length. It is modelled by using half of a sine curve with half the amplitude determined by Equation 7.5.

No intentional eccentricity was set for the axial force which was assumed to be applied in the middle of the cross section.

7.2.4 Loading

The degree of loading was taken as a percentage of the design load at room temperature. This proved to be a problem as no applicable design rules for HPC were ready at the time these calculations were carried out. To obtain values that could serve as start values for the computer simulations, equations for calculation of OPC loading were used (BBK 94, /1994/) and the necessary values were extrapolated to serve for HPC. These were set as the ”ultimate load” (100 % load) and reduced or increased to obtain a variety in the loading.

7.2.5 Fire Engulfment

The columns were exposed to a temperature time curve according to ISO-834 /1975/. All of the columns were exposed on 100 % of their perimeter i.e. 4-side exposure.

7.3 COMPUTER CALCULATION

In Sections 7.1 and 7.2 the background of the computer calculations of columns was explained as well as the assumptions for the calculations. In this section the calculation procedures are explained and programs used in the calculation are introduced.

Totally 86 simulations have been carried out for columns for defining and verifying the design rules. Furthermore several calculations have been done in order to verify and compare the program CONFIRE with tests performed in Japan and Germany.

7.3.1 Calculation Procedures

For a column the calculation procedure is much more complicated than for beams and slabs. This is due to 2nd order effects that have to be taken into account in the calculation. Parameters like length, slenderness and load eccentricity, not only have to be considered in order to determine the load bearing capacity, but also result in increasing complexity of the programs needed for the calculation. Important steps for visually determining the fire resistance of a column can be seen in Figure 7.5.

It is important to emphasise that the main effort is to compare the True relative strength curve to the single isotherm curves (the 400 and 500 ºC curves respectively). These three curves are therefore plotted in the same diagrams to gain an understanding of their differences and similarities with respect to each plotted factor.

As with beams and slabs is was desired to use the already accepted OPC design rules for HPC with some modifications.

7.3.2 Computer Model

The basic computer programs used in the simulations are; SUPER-TEMPCALC, and CONFIRE. In order to make these compatible and convert output data from one program to input data to another, use has been made of a couple of conversion programs, namely CFCONV and CONREAD. MATLAB and Microsoft EXCEL have been used for visualisation of the final output from CONFIRE.

A short description of the programs follows. A more detailed description can be found in Appendix D.

CONFIRE

CONFIRE is a finite element program for the analysis of fire exposed plane frames consisting of reinforced concrete sections divided into rectangular elements. The program requires several kinds of input data; cross-sectional measures, mechanical data for concrete and reinforcement, load and eccentricities, structural data including topology, boundary conditions including information on supports as well as information about the incremental iteration process and time increments. Some of the important factors are shown in Figure 7.6.

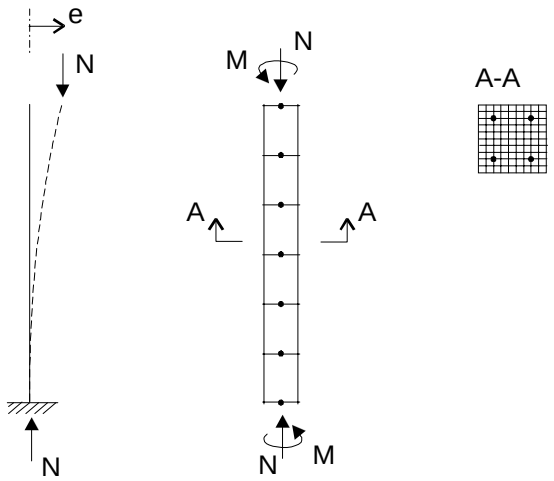

Figure 7.6
Simplified structure model and cross-section used in CONFIRE.

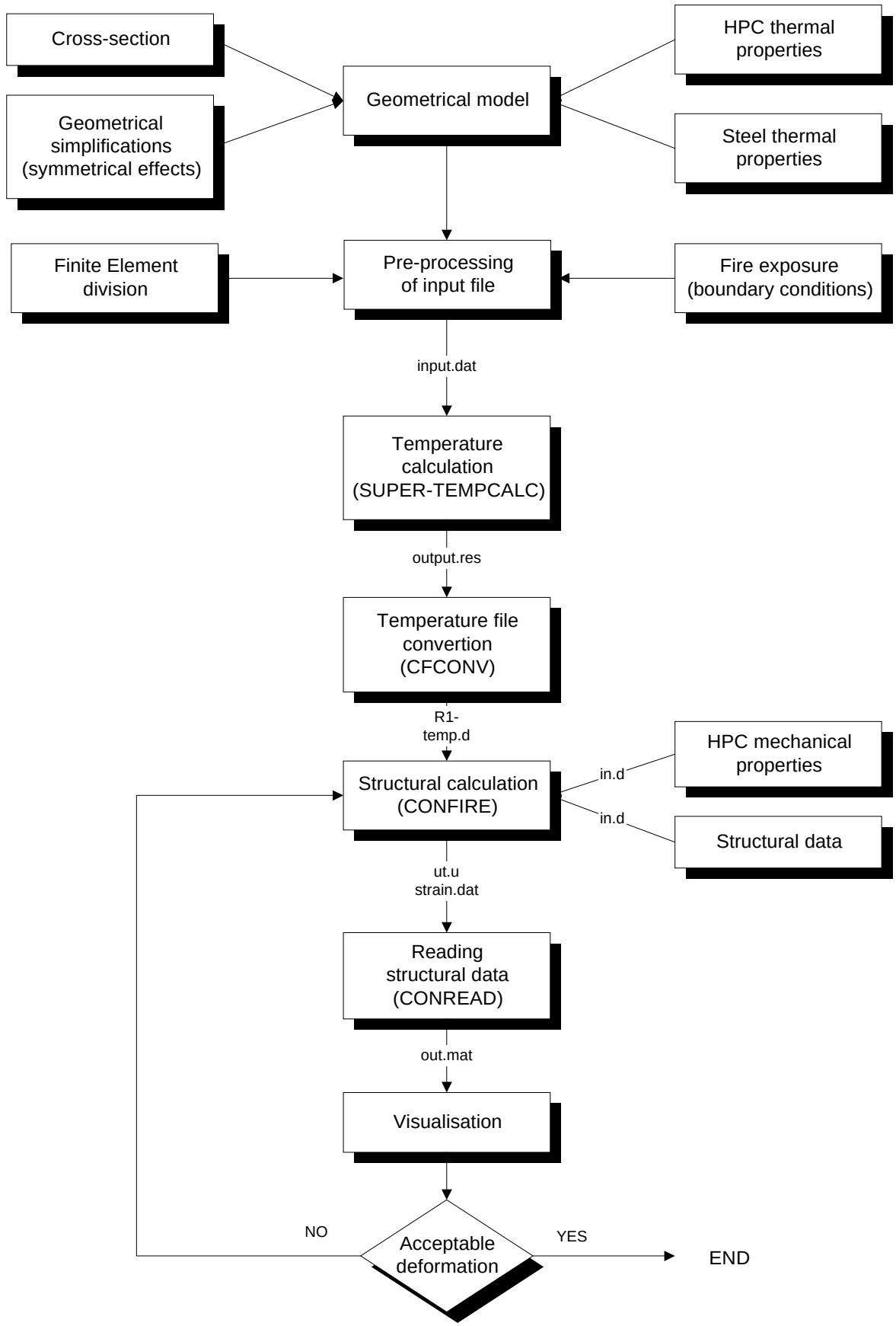

Figure 7.5 *Detailed calculation procedure for fire resistance of a concrete column*

The node temperatures in the cross-section are supplied by SUPER-TEMPCALC (see Section 5.1.3) for each time step and are applied over the total height of the column. The mechanical properties for concrete and steel are updated for each change of temperature. The output from the program consists of time to failure for the current load, deformations, strains and stresses. The program was developed by Nils Erik Forsén in Norway. For further reference see Forsén /1982/.

Conversion Programs

As mentioned before, two of conversion programs were used in the column analysis. These are CFCONV and CONREAD. CFCONV converts the SUPER-TEMPCALC temperature output file into an input file to CONFIRE. The temperature reported from the SUPER-TEMPCALC calculation represents every node of the element mesh. This format does however not comply with the request of input data to CONFIRE, and thus a conversion is necessary. CFCONV calculates average temperatures from the node points and arranges them in a way that agrees with the input format to CONFIRE. CONREAD is a utility which reads and converts the CONFIRE output file into MATLAB format from which graphical analysis easily can be done.

7.4 RESULTS

In this Section the result of every column calculation will be put forward and discussed. For each calculation, a number of diagrams have been drawn to ease the interpretation of the simulation results and to give a better understanding of how the design rules were developed. This includes both temperatures in the sections as well as the time to failure for the actual column.

7.4.1 Temperatures in the Cross-sections

For columns it is very important to analyse the temperatures in the cross-section and specially in the reinforcing steel as discussed in Section 7.1.4. In the following section follows a discussion of the actual temperatures and the consequences they have depending on the different cross-sections.

Cross-section of 150x150 mm

For such a small cross-section as 150x150 mm the corner effect of the temperature field will play a dominant role in the behaviour of the column as the corner reinforcement will gain higher temperatures than in a larger section where the one dimensional heat flow (not affected by the corners) are responsible for a large part of the total temperature field. Analysed nodes in the cross-section are shown in Figure 7.7. The reinforcement diameter is ϕ16 and the steel quality is as described in Section 7.2.

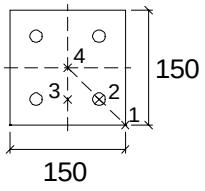

Figure 7.7
Temperature reading locations for Figure 7.6. Points 1, 2 and 4 are on the diagonal line from the corner to the centre of the cross-section and point 3 is on the centre line of the cross-section in the same height as the reinforcement.

In Figure 7.7 thermocouple number 1 is located on the corner of the cross-section to describe the boundary temperature (ISO-834). This node has been included in order to be able to se how the other node temperatures behave in relation to the boundary time-temperature curve. Point 2 is at the centre of the reinforcement but notice that the temperature calculations are conducted in the absence of the reinforcement for reasons discussed in Chapter 5. The temperatures of the nodes in Figure 7.7 are shown in Figure 7.8.

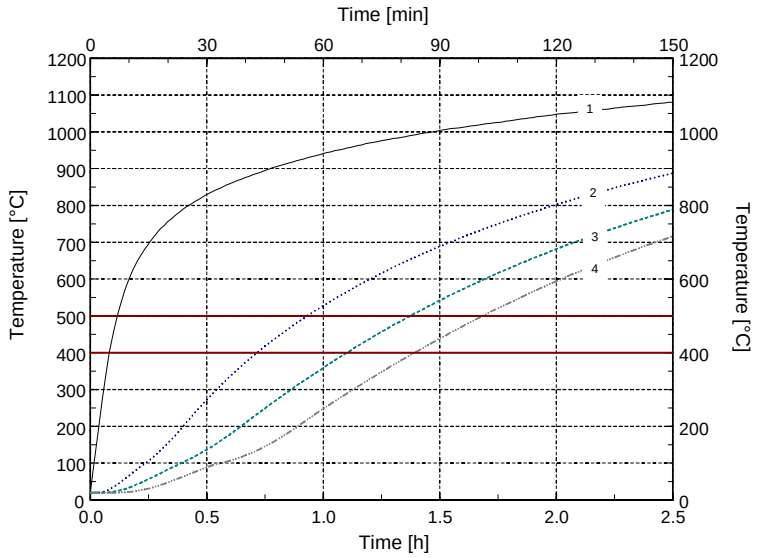

Figure 7.8
*Temperature in the 150*150 mm cross-section as a function of time. Location of the points 1 to 4 is according to Figure 7.7.*

The temperature rises dramatically from the start as a result of the small cross-section. Notice the relatively small difference of the temperature at points 2 and 1. The difference at points 2 and 3 are due to the two-dimensional effect of the corner when the temperature flow is from both sides. This effect is vital for the load bearing capacity of the column and the time to failure, especially in a small cross-section.

Cross-section of 300x300 mm

The 300x300 mm cross-section has four reinforcement bars at each side with diameter ϕ25 mm as shown in Figure 7.9. This will mean that the total reinforcement area will heat up slower than for the same cross-sections with only corner reinforcement and hence the reinforcement will have a greater influence on the total strength of the column and the time of failure (see Chapter 5).

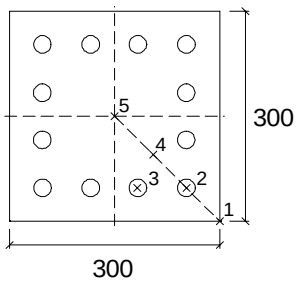

Figure 7.9
Temperature reading locations for Figure 7.13. Points 1, 2, 4 and 5 are on the diagonal line from the corner to the centre of the cross-section and point 3 is at the centre of the side reinforcement.

There are five points in the 300x300 mm cross-section for which the temperature has been shown in Figure 7.10. Point number 1 is used as usual to show the boundary temperature to compare to the node temperatures further in the section.

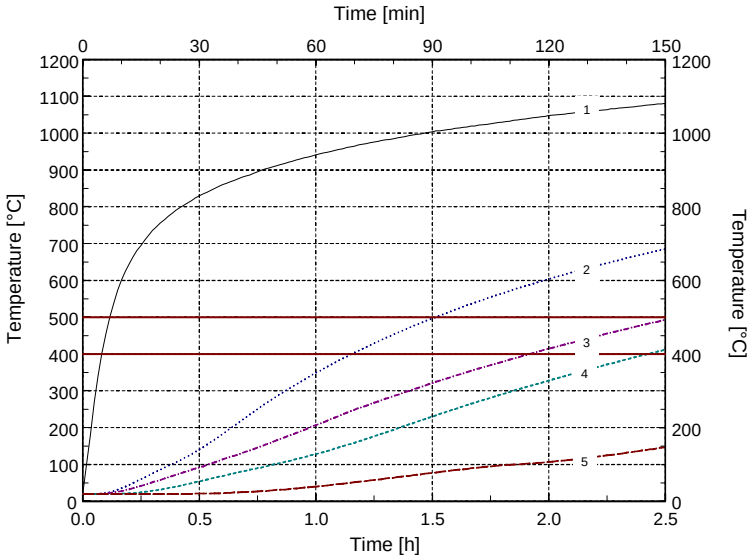

Figure 7.10
Temperature in the 300x300 mm cross-section as function of time. Locations of the points 1 to 5 are according to Figure 7.9.

Observe the increasing difference between the boundary temperature and the temperature further in the section when compared to the 150x150 mm cross-section where the whole section has reached temperatures of over 600 ºC after 2 hours. For the 300x300 mm cross-section the core temperature in the centre has only reached 105 ºC after 2 h.

Cross-section of 400x400 mm

The 400x400 mm cross-section has five reinforcement bars at all sides as shown in Figure 7.11. The great amount of reinforcement in this cross-section means that the corner reinforcement will have very little influence of the total fire resistance as it will heat up quickly compared to the other reinforcement bars (Hansson, /1993/). The temperature flow will be more like in a one dimensional case where the 400 mm sides behave somewhat like slabs.

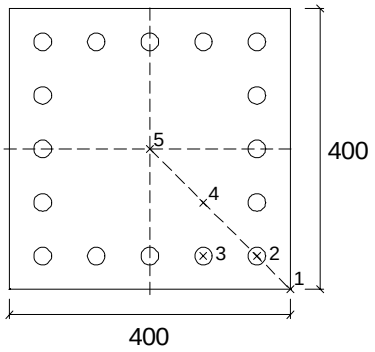

Figure 7.11
Temperature reading location a 400x400 mm cross-section. Points 1, 2, 4 and 5 are on the diagonal line from the corner to the centre of the cross-section whereas point 3 is at the centre of the side reinforcement.

The temperature of points 1 to 5 in Figure 7.11 are shown in Figure 7.12.

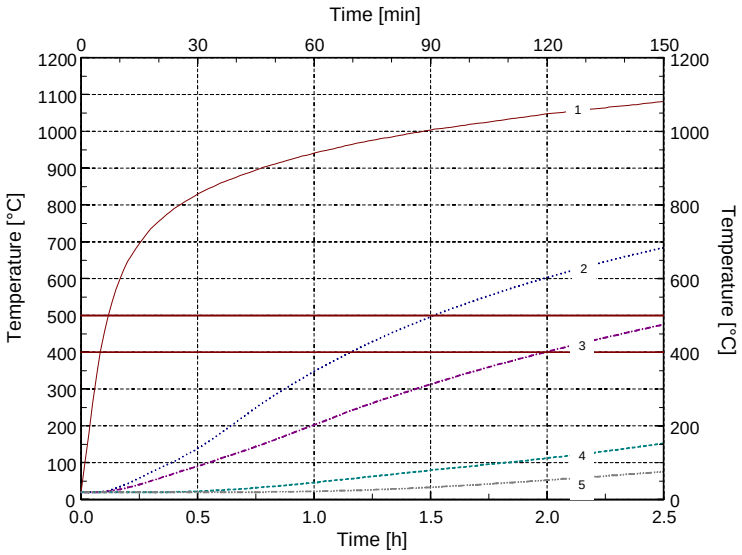

Figure 7.12
Temperature in the 400x400 mm cross-section as function of time. Placement of the points 1 to 5 are according to Figure 7.11.

The temperature at locations 4 and 5 are only reaching about 50 and 110 °C respectively after 2 hours while the reinforcement is up to approximately 400 and 600 °C. The slow heat up of the inner concrete will result in increasing influence of the reinforcement in the total strength of the column as is reduces quicker than the compression strength of the main core of the concrete. It is also interesting to notice that for a large cross-section there is a greater zone that have temperatures in the interval 100 to 300 °C which is critical in the case of HPC when it comes to simplifying the True relative strength curve with the single isotherm curves. This has been discussed in Section 6.4 (see Figure 6.10 and 6.14).

7.4.2 Time to failure

In any normal case the computer simulation is interrupted when the column has failed to bear the applied loads, due to escalating eccentricity and diminishing strength and stiffness that originates from elevated temperatures. By trying to establish general effects based on specification of the failure time results, it is possible to find a pattern of how the difference in load parameters and the combined influence from other parameters go together. Other factors that may influence interruption in the computer analysis is the instability of the program due to input data parameters like the relative strength versus temperature.

The curves for relative strength versus temperature, the 400 and 500 curves, can be a reason for this interruption as it has a steep descend, e.g. from 100 % strength relative ambient strength at 399 ºC to 0 % at 400 ºC. It can be difficult computationally to simulate this as the strength of an element suddenly is reduced so abruptly. This has been experienced in the simulations and it has helped in several cases to smooth the descent by allowing the completion of the reduction process a broader temperature interval. This has fortunately little influence on the time to failure, but can in certain cases prove to be a little bit on the safe side by giving time to failure 1 or 2 minutes earlier than using a straight line on a 1 degree interval.

7.4.3 Slenderness Ratio 13

Cross-section of 150x150 mm

The 150x150 mm cross-section of the length 1 meter and with a fixed end boundary gives a slenderness ratio of 13. The configuration of this column is shown in Figure 7.13.

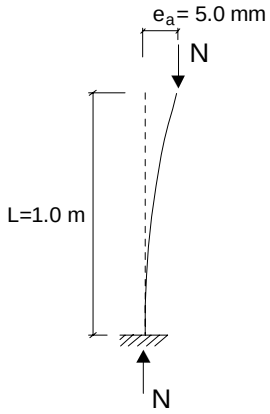

Figure 7.13
Geometrical properties of a column with 300x300 mm cross section, showing the length, initial out of straightness as well as the fixed end boundary condition.

The initial out of straightness is a function of the length and according to Equation 7.5 it becomes approximately 5.0 mm for 1 meter as shown in Figure 7.13. The time to failure was calculated for four different load combinations. These are, as shown in Figure 7.14: 1141.0, 912.8, 684.6 and 456.4 kN.

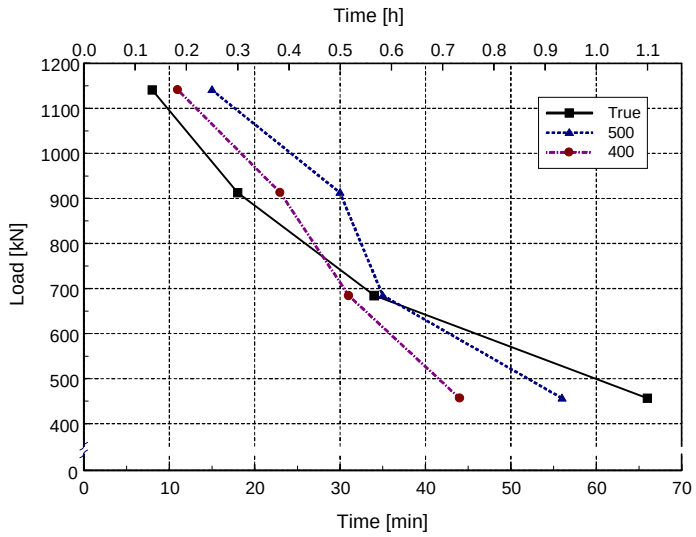

Figure 7.14
Time to failure for a column of length 1 m and with a cross-section 150x150 mm.
Intersection between True and 400-curve occurs at 28 minutes while True has an intersection with 500-curve at 38 minutes.

The similarity between the 400 and 500 curves is not surprising as they both have the same form, 100% relative compression strength to a certain temperature and zero after that. As expected there is only a certain time delay between these curves, the 400 curve being more conservative than the other. The True curve has on the other hand a different slope or curvature, less steep than the single isotherm curves. The single isotherm curves are non conservative for greater loading, when the temperatures in the cross-section are low. For low temperatures, the difference between the True and single isotherm curves, in terms of relative strength, is greatest. By low temperature is meant the interval 100 to 350 °C. This is evident by looking at Figure 6.10. When the

temperatures in the cross-section increases and a larger part of the cross-section gains temperatures above 400 or 500 °C the single isotherm curves become more conservative.

Due to the phenomena mentioned above there is an intersection between the True and the two other curves. That intersection happens at about 28 minutes for the 400 curve and at about 37 minutes for the 500 curve. The exact time can not be estimated from Figure 7.14 due to limited number of calculations and other uncertainties but it should be safe to say that the time of interaction for the 400 curve is less than 30 minutes. This be important to notice as concrete columns always have a load bearing function in a structure and are, as such, never designed for less than 30 minutes of fire resistance. Furthermore and 60 minutes is in fact the usual minimum requirement for a load bearing structure.

Cross section of 300x300 mm

A cross-section of 300x300 mm, and a length 2 meters is calculated to have a slenderness ratio of 13. The configuration of this column is seen in Figure 7.15.

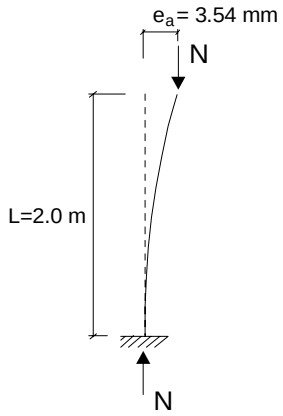

Figure 7.15
Geometrical properties of column showing the length, initial out of straightness as well as the fixed end boundary condition.

The time to failure for the column in Figure 7.15 is given in Figure 7.16.

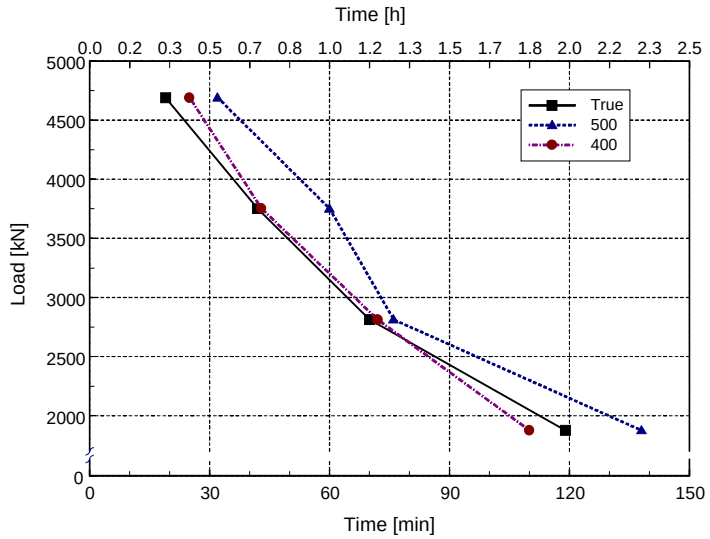

Figure 7.16
Time to failure for a column of the length 2 m and with a cross-section 300x300 mm. Intersection between True and 400 curve is at time 78 minutes while True has no intersection with 500 curve.

For the same reasons as observed for the columns with 150x150 mm cross section the 400 and 500 relative strength curves have similar form but with a offset in time. The observed time delay between the 400 and 500 curves is on the other hand not as trivial as for the smaller cross-section.

As the temperature in the 400x400 mm cross-section is lower than that for smaller cross-sections the influence from cutting off concrete higher than certain temperature will not have the same drastic effects and might be more dependent on the reinforcement temperatures. Hence the difference between the single isotherm strength curves and the True curve will not be as great as before. Still the difference increases with increasing temperature and the intersection between 400 and True curve happens at 78 minutes. It is important to notice how close the two curves are, giving similar time to failure at most load combinations but the tendency is, as before, that the 400 curve becomes more conservative than the 500 curve with increasing time. The 500 curve is always on the unsafe side.

7.4.4 Slenderness Ratio 27

The 150x150 mm cross-section, the length 2 m and a fixed end boundary gives a slenderness ratio of 27. The initial out of straightness is a function of the length and according to Equation 7.5 becomes for this length 3.54 mm as shown in Figure 7.17 where the geometry of the 2 m column is shown.

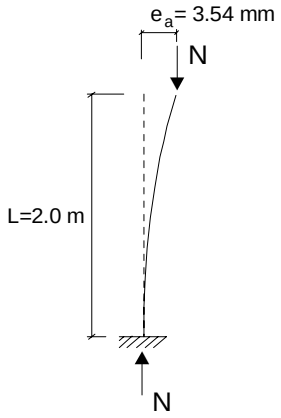

Figure 7.17
Geometrical properties of column showing the length, initial out of straightness and a fixed end boundary condition.

The time to failure was calculated for four different load combinations. These are, as shown in Figure 7.18, in kN: 330, 264, 198 and 132 kN.

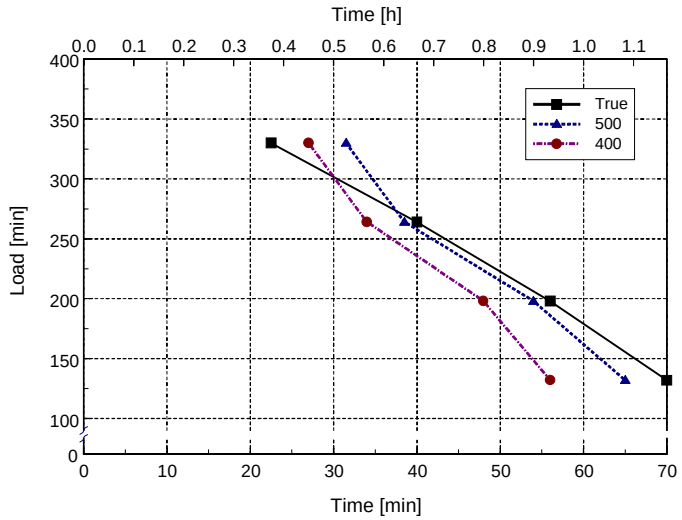

Figure 7.18
Time to failure for a column of length 2 m and with a cross-section 150x150 mm. Intersection between true and 400 curve occurs at 30 minutes while true has an intersection with 500 curve at 38 minutes. As observed for the 1 m column there is similar curvature for the 400 and 500 curves.

The 400 and 500 curves are more conservative for this 2 m long column than for the column of the length 1 m. When the temperature increases, the single isotherm curves increases the slenderness of the column at a faster rate than the True curve as the strength increases again up to 400 °C after a local minimum at about 200 ºC. This influence on the slenderness for an already slender column is a crucial factor for the total fire resistance time.

It must be emphasised that the minimum slenderness ratio for which column fire resistance time has been calculated is 13. For columns with even lower slenderness numbers a special calculation based on the True curve is necessary and the results obtained here should not be directly applied.

7.4.5 Slenderness Ratio 40

Cross-section of 300x300 mm

The 150x150 mm cross-section, the length 2 m and a fixed end boundary gives a slenderness ratio of 27. The initial out of straightness is a function of the length and according to Equation 7.5 becomes for this length 3.54 mm as shown in Figure 7.17 where the geometry of the 2 m column is shown.

The configuration of the 300x300 mm column of length 6 m is shown in Figure 7.19.

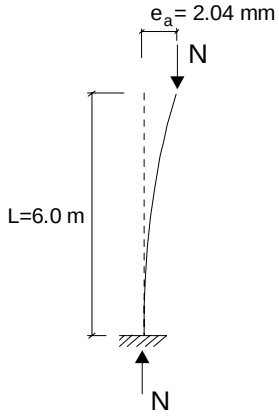

Figure 7.19
Geometrical properties of a 300x300 mm column showing the length, initial out of straightness as well as the fixed end boundary condition. The slenderness ratio is 40.

The time to failure for the column in Figure 7.19 is shown in Figure 7.20.

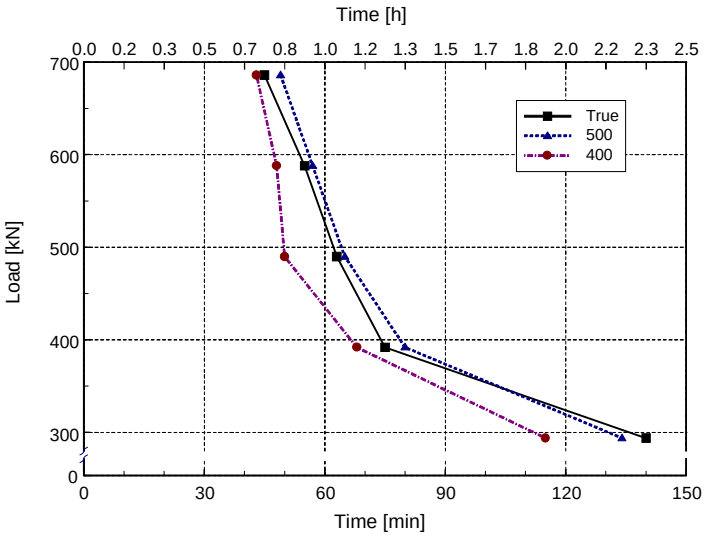

Figure 7.20
Time to failure for a column of the length 6 m and with a cross-section 300x300 mm.
The 400 curve gives for any load shorter time to failure, True has an intersection with 500 curve at time 104 min.

An indication from Figure 7.20 is that for slender columns, the single isotherm curves become more conservative than for less slender columns. Comparison to Figure 7.16 for a 2 meter long, 300x300 mm column, shows that. The reason is the increasing importance of the single isotherm strength curve for slender columns in comparison to the short columns (see Section 7.1.4). The 400-curve proves to be conservative at all times whereas the 500 curve only interacts with the True curve at approximately 110 minutes.

Cross-section of 400x400 mm

The configuration of the 8 m column is seen in Figure 7.21.

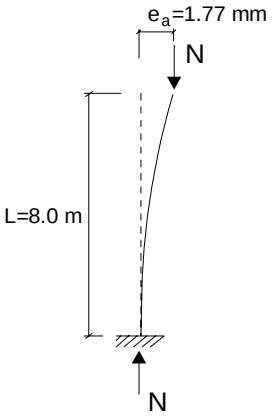

Figure 7.21
Geometrical properties of 400x400 mm column showing the length, initial out of straightness as well as the fixed end boundary condition. The slenderness ratio is 40.

The time to failure for the column of 400x400 cross-section and length 8 m is given in Figure 7.22.

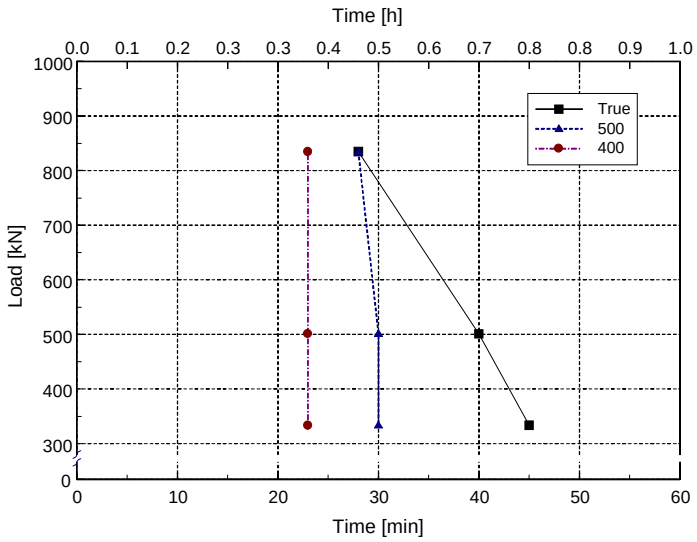

Figure 7.22
Time to failure for a column of the length 2 m and with a cross-section 400x400 mm.
The strange form of the curves is to a certain extent dependent on the great cross-section and has to be viewed in a critical manner.

For great cross-sections CONFIRE (see Section 7.3.2) seems to have problems with the convergence, especially when there is large amount of reinforcement involved. Figure 7.24 reveals this problem where the number of converged tests were few. It was only for the True curve that an acceptable displacement was obtained in all cases. The starting point of the other curves can however give a hint of were they stand with regard to the time of failure in comparison to the True curve and it looks like the 400 curve is on safe side once again. This comparison must be taken with great precaution as the convergence of these tests were bad and similar time to failure was obtained in each of the calculations of the 400 and 500 curves.

7.5 DESIGN METHOD

In Section 7.3 the calculations that will form the basis for the design rules were introduced. The time to failure at different load levels were noted for each of the six columns in question. In this Section the results obtained will be used to construct design rules for practical purposes.

7.5.1 General Results from Calculation

The results found in Section 7.4 were that the 400 curve would give a conservative fire resistance time in most cases and these predicted times of failure were shorter than when the True curve was used.

In one case the 400 curve was not conservative with respect to the fire resistance time. This is for the 2 m long column with cross section 300x300 mm, slenderness 13. The calculated fire resistance times can be seen in Figure 7.14. The difference in time between using the 400 and True curves are however very small (1 or 2 minutes) and is therefore considered acceptable.

For very large axial loading where the times to failure for the column were lower than 30 minutes, concrete with cross sections reduced in accordance with the 400 curve were a bit on the unsafe side in some cases. Shorter fire resistance times than 30 minutes are however of limited importance in practice.

In all cases the 400 isotherm curve becomes more conservative (in comparison of the True curve) when the temperatures in the cross-section increases. Especially for the more slender columns.

The above indicates that for very slender columns and long fire resistance time, reduction according to the 400 curve might become very conservative. It has not be possible to analyse this within the scope of this report.

7.5.2 Thermal Calculation

For calculation of the thermal field of a HPC cross-section the reader is referred to Section 6.5.3.

OPC thermal properties can be used for HPC if the penetration is increased by 20 %, and the temperatures in the reinforcement is also increased by 20 % (see Section 5.2.3).

7.5.3 Design Method

The structural strength of a column shall be calculated based on reduced cross-section and reduced steel reinforcement strength. The penetration shall be according to the 400 °C isotherm. This penetration has to be done for the time for which the structure is to be designed; 30, 60, 90, 120 or 240 minutes in most cases.

The reduction can also be accomplished by applying the 500 ºC isotherm with an increased penetration of 35 %. In that case the penetration will therefore be as according to Equation 7.6.

$$a = 1.35 * a_{500} \quad (7.6)$$

where

a	is the actual reduction of the cross-section
a_{500}	is the reduction of the cross-section according to the 500 isotherm.

The reinforcement strength has to be reduced according to Figure 3.11 with a method presented in Section 6.5.4.

7.6 SIMULATION OF FULL SCALE TESTS

In this project some modifications have been made of a pre-existing structural calculation program CONFIRE (Forsén, /1982/) to account for the properties and behaviour of HPC. These modifications need to be verified and in this sense, simulation of tests are the best way.

For the time being, tests on fire exposed HPC columns are very rare. Moreover the bulk of all tests that have been carried out on HPC today aim at investigating the spalling phenomena. As spalling reactions of columns ruin the specimens for general mechanical testing, the spalling phenomena has to be accounted for before other tests can be undertaken. The spalling can be counteracted by adding capillary forming chemicals in the concrete mix and often precipitated siliceous acid. This way the spalling may be significantly reduced.

In order to verify the ability of the CONFIRE software to accurately predict the structural behaviour of columns subjected to fire, two tests conducted in Japan and Germany respectively were simulated. The tests involve full size columns of 3.5 and 5.59 metres and concrete cube compression strengths of 118.9 and 109.1 MPa respectively. The documentation of these tests

were not totally satisfactory, e.g. no measurements of horizontal displacements were undertaken, and thus the time to failure was the factor that had to be relied on for comparison.

All the tests were carried out transiently, i.e. the load was kept constant and the temperature increased (according to the ISO-834 /1975/ standard fire exposure curve) until failure.

7.6.1 Test in Japan

This test was carried out at the Technology Research Center (TRC), Yokohama, Japan

Test configuration and choice of column

At TRC, several full scale tests have been carried out on HPC as shown in table 7.2.

Table 7.2 *General information about the columns tested in Japan (Michikoshi, /1995/)*

Number	Name	Cross section [mm]	Length [mm]	Compression strength (cube) [MPa]	Load factor (N/F_cbD) [kN]	Time to failure [min]
1	RC30-12	300 x 300	3.5	118.9	0.12	264
2	RC30-27	300 x 300	3.5	118.9	0.27	176
3	RCC30-27	300 x 300	3.5	118.9	0.27	214
4	RC45-12	450 x 450	3.5	118.9	0.12	360
5	RC75	750 x 750	2.5	98.5	-	-
6	RC75*	750 x 750	2.5	98.5	-	-
7	RCC75	750 x 750	2.5	118.9	-	-
8	RC100	1000 x 1000	2.5	118.9	-	-

As seen in Table 7.2 only the first four columns gave some results with respect to structural collapse. The other four columns (cross-section 750x750 mm and 1000x1000 mm) did not collapse under the testing time of 360 minutes. Only collapsed columns were considered interesting as the time to collapse could be compared between the test and the simulation.

The loading of the columns were set as a percentage of the maximum concrete compression strength of the cross-section (F_cbD, see Figure 7.26), e.g. 1080 kN for the RC30-12 column and 2430 kN for the RC30-27 column. The column named RCC30-27 has the same configuration as the RC30-27 column but has a extra mortar cover of 20 mm on the whole circumference.

It must be pointed out that these simulations were conducted to verify a computer program and therefore it is important to look at the mechanical differences that can take place in the different tests. For RC30-12 and RC30-27 the only difference is the axial load, hence the same phenomenon will take place in the two columns but with a slight time delay in the column with lower axial load. RC30-27 and RCC30-27 do have the same configuration except that the RCC30-27 is insulated with mortar finish and therefore will be subjected to a slower concrete temperature field development than if not insulated and the mechanical changes will accordingly take place at a slower rate.

Due to a long fire resistance time of column RC45-12 (360 min) the simulation of it proved difficult to complete as the time steps had to be extended due to a limitation of number of time steps in CONFIRE. This on the other hand created some convergence problems as the temperature increase between time-steps in some nodes became too large.

Based on the above only one column from Table 7.2 was simulated and that was column RC30-27.

The geometry of the column is described in Figure 7.26 (all lengths in mm) *(Michikoshi, /1995/).*

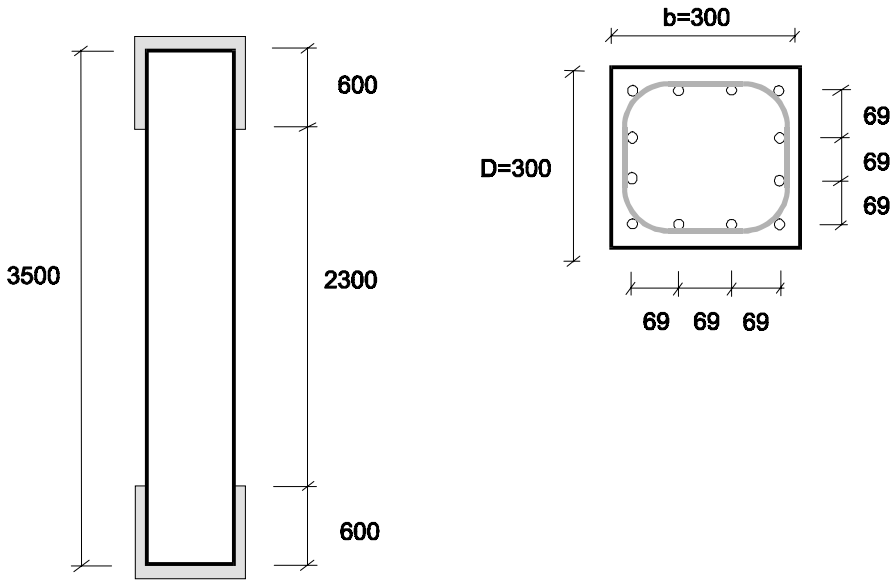

Figure 7.23 *Geometrical data for column RC30-27 (Michikoshi, /1995/).*

The concrete cover is 40 mm.

The configuration of the column is given in Table 7.3.

Table 7.3 *Detailed description of column RC30-27 (Michikoshi, /1995/).*

RC30-27:	Value	Unit
Structure		
Cross-section	300 x 300	[mm]
Eccentricity	0	[mm]
Load factor	12	% of total cross-section compression strength
Axial load	2430	[kN]
Concrete		
Compression strength (cube)	118.9	[MPa]
Modulus of elasticity	40.7	[GPa]
w/c ratio	22	[%]
Reinforcement		
Diameter	13	[mm]
Ultimate tension strength	624	[MPa]
Modulus of elasticity	185	[GPa]

The time to failure in the test was measured 176 minutes.

Test simulation

The best way to compare a computer simulation and a full-scale test of columns is by comparing the horizontal displacement, which is much more reliable than comparing vertical displacement. Vertical displacement is proportionally much more dependent on the mechanical expansion of the aggregate and the displacement in the vertical direction is smaller than in the horizontal direction (Anderberg, /1976/).

The information available for the columns in question are limited and the comparison between the tests and the computer simulation is done by comparing the time to failure, 176 minutes.

The RC30-27 column had to be simulated with some simplifications. Simplifications regarding the exposed surface of the column were made since CONFIRE only allows one type of cross-section to represent the column's section. This was taken to be the fire exposed surface and thus the insulated ends (see Figure 7.23) were not taken into consideration. The column was therefore shortened by the length of the insulated ends.

Boundary conditions are always difficult to simulate. Often these are not known and sometimes a combination of fixed end and free rotation boundary is relevant. By judging from the pictures and the way the column failed, the boundary conditions were set as free to rotate at top and bottom.

The upper half of the column is simulated by setting the lower end fixed and the other end free (see Figure 7.3 c)). This can be considered as representative for the column in question as the displacement in the middle of the real column will be the same as at the top of the simulated one (half the length) if the lower boundary is kept fixed.

The temperature distribution in the cross-section of the RC30 column (300x300 mm) was calculated with SUPER-TEMPCALC (Anderberg, /1991/) for a duration of 240 min.

The horizontal displacement of the simulated column (see Figure 7.24) will be the same as the mid-displacement of the real column. This deflection gives information about the structural stability and behaviour of the column. When the deflection ratio approaches infinity the structure fails.

The horizontal deflection is shown as a function of time in Figure 7.24.

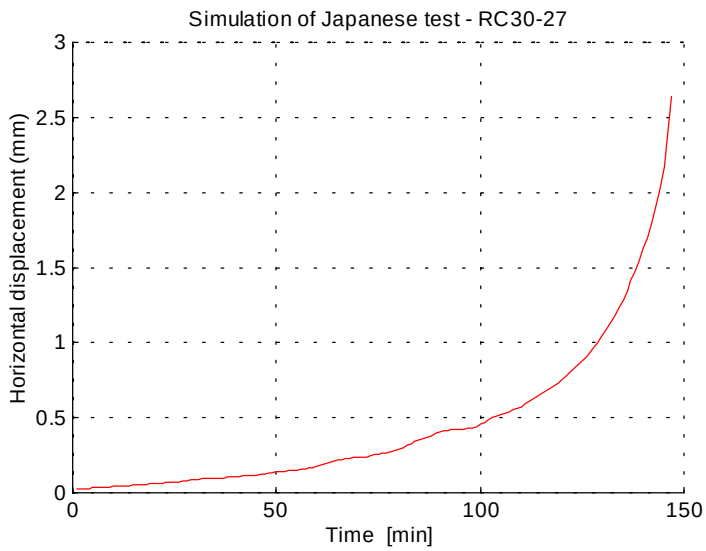

Figure 7.24
Calculated horizontal displacement of the RC30-27 column.

In Figure 7.24 the time to failure can be determined to be 147 minutes. This is to be compared to the 157 minutes that were obtained in the Japanese test.

From the above it can be concluded that CONFIRE provides an acceptable prediction of the behaviour of the column within the test. It is however important to realise that there are many uncertainties in this simulation as mentioned earlier.

7.6.2 Test in Germany

This test was carried out at The Institut für Baustoffe, Massivbau und Brandschutz, TU Braunschweig, Germany.

Test configuration and choice of column

Several small scale tests of columns with the length of 1 m were carried out to obtain information about any necessary precautions for prevention of spalling in a fire. Two full scale tests were carried out after these tests, one with fibre addition and one with anti spalling mesh. The one with anti spalling mesh failed due to severe spalling and will therefore not be suitable for simulation. The other column reached a fire resistance time of 181 minutes and that test will be simulated in this Section *(Diederichs, /1995/).*

The Geometry of the column is shown in Figure 7.25 *(Diederichs, /1995/).*

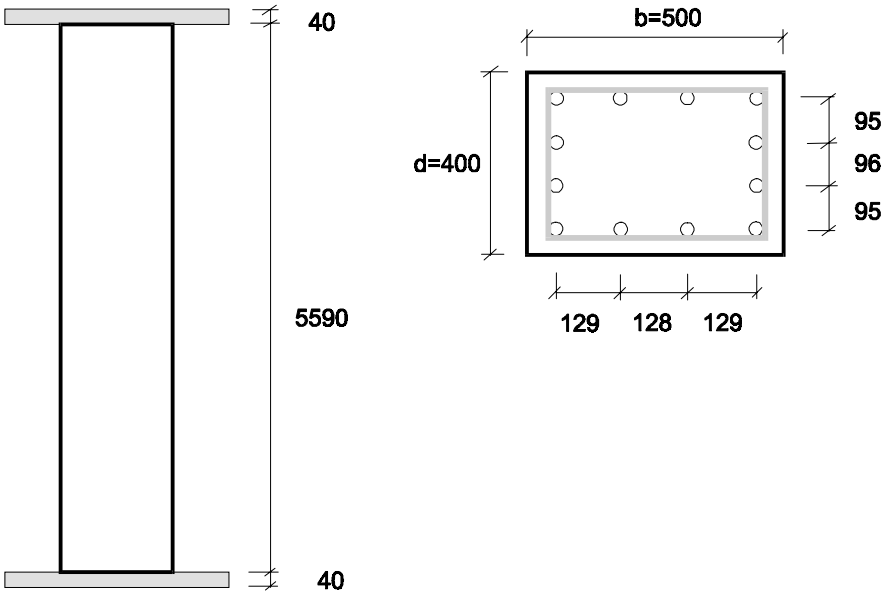

Figure 7.25
Geometrical data of the simulated column (Diederichs, /1995/).

Note that the rectilinear binding is not shown in Figure 7.25.

The configuration of the column can be viewed in Table 7.4.

Table 7.4 *Detailed description of the tested column from Germany (Diederichs, /1995/).*

	Value	Unit
Structure		
Cross-section	400 x 500	[mm]
Eccentricity	133.3	[mm]
Axial load	2400	[kN]
Concrete		
Compression strength (cube)	109.1	[MPa]
Modulus of elasticity	42.1	[GPa]
w/c ratio	25	[%]
Fibre	5.4	kg/m^3
Reinforcement		
Diameter	25	[mm]
Ultimate tension strength	500	[MPa]
Modulus of elasticity	185	[GPa]

Test simulation

As for the Japanese column the simulation was done by assuming that the end boundary was fixed in the horizontal direction and then simulating the upper half of the column.

The cross-section of 400 x 500 mm is relatively large and therefore the temperature field in the cross-section will not play a significant role on the structural stability of the column until several tenths of minutes have passed.

The great cross-section will also have effects on the calculation process where convergence problems may arise. This can be seen on the horizontal displacement of the column where the curve has not as clear approach to failure as for smaller cross-sections. This of course means that the reliability of the simulated displacement will not be as high as for a curve showing more rapidly increasing displacement.

The horizontal displacement as a function of time can be seen in Figure 7.26.

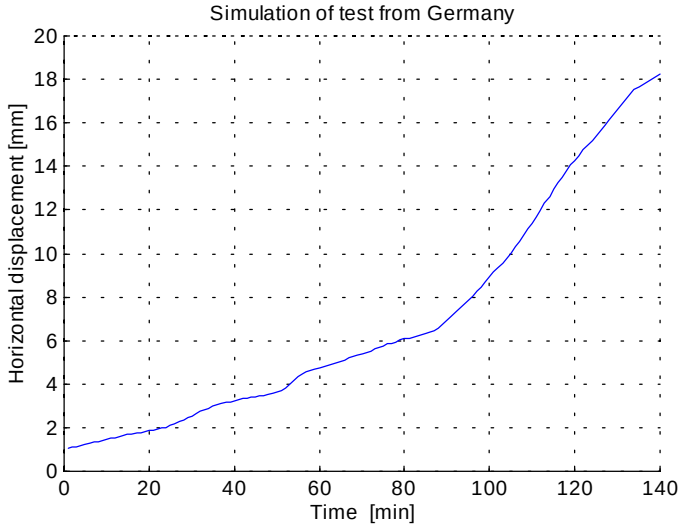

Figure 7.26
Horizontal displacement of a column tested in Germany

The displacement at the time of failure is quite large which supports that the simulation is reliable. The time of failure in the simulation is 140 min compared to the 180 min in the test.

The reasons for the differences in time to failure can be many. The exact boundary conditions are not known and a difference between the simulated ones and the tested can be of extreme importance. The furnace temperature in the test is supposed to be according to the ISO-834 standard temperature curve but as no temperature relation in the test is documented this is hard to verify. The ISO-834 curve is quite extreme and can be difficult to obtain in a practical test.

7.6.3 General Results from Simulation

As a result of the test simulations it can be confirmed that CONFIRE gives acceptable results with concern to time to failure. Furthermore the program gives conservative failure times in both cases.

It must be noted that in order to accurately simulate a test, all test parameters must be well defined and followed in the test. This is seldom the case as in mechanical testing, the equipment is often hard to control in every detail. Furthermore, these parameters must be possible to simulate with the existing program codes. The best results are obtained when
Many uncertainties are thus involved in a simulation of a test.

7.7 INTERACTION DIAGRAM

In this Section an interaction diagram (see Section 7.1.3) incorporating force and moment will be put forward in order to improve the understanding of the overall behaviour of columns. The Section furthermore explains how interaction diagrams are used in the design in a practical sense.

Interaction diagrams can give considerable information on the overall behaviour of a column in a practical situation. Interaction diagrams have been made for OPC columns at room temperatures but they are not available for fire exposed columns. For HPC columns no interaction diagrams have been produced.

Usually interaction diagrams have normalised axial force on the vertical axis and normalised moment or axial force times eccentricity on the horizontal axis. For a specific cross-section a line may then be drawn for all the load-moment combinations which causes failure in the column. A combination of such lines makes up a design chart for a column with different reinforcement area, cross-sectional area, concrete strength and the strength of the reinforcement steel.

As mentioned in former chapters, increase in the temperature modifies the mechanical and thermal properties for both concrete and reinforcement. As these properties change, as a function of temperature, an interaction design chart would have to be made for each temperature combination in the cross section, meaning that these diagrams would be a function of cross-section and temperature field. The task to construct design charts for concrete columns under fire exposure is therefore overwhelming.

In spite of the above, one interaction line has been calculated for a specific column in order to gain a better understanding of the behaviour of fire exposed concrete columns. It has not been

the intention to build a design basis using such charts, but merely to confirm the general form of the interaction diagram observed for concrete columns at ordinary temperatures.

Figure 7.27 shows the geometry of the cross section and the fire exposure for the column used in obtaining the interaction diagram.

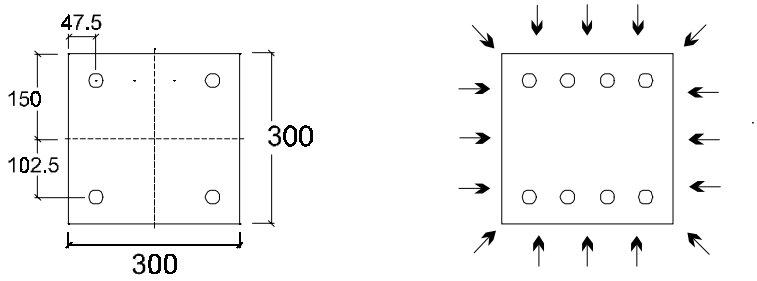

Figure 7.27
Cross-sectional geometry and fire exposure of the column used for the interaction diagram.

Four reinforcement bars were placed in the corners of the cross section with a concrete cover of 47.5 mm. The yield strength of the reinforcement steel was 500 MPa.

Figure 7.28 displays the length (2.4 m), boundary condition and loading situation of the column.

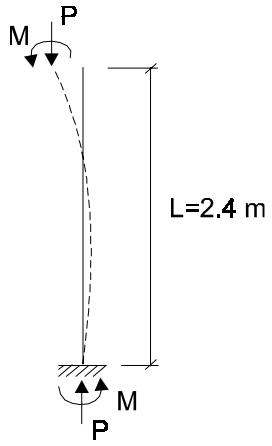

Figure 7.28
Structural data for the column in question showing length, initial out of straightness and the boundary conditions.

The time for which the load-moment combination is calculated is 90 minutes. About 10 iterations were needed for each point in the diagram thus resulting in 80 iterations in total. The interaction diagram is shown in Figure 7.32.

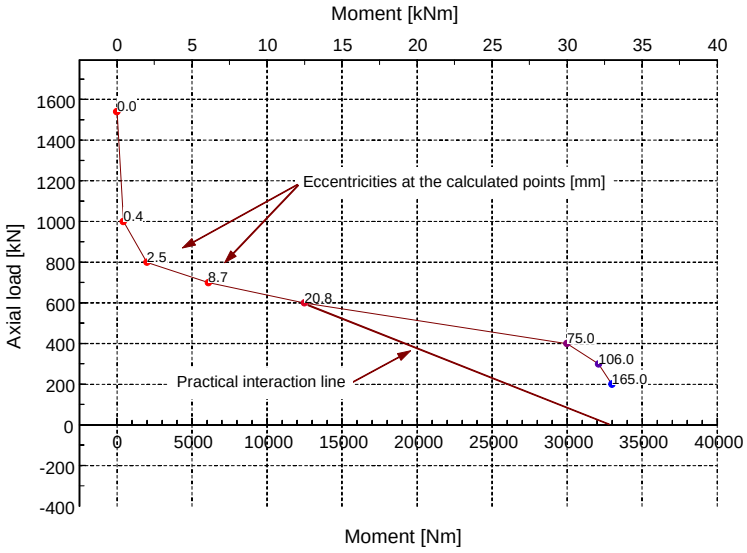

Figure 7.29
Interaction diagram for a column with a four sided fire exposure according to ISO-834. The time at which the failure is calculated is 90 minutes. Note that in a practical situation the left end of the diagram is unimportant as a minimum eccentricity is applied in design codes.

When only axial force acts on a column without any significant moment it behaves like a short column not affected by the slenderness. This is quickly changed when external moment is applied to the column ends imposing an eccentricity for the axial force. Observe the temperature in the cross-section after 90 minutes shown in Figure 7.10. Because of the high temperatures in the cross-section the influence of the moment is crucial concerning the overall behaviour of the column and the risk for buckling failure.

CONFIRE does not allow the column to be loaded with axial force only, as convergence problems arise. The moment applied for the maximum axial force is however only 10 Nm to gain convergence. A similar problem arises at the other end of the diagram where the axial load approaches zero and the vertical force is not sufficient for convergence.

It is important to notice that the part to the left of the diagram where the axial force dominates is irrelevant from a practical point of view as a certain minimum out of straightness has to be applied in design. In Sweden h/30 or a minimum of 20 mm has to be applied (BBK 94, /1994/). As can be seen in Figure 7.32 the 20 mm fictitious eccentricity is near the middle of the diagram.

The practical interaction line, from the minimum allowed moment-force combination, to a pure moment load gives an approximation for allowed force-moment combinations. This line gives, according to the diagram, a conservative failure time as this practical curve lies totally within the calculated one.

8. CONCLUDING REMARKS

Up till now, HPC has only been used in very special applications. To be able to expand the usage and acceptance of HPC, extensive research has to be undertaken and design methods have to be developed. This report deals with the latter subject, i.e. to develop design guide lines for HPC structures exposed to fire.

The report also gives a methodology for the development of simplified design methods. The methodology differs somewhat for beams and slabs, and columns where structural factors have to be taken into consideration.

This thesis will hopefully contribute to the increased application of HPC structures and ease its design process.

8.1 GENERAL RESULTS

In Chapter 3 mechanical properties of HPC were listed. It is revealed that there is a great difference in the relative strength of HPC in comparison to OPC. This difference will strongly influence the design rules adopted but this will be further discussed later on. The initial modulus of elasticity varies also and for the same stress, HPC will have 40% less strain than OPC. In this Chapter a model, developed for OPC, was modified to account for the HPC properties. This model is the basis for the structural calculation program CONFIRE and even incorporates mechanical properties for steel also given in Chapter 3.

Chapter 4 outlines thermal properties of HPC with a great effort spent to compare HPC to OPC. Factors of importance are thermal conductivity and thermal capacitivity. This basic thermal analysis is then used in Chapter 5 to calculate differences in the temperature field as a function of time. It is demonstrated that the heating of a cross-section happens approximately 20 % faster in HPC than in OPC. Chapter 5 also lists the theory for thermal calculation and the numerical approach.

The fire engineering design methods for HPC differ somewhat from the OPC design methods in the way that they require increased protection to mitigate spalling in case of fire. It is possible to apply the same general methodology for mechanical design of HPC as for OPC for all kinds of structures analysed in this report, namely the reduction by a single isotherm strength curve. However, some partial modifications have to be made in some cases. This also allows the designer to be quickly familiarised with the new methods.

Due to differences in structural properties for beams, slabs and columns, these have to be assigned different design methods. In Chapter 6, beams and slabs are analysed. The analysis performed on beams and slabs is on a member level where the moment capacity of the cross-section is calculated and compared, using different relative strength curves, the True and single isotherm curves respectively. The resulting design recommendation is that beams and slabs are designed by using the 500 curve (Figure 2.1) but the moment capacity of the cross-sections where the compression zone is exposed to fire is reduced by 5 to 10 % depending on the kind of structure (slab or beam) and whether the structure has reinforcing steel or pre-stressing steel.

The necessary reduction in the moment capacity can partly be explained by the complex variation of the relative strength of HPC as a function of temperature, the True curve. This curve, has a unique reduction in the relative strength at temperatures between 100 and 350 °C with a local minimum of 60 % of the original value at 200 °C. This is different from what has been observed for OPC where the relative strength curve has a simpler form. How much exactly this form of the curve influences the mechanical response of a member is difficult to say.

Analysis of the phenomena arising in the members due to variation in different parameters has resulted in a firm bases for the design recommendations. This variation applies to cross-sections, steel type and amount, as well the type of fire exposure.

There are some limitations in the assumptions adopted in the calculations. This applies among other things to the ISO fire exposure where only similar heat regimes can be accepted for the design rules. This time-temperature regime is on the other hand by far the most common for the design of structures.

Design methods for columns where put forward in Chapter 7. The same general approach has been chosen for columns as for beams, i.e. reduction according to a single isotherm curve. The calculation procedure is however somewhat more complicated as structural factors have to be taken into consideration. The comparison of relative strength curves revealed that the simplified 400 curve was sufficient to give a conservative result in comparison to the curve obtained in tests of HPC (the True curve).

The columns were reinforced as could been expected in columns of respective size and length. Note that this combination results in larger amount of reinforcement for HPC than for OPC because of the higher compression strength.

The columns have only be axially loaded with slight initial out of straightness. Section 7.7 reveals on the other hand how the interaction design chart (moment capacity versus axial force) will give conservative results for other axial load and moment combinations.

The verification of tests done in Japan and Germany was carried out for CONFIRE, where the program proved to give quite acceptable and conservative results.

8.2 FUTURE WORK

A discussion has been given of the influence of HPC properties on the beam and slab behaviour but a theoretical model incorporating these new properties would allow a better understanding of phenomena arising under a fire. A construction of such a theoretical model has not been possible within the scope of this project.

Research efforts have only recently been focused on HPC columns. Tests of HPC columns under fire exposure are rare but some are planned in the near future. Those available have usually been carried out to analyse the spalling phenomenon and not mechanical response under fire. It would be very interesting to be able to simulate more tests in order to verify the existing models for calculation with respect to fire but also in the overall sense.

More detailed design charts involving columns of varying sizes and configuration would give a deeper knowledge of the overall behaviour of columns. These are on the other hand very time consuming as iterations, varying load and moment combinations, are needed to obtain a failure at the desired time (i.e. 30, 60, 90 or 120 minutes).

9. REFERENCES

Anderberg, Y., /1976/, ”Fire-exposed hyperstatic concrete structures - An experimental and theoretical study” , Division of Structural Mechanics and Construction, Lund Institute of Technology, Bulletin 55, Lund.

Anderberg, Y., Thelandersson, S., /1976/, ”Stress and Deformation Characteristics of Concrete at High Temperatures”, Division of Structural Mechanics and Construction, Lund Institute of Technology, Lund.

Anderberg, Y., Forsén, N.E.., /1982/, ”Fire Resistance of Concrete Structures” , Division of Structural Mechanics and Construction, Lund Institute of Technology, report LUTVVDG/(TVBB-3009), Lund.

Anderberg, Y. (editor), /1983/, ”Properties of Materials at High Temperatures, Steel”, RILEM-PHT 44-Report, Division of Building Fire Safety and Technology, Lund Institute of Technology, ISSN 0282-3756, Lund.

Anderberg Y., /1991/, ”SUPER-TEMPCALC”, A Commercial and User-Friendly Computer Program with Automatic FE-Generation for Temperature Analysis of Structures Exposed to Fire”, Fire Safety Design, Lund.

Anderberg, Y., /1992/, ”Temperaturbilagan”, Byggforskningsrådet, ISBN 91-540-5448-6, Stockholm.

Anderberg, Y., Pettersson, O., /1992/, ”Brandteknisk dimensionering av betongkonstruktioner”, Byggforskningsrådet, ISBN 91-540-5448-6, Stockholm.

Anchor, R.D. (editor), et.al., /1986/, ”Design of Structures against Fire”, Elsevier Applied Science Publishers LTD, ISBN 1-85166-012-7.

Atlassi, E., /1994/, ”Water vapour sorption isotherms and related properties of mature silica fume mortar”, Department of Building Materials, Chalmers Institute of Technology, Gothenburg.

”Betonghandboken”, /1990/, Konstruktion, utgåva 2, Svensk byggtjänst, ISBN 91-7332-533-3, Stockholm.

”BBK 94”, /1994/, Boverket´s handbook for concrete structures ((S) Boverket´s handbok om Betongkonstruktioner) Boverket, Karlskrona.

”BBR 94”, /1995/, Boverket´s Building regulations ((S) Boverkets Byggregler), 94:3, Karlskrona.

”BKR 94”, /1995/, Design Regulations of the Board ((S) Boverkets Konstruktionsregler), 94:2, Karlskrona.

Buchanan, A.H., Munukutla V.R., /1991/, ”Fire Resistance of Load-Bearing Reinforced Concrete Walls”, Fire Safety Science - Proceedings of the Third International Symposium, Elsevier Applied Science, pp. 771-780.

CEB, /1991/, ”Fire Design of Concrete Structures in Accordance with CEB/FIB Model Code 90 (Final Draft)”, Bulletin d’Information, No. 208, Lausanne.

Claesson, C., /1995/, ”Behaviour of Reinforced High Strength Concrete Columns”, Licentiate thesis, Publication 95:1, Division of Concrete Structures, Chalmers university of Technology, Göteborg.

”Design Handbook”, /1996/, High Performance Concrete, A Swedish Program for Research and Development, Draft 2.

Diederichs U., Jumppanen U.M., Schneider U., /1995/, ”High Temperature Properties and Spalling Behaviour of High Strength Concrete”, Fourth International Workshop for High Performance Concrete - Characteristic Properties and structural Performance, Weimar.

Ehm, H., /1967/, ”Betrag zur rechnerischen Bemessung von brandbeanspruchten balkenartigen Stahlbetonbauteilen”, Dissertation, Technische Universität Braunschweig.

ENV 1991-2-2, /1994/, ”Basis of design and actions on structures, Part 2-2 Actions on structures exposed to fire”, CEN, Brussels.

ENV 1992-1-1, /1993/, ”Design of concrete structures, Part 1-1: General rules and rules for buildings”, CEN, Brussels.

ENV 1992-1-2, /1995/, ”Design of concrete structures - Part 1-2: General rules - Structural fire design”, CEN, Brussels.

ENV 1993-1-2, /1995/, ”Design of steel structures - Part 1-2: General rules - Structural fire design”, CEN, Brussels.

Forsén, N.E., /1982/, ”A Theoretical Study of the Fire Resistance of Concrete Structures”, FCB-SINTEF, report STF65 A82062, Trondheim.

Glavind, M., Stang, H, /1991/, ”Evaluation of the complete compressive stress-strain curve for high strength concrete”, Department of Structural Engineering, Technical University of Denmark. Published in RILEM, ”Fracture Processes in Concrete, Rock and Ceramics,”, E. & F.N. Spon, London.

Göransson U., /1996/, ”Mechanical Properties of High Strength Concrete at Elevated Temperatures, A Strain Model”, M7:6, Lund.

Hansson, H., /1993/, ”Betongpelare vid brand; Simulering av försök och dimensioneringsanvisning”, Institute of Technology, Department of Fire Safety Engineering, ISSN 1102-8246, ISRN LUTVDG/TVBB-5002-SE, Lund.

Hertz, Kristian, /1985/, ”Analysis of Prestressed Concrete Structures Exposed to Fire”, Technical University of Denmark, DK-2800, Lyngby.

Holman J.P., /1986/, ”Heat transfer”, sixth edition, McGraw-Hill, New-York.

Holst F., /1994a/, ”Mechanical Properties of High Strength Concrete at Elevated Temperatures”, M7:2, Lund.

Holst F., /1994b/, ”Thermal Properties of High Strength Concrete at Elevated Temperatures”, M7:3, Lund

ISO-834**, /**1975**/, ”**Fire Resistance Tests. Elements of Building Construction”, International Standards Organisation, Geneva.

Johannesson, P., Vretblad, B., /1993/, ”Byggformler och tabeller”, Liber Utbildning AB, Uppsala.

Jumppanen, U., et al., /1989/, ”Behaviour of high strength concrete at high temperatures”, Report 92, Helsinki University of Technology, Department of Structural Engineering.

Lie, T.T. and Lin, T.D., /1985/, ”Fire Performance of Reinforced Concrete Columns”, Fire Safety: Science and engineering, ASTM STP 882, T.Z. Harmathy, Ed., American Society for Testing and Materials, Philadelphia, pp. 176-205.

Mårtensson, A., /1994/, ”Bärande Konstruktioner; Betongkonstruktioner”, Bärande Konstruktioner, Lunds tekniska högskola.

Michikoshi, S. et.al, /1995/, ”Fire-Proof Test of RC-columns with High Strength Concrete”, Technology Research Center, Taisei Corporation, Yokohama.

Oredsson J., /1995/, ”CBEAM version 3.0, Users Manual”, Fire Safety Design, Lund.

Oredsson J., /1997/, ”Tendency to Spalling of High Strength Concrete”, M7:4, Lund.

Park, R., Paulay, T., /1975/, ”Reinforced Concrete Structures”, John Wiley & Sons.

Thelandersson S., /1994/, Betonghandboken Material Kapitel 25 Brandbeständighet, AB Svensk Byggtjänst, Stockholm.

Yatagai Ken, et.al, /1995/, ”Study on Fire Resistance of RC columns of High-Strength Concrete (Part 2)”, Technology Research Center, Taisei Corporation, Yokohama.

APPENDICES

A CROSS-SECTIONS
A1 Beams and slabs

Name	Type of steel		Cross-section
	Rein-forcing	Pre-stressed	
A 1, 2	X	X	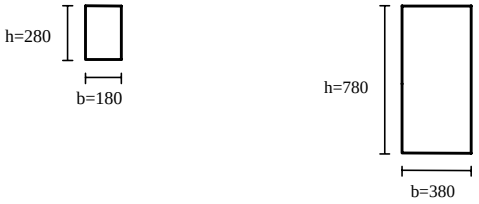
B 1, 2		X	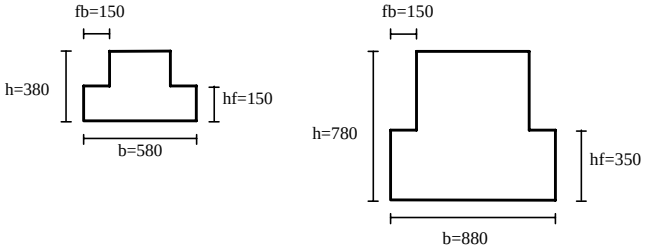
C 1, 2, 3		X	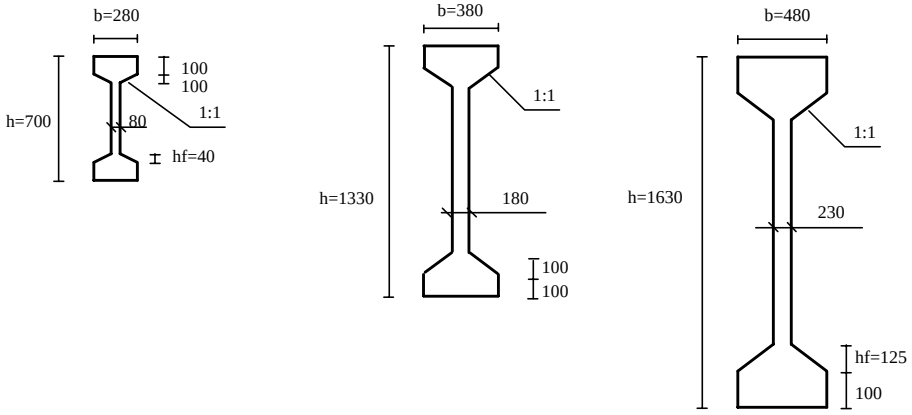
D 1, 2		X	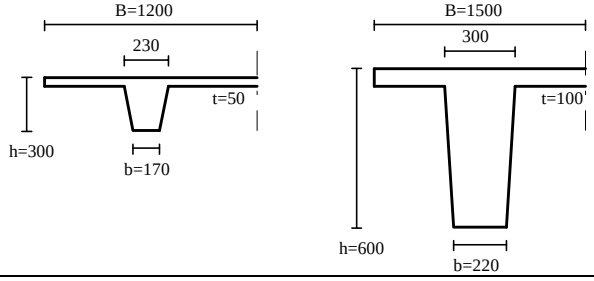

E 1, 2	X	X	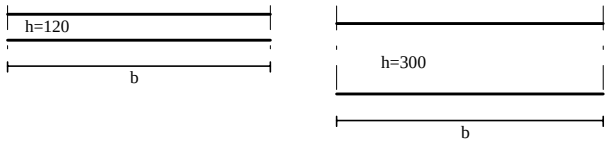
F 1, 2, 3		X	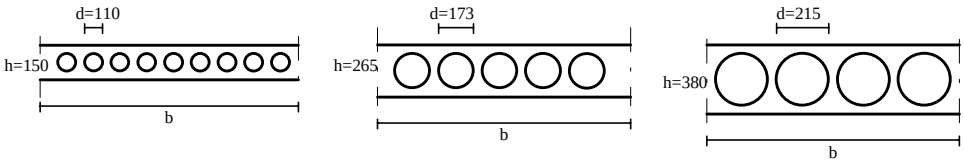

A2 Columns

All columns are reinforced.

Column 150x150 mm

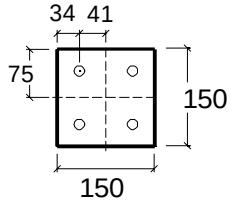

Column 300x300 mm

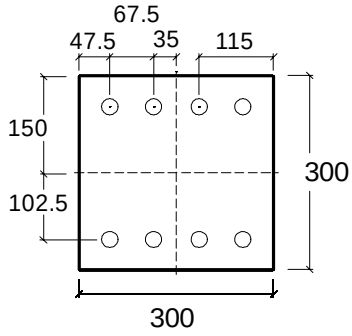

Column 400x400 mm

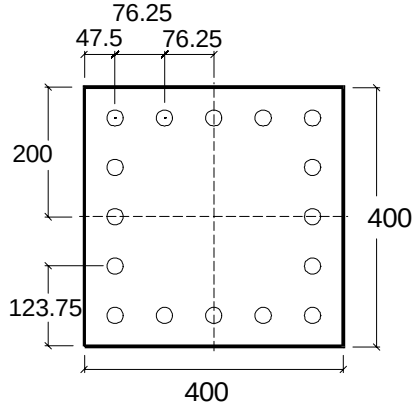

B MOMENT CAPACITY CALCULATION OF BEAMS AND SLABS

B1 Figures

A1ri

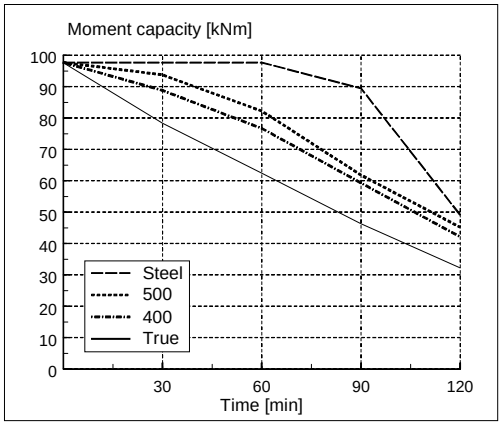

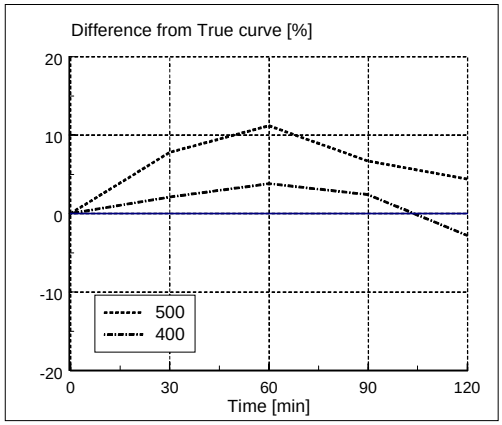

A1rii

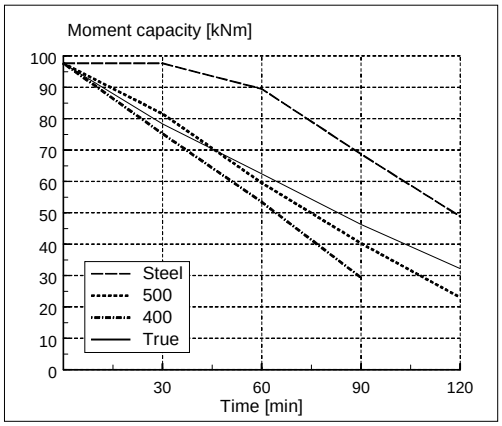

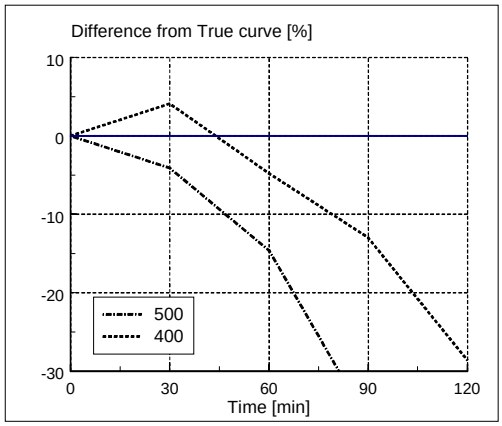

A1rib

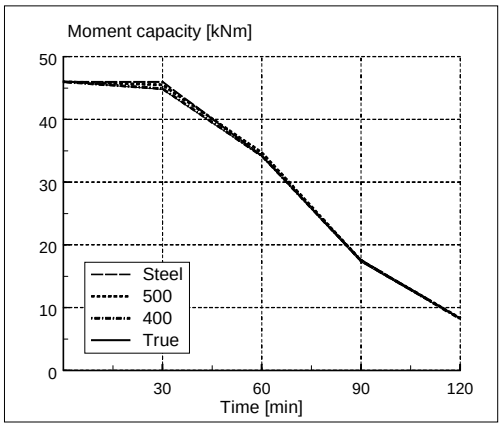

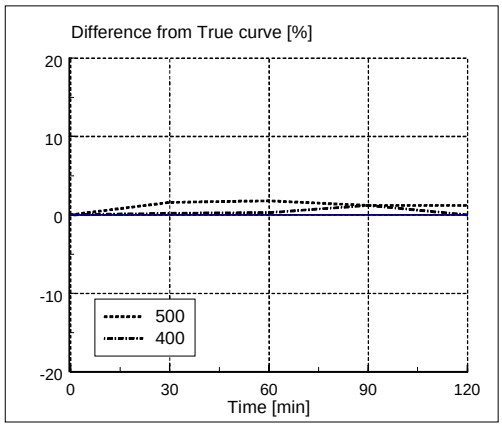

A1pi

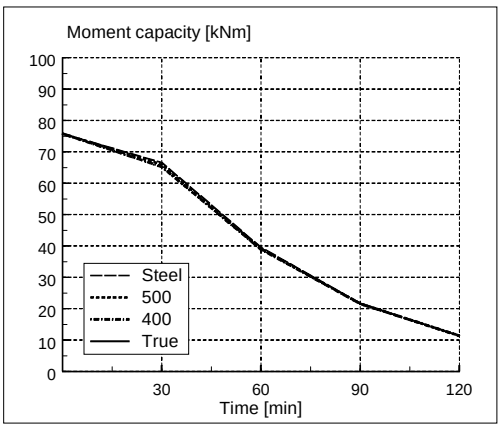

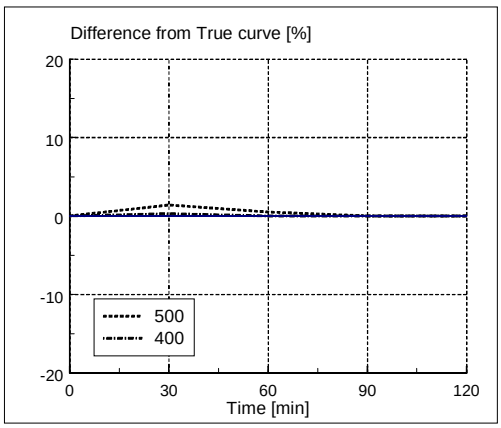

A1pii

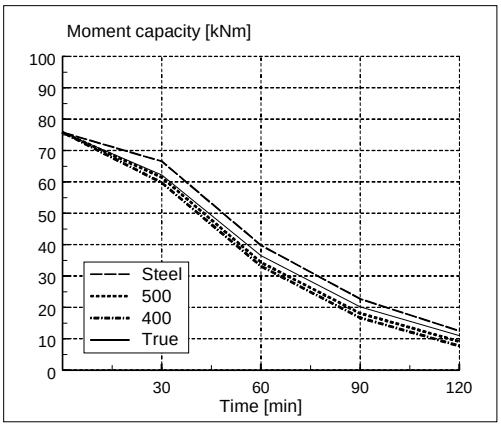

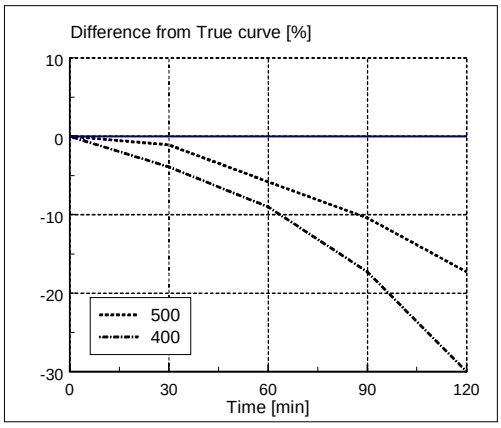

A2ri

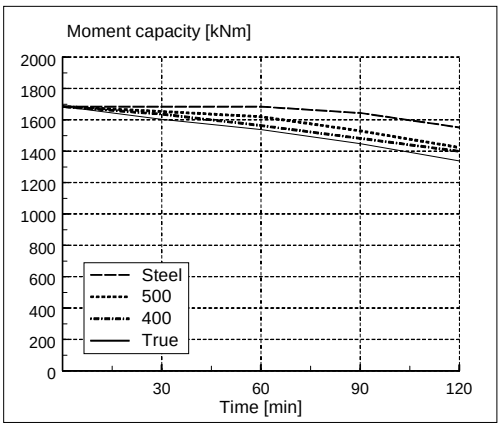

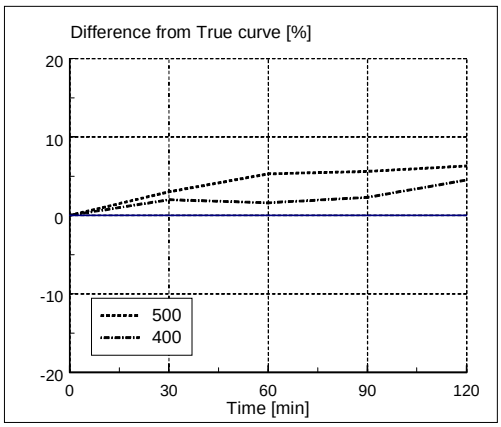

A2rii

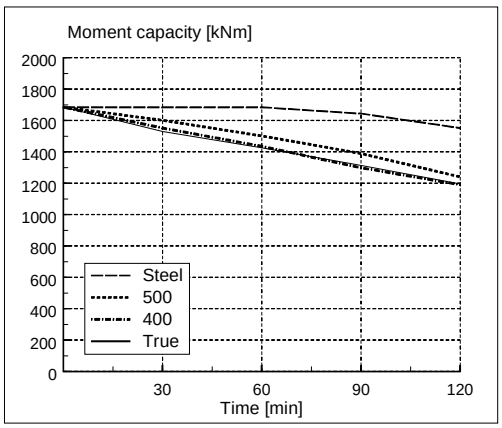

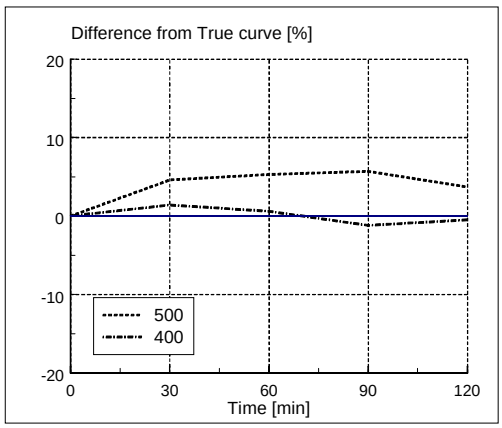

A2pi

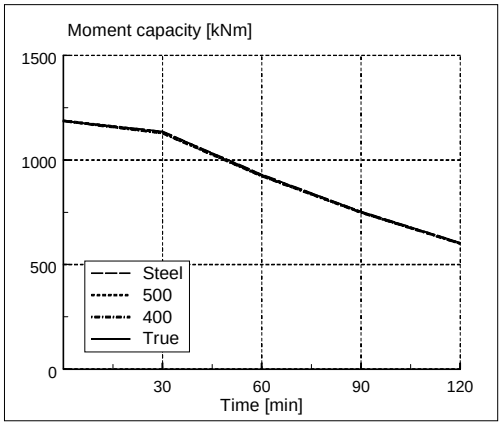

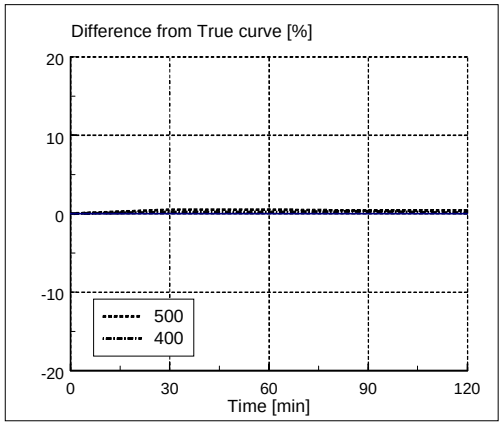

A2pii

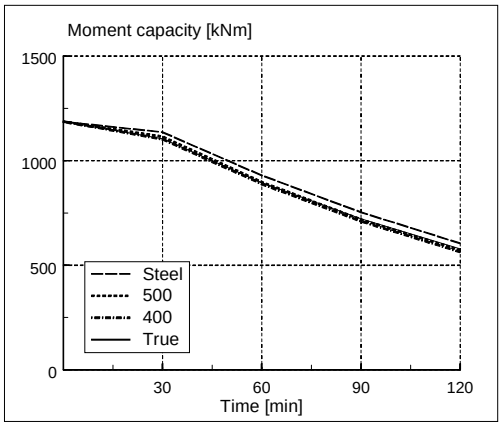

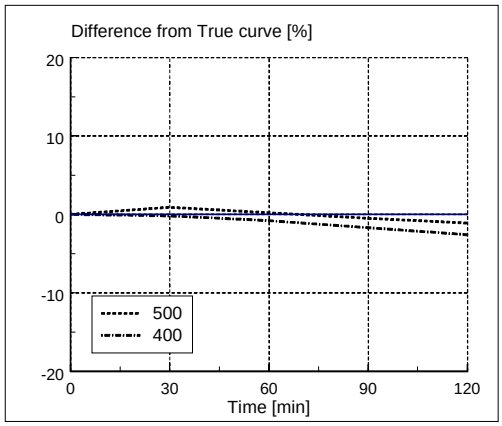

B1pi

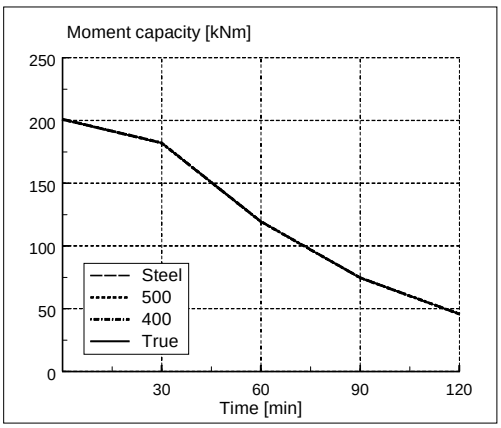

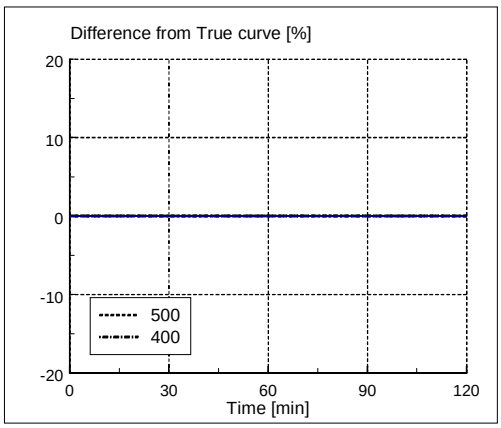

B1pii

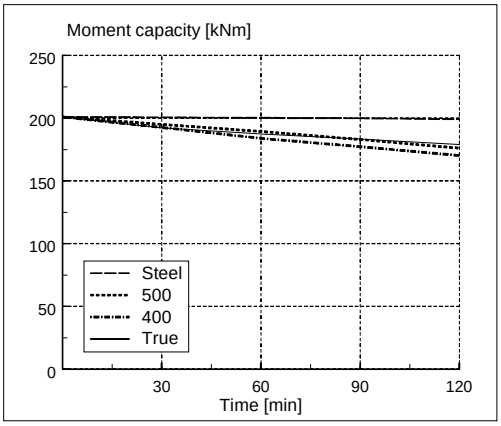

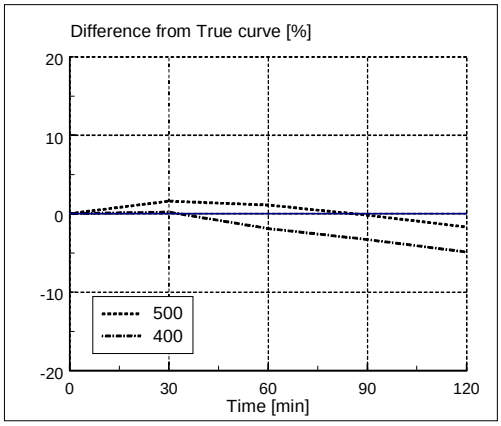

B2pi

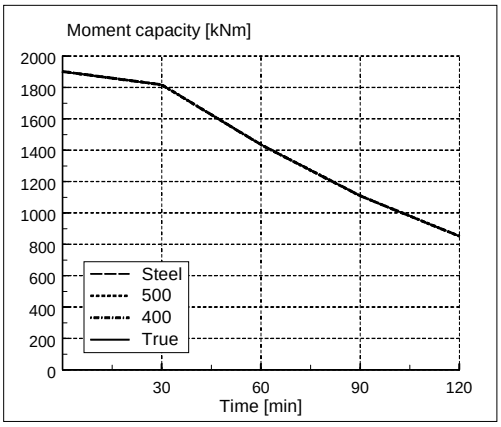

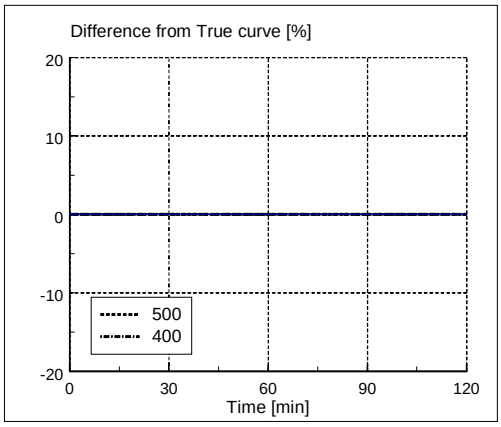

B2pii

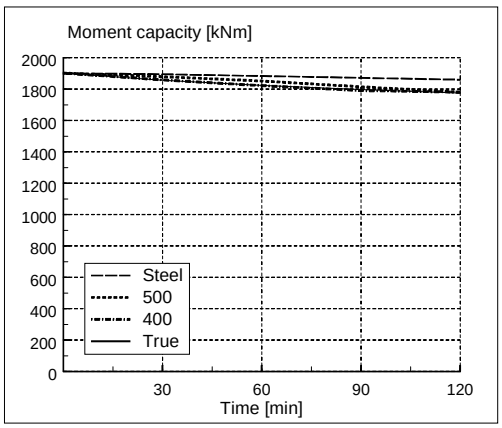

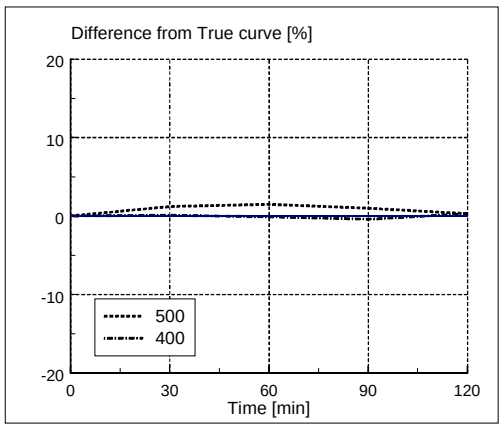

C1pi

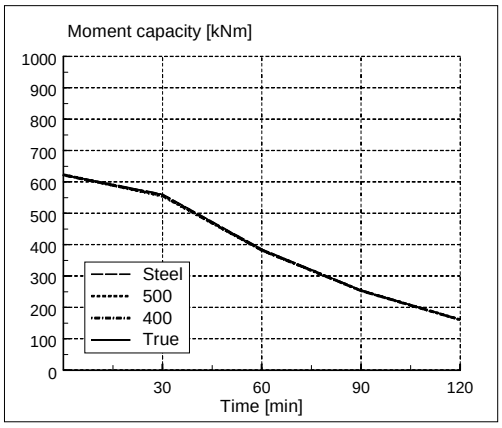

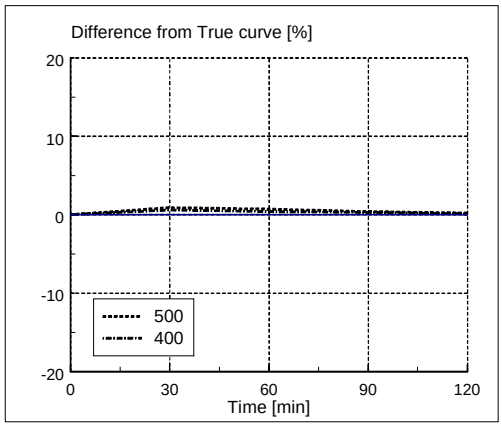

C2pi

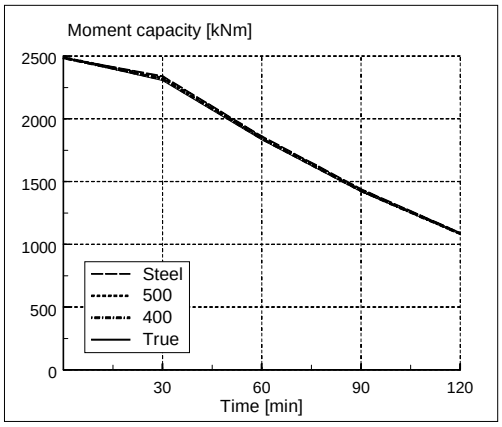

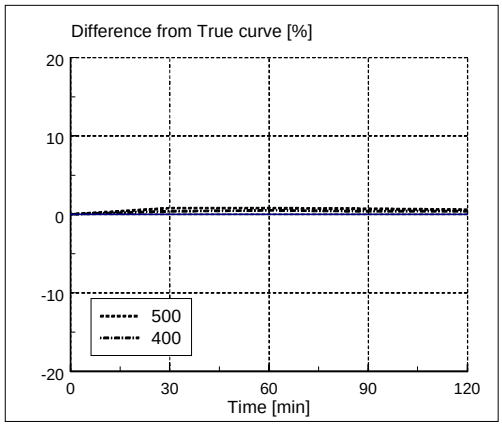

D1pi

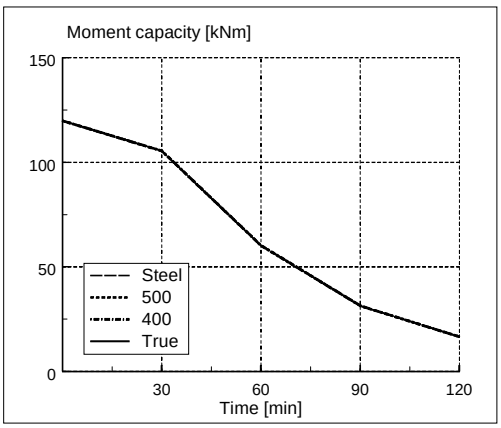

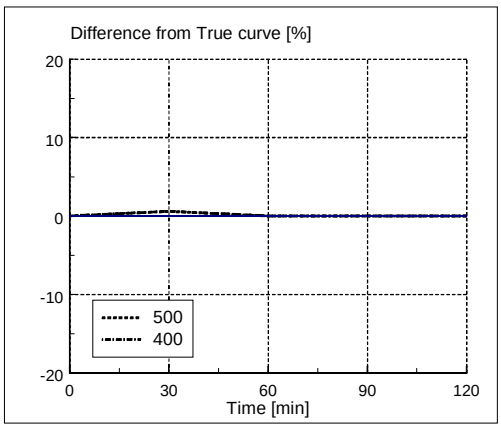

D1pii

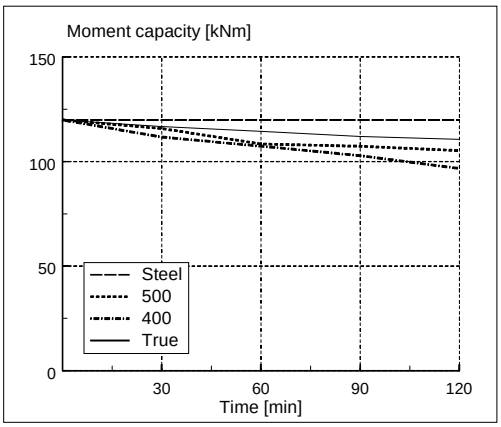

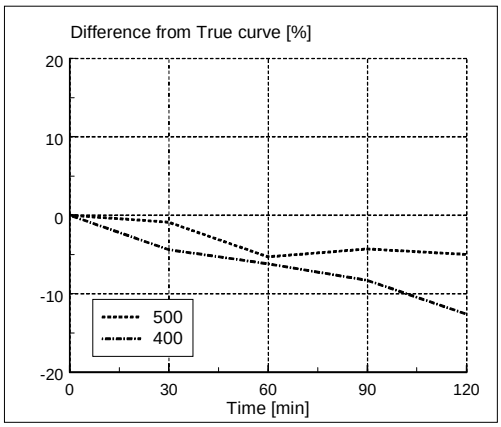

D2pi

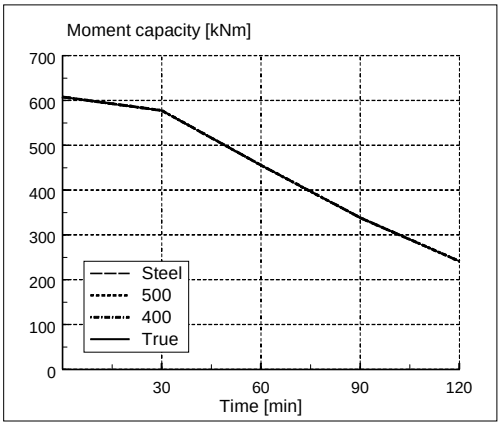

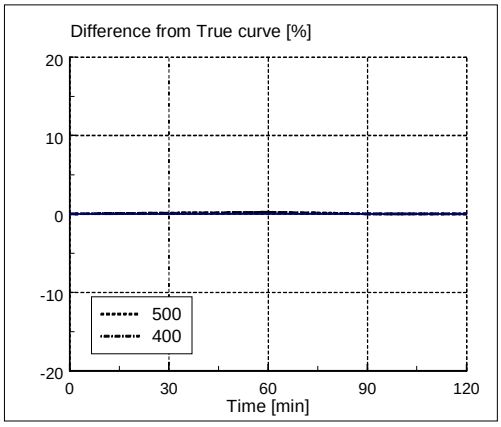

D2pii

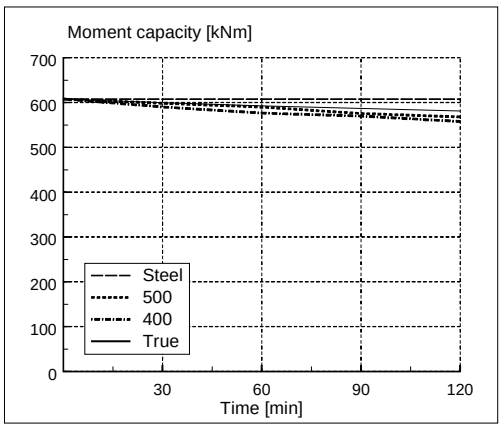

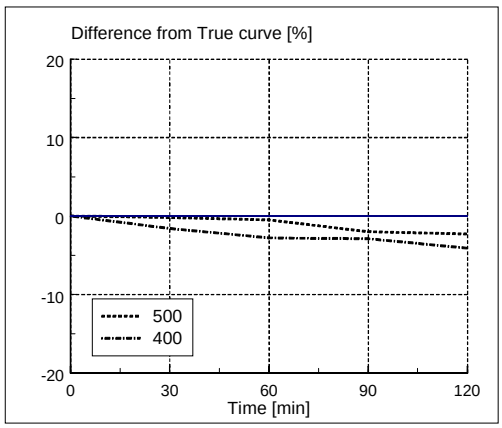

E1ri

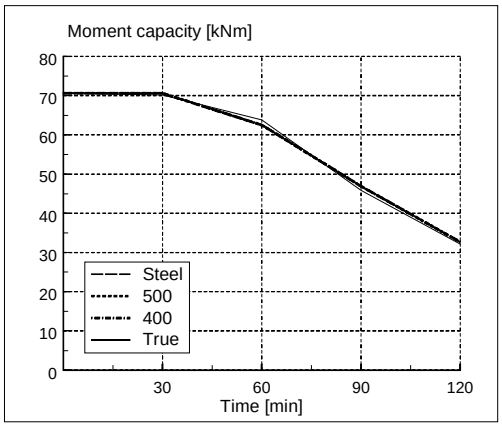

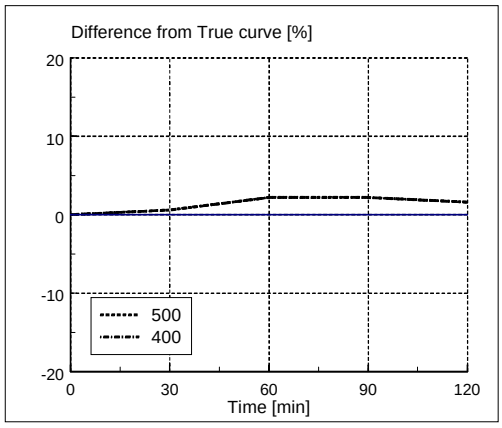

E1rii

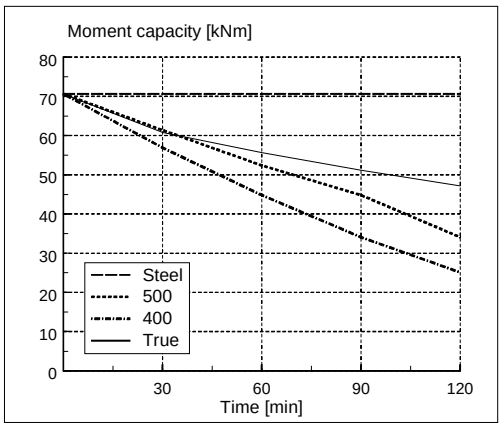

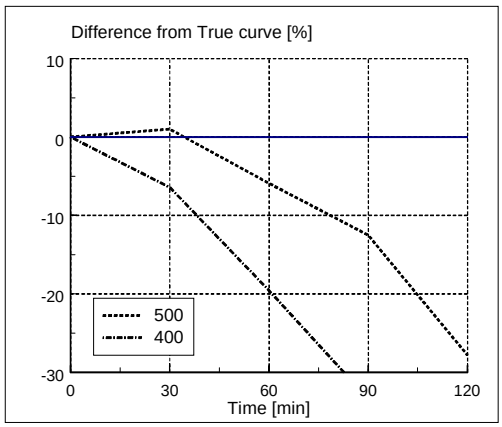

E1pi

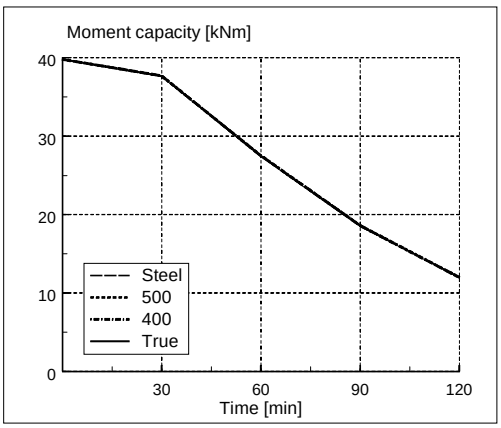

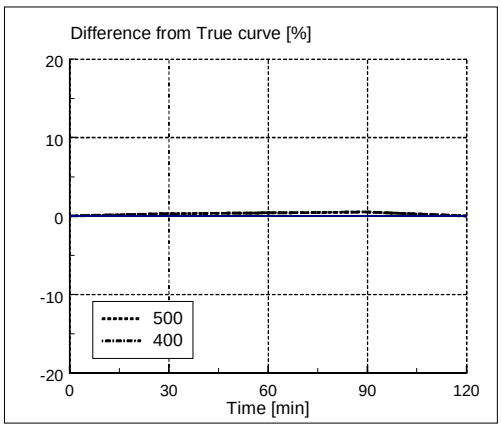

E1pii

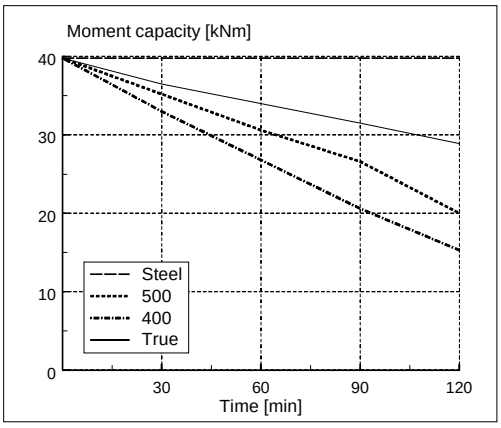

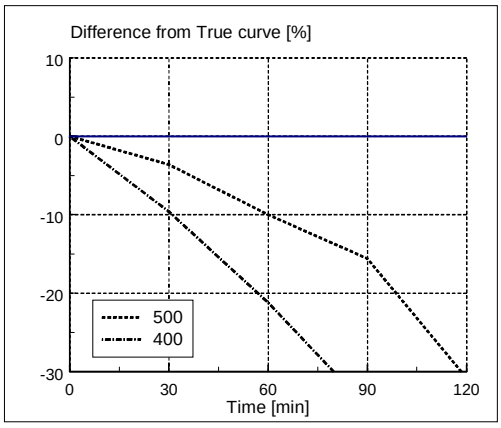

E2ri

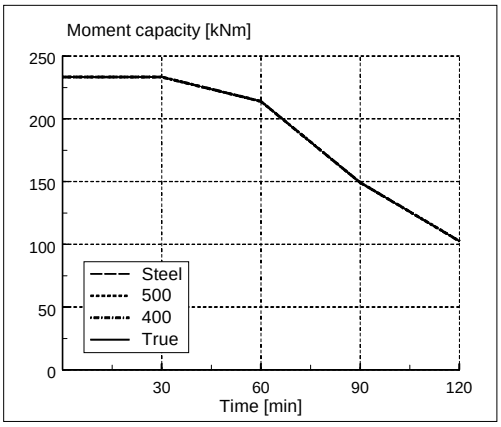

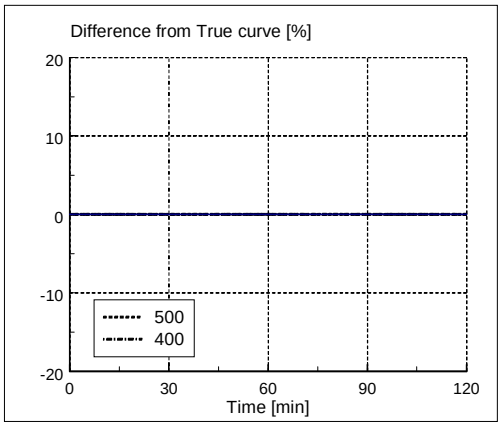

E2rii

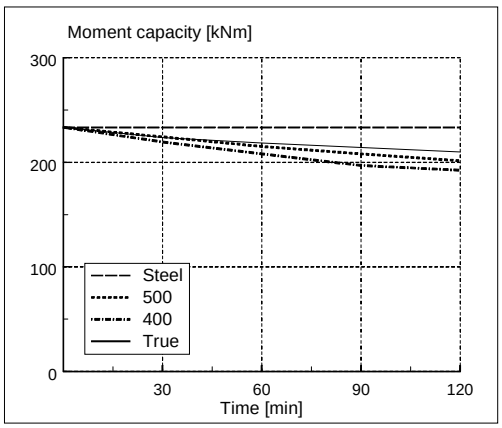

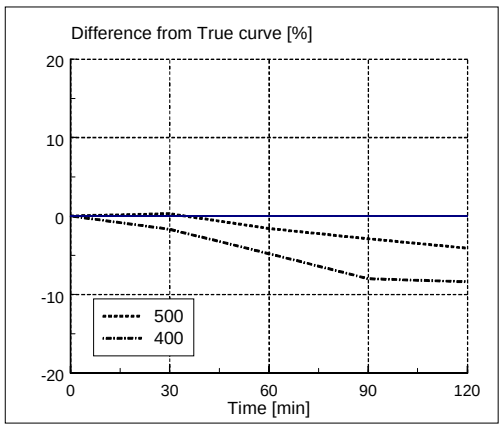

E2pi

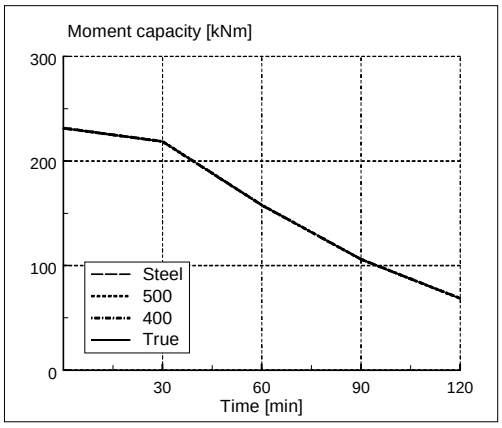

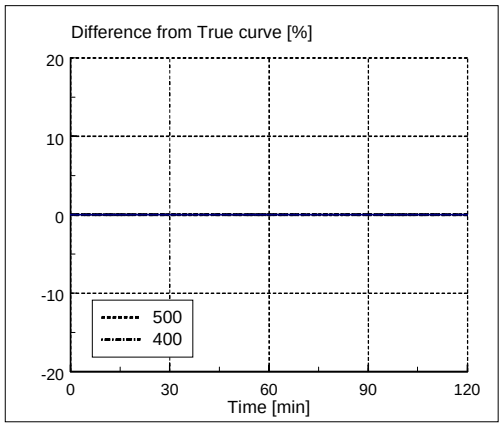

E2pii

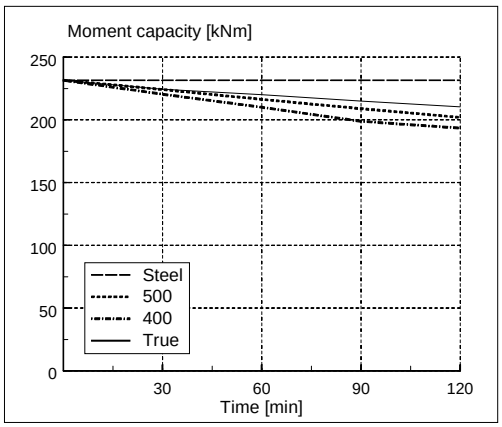

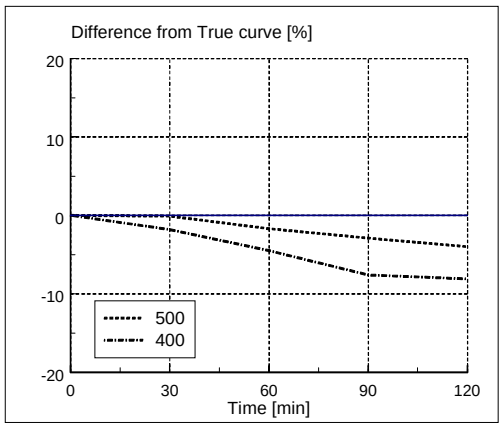

F1pi

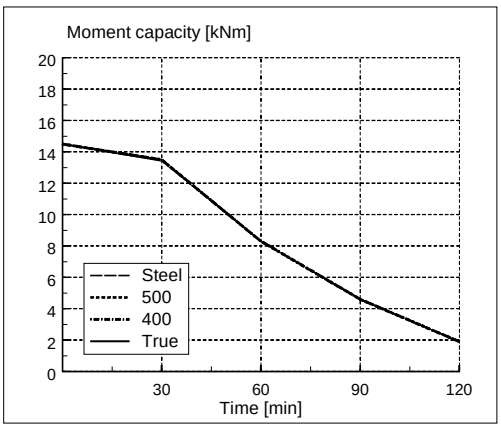

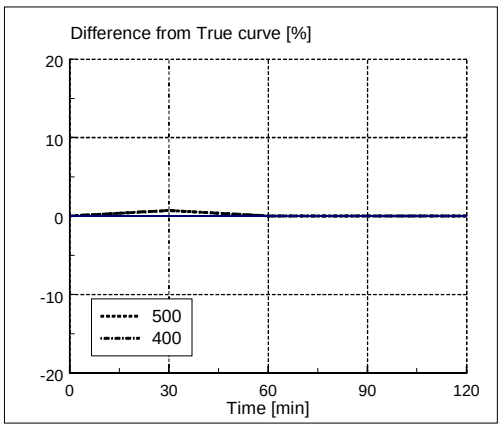

F1pii

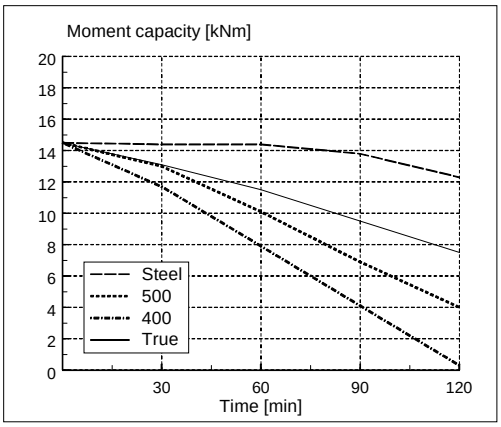

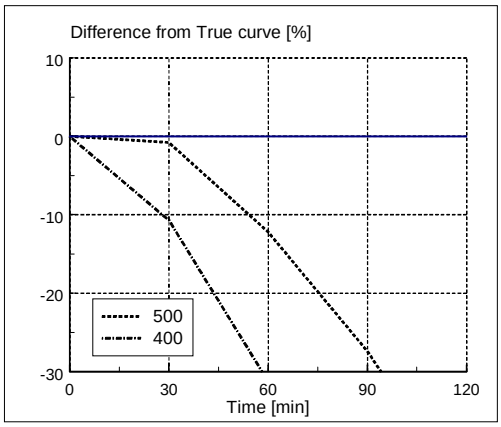

F2pi

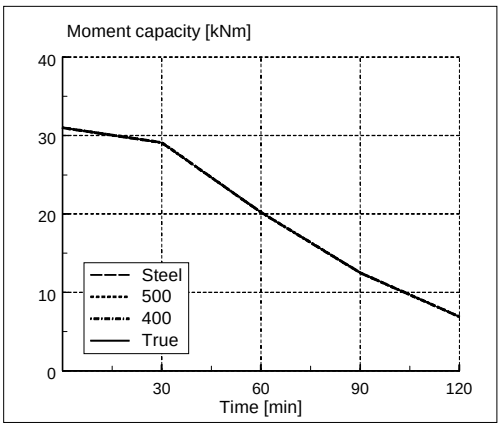

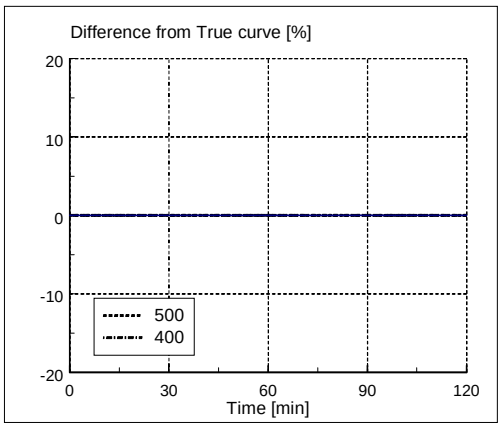

F2pii

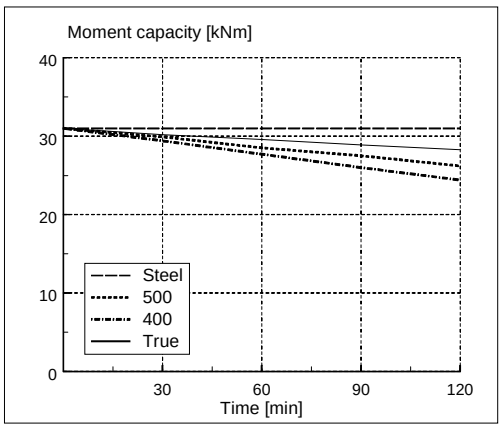

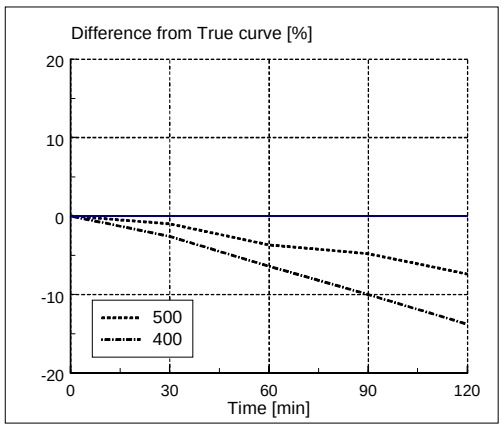

F3pi

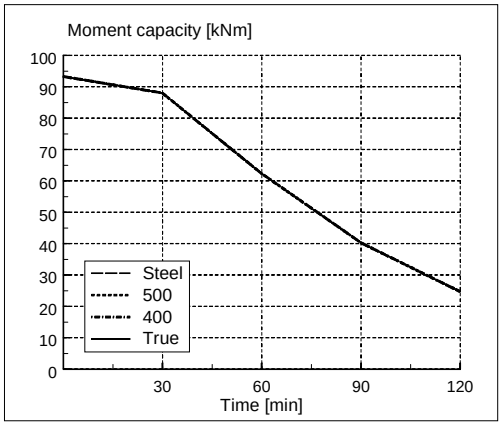

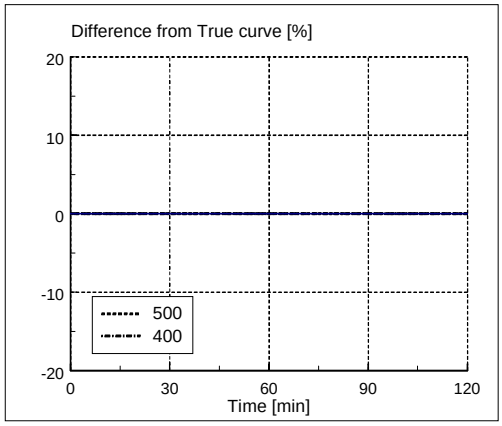

F3pii

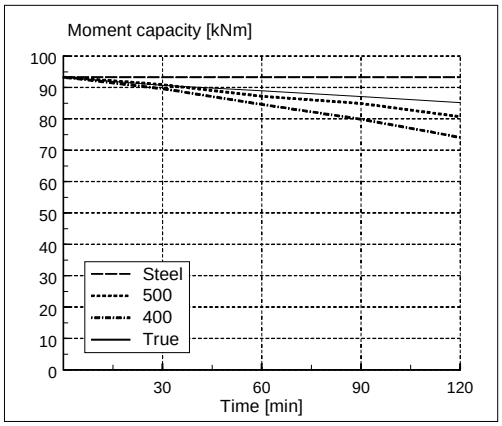

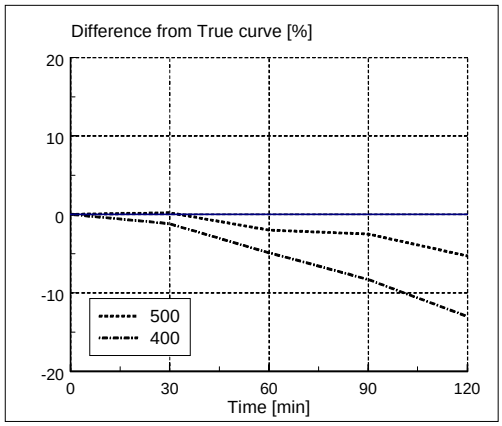

B2 Tabulated Values

The following applies to different columns in the Table below:

1. Cross-sections as given in Appendix A
2. Time for which the moment capacity is calculated.
3. Relative moment capacity using the True curve
4. Relative moment capacity using the 350 isotherm curve
5. Percentage difference between the True curve and the 350 isotherm curve
6. - 9. Similar for the 400 and 500 isotherm curves
10. Relative moment capacity using the 1500 isotherm curve (equal to the reduction in the steel).

1	*2*	*3*	*4*	*5*	*6*	*7*	*8*	*9*	*10*	*11*
	Time	Relative moment capacity	350 curve	Procent. Diff.	400 curve	Procent. Diff.	500 curve	Procent . Diff.	1500 curve	Procent . Diff.
A1rii	0	**97,7**								
	30	**78,4**	72,7	-7,3%	75,2	-4,1%	81,6	4,1%	97,7	24,6%
	60	**62,5**	45,7	-26,9%	53,4	-14,6%	59,5	-4,8%	89,5	43,2%
	90	**46,3**	-	-	29,4	-36,5%	40,3	-13,0%	68,7	48,4%
	120	**32,2**	-	-	-	-	23	-28,6%	48,8	51,6%
A1ri	0	**97,7**								
	30	**87**	88,8	2,1%	88,8	2,1%	93,8	7,8%	97,7	12,3%
	60	**73,9**	75,3	1,9%	76,7	3,8%	82,2	11,2%	97,7	32,2%
	90	**57,9**	55	-5,0%	59,3	2,4%	61,8	6,7%	89,5	54,6%
	120	**43,3**	38,3	-11,5%	42,1	-2,8%	45,2	4,4%	49,1	13,4%
A1rib	0	**46**								
	30	**44,8**	44,9	0,2%	44,9	0,2%	45,5	1,6%	46	2,7%
	60	**34,1**	34,2	0,3%	34,2	0,3%	34,7	1,8%	34,2	0,3%
	90	**17,3**	17,4	0,6%	17,5	1,2%	17,5	1,2%	17,6	1,7%
	120	**8,2**	8,2	0,0%	8,2	0,0%	8,3	1,2%	8,3	1,2%
A2rii	0	**1684,3**								
	30	**1530,9**	1533,9	0,2%	1552,1	1,4%	1601,3	4,6%	1684,3	10,0%
	60	**1426,6**	1404,1	-1,6%	1435,4	0,6%	1501,6	5,3%	1684,3	18,1%
	90	**1314,3**	1265,6	-3,7%	1298,2	-1,2%	1389,8	5,7%	1643,9	25,1%
	120	**1195,6**	1115,1	-6,7%	1190,1	-0,5%	1239,5	3,7%	1551,8	29,8%
A2ri	0	**1684,3**								
	30	**1604,5**	1619,9	1,0%	1636,5	2,0%	1653,3	3,0%	1684,3	5,0%
	60	**1538,8**	1563,5	1,6%	1563,5	1,6%	1619,9	5,3%	1684,3	9,5%
	90	**1447,6**	1472	1,7%	1481,5	2,3%	1529,3	5,6%	1643,9	13,6%
	120	**1338,8**	1352,5	1,0%	1399	4,5%	1423,7	6,3%	1551,8	15,9%

A2pii

0	**1186,9**								
30	**1104,9**	1101	-0,4%	1102,4	-0,2%	1114,9	0,9%	1136,1	2,8%
60	**895,5**	877,9	-2,0%	888,6	-0,8%	897,2	0,2%	929,6	3,8%
90	**722,5**	704	-2,6%	710,4	-1,7%	718,8	-0,5%	753,5	4,3%
120	**578,8**	557,9	-3,6%	564	-2,6%	572,4	-1,1%	605,1	4,5%

A2pi

0	**1186,9**								
30	**1127,2**	1128,9	0,2%	1128,9	0,2%	1132,8	0,5%	1136,2	0,8%
60	**921,5**	923,4	0,2%	923,6	0,2%	926,3	0,5%	930,4	1,0%
90	**747,2**	747,9	0,1%	749,4	0,3%	750,1	0,4%	753,8	0,9%
120	**599,7**	600,4	0,1%	600,5	0,1%	602	0,4%	604	0,7%

A1pii

0	**75,8**								
30	**62,2**	58,9	-5,3%	59,8	-3,9%	61,5	-1,1%	66,6	7,1%
60	**36,5**	31,8	-12,9%	33,2	-9,0%	34,4	-5,8%	39,8	9,0%
90	**20,2**	15,6	-22,8%	16,7	-17,3%	18,1	-10,4%	22,7	12,4%
120	**11**	6,7	-39,1%	7,7	-30,0%	9,1	-17,3%	12,5	13,6%

A1pi

0	**75,8**								
30	**65,1**	65,3	0,3%	65,3	0,3%	66	1,4%	66,6	2,3%
60	**38,9**	38,9	0,0%	38,9	0,0%	39,1	0,5%	39,5	1,5%
90	**21,6**	21,6	0,0%	21,6	0,0%	21,6	0,0%	21,7	0,5%
120	**11,4**	11,4	0,0%	11,4	0,0%	11,4	0,0%	11,4	0,0%

B1pi

0	**200,9**								
30	**182,1**	182,1	0,0%	182,1	0,0%	182,1	0,0%	182,1	0,0%
60	**119,4**	119,4	0,0%	119,4	0,0%	119,4	0,0%	119,4	0,0%
90	**74,7**	74,7	0,0%	74,7	0,0%	74,7	0,0%	74,7	0,0%
120	**45,9**	45,9	0,0%	45,9	0,0%	45,9	0,0%	45,9	0,0%

B1pii

0	**200,9**								
30	**192,3**	190,1	-1,1%	192,7	0,2%	195,4	1,6%	200,7	4,4%
60	**187,4**	181,6	-3,1%	183,9	-1,9%	189,4	1,1%	200,3	6,9%
90	**183,4**	171,7	-6,4%	177,3	-3,3%	183	-0,2%	199,9	9,0%
120	**179**	164,4	-8,2%	170,2	-4,9%	176	-1,7%	199,3	11,3%

B2pi

0	**1901,6**								
30	**1817,2**	1817,2	0,0%	1817,2	0,0%	1817,2	0,0%	1817,2	0,0%
60	**1435**	1435	0,0%	1435	0,0%	1435	0,0%	1435	0,0%
90	**1109,9**	1109,9	0,0%	1109,9	0,0%	1109,9	0,0%	1109,9	0,0%
120	**852,6**	852,6	0,0%	852,6	0,0%	852,6	0,0%	852,6	0,0%

B2pii

0	**1901,6**								
30	**1856,4**	1858,4	0,1%	1858,4	0,1%	1878,9	1,2%	1895,4	2,1%
60	**1824**	1822,3	-0,1%	1822,3	-0,1%	1851,9	1,5%	1883,8	3,3%
90	**1797,5**	1790,1	-0,4%	1790,1	-0,4%	1814,9	1,0%	1872	4,1%
120	**1774,7**	1757,6	-1,0%	1780,9	0,3%	1780,9	0,3%	1860,4	4,8%

C1pi

0	**622,6**								
30	**552,8**	554,8	0,4%	555,9	0,6%	557,5	0,9%	560,2	1,3%
60	**380,4**	381,4	0,3%	382	0,4%	383,2	0,7%	385,2	1,3%
90	**252,7**	253	0,1%	253,4	0,3%	253,8	0,4%	254,8	0,8%
120	**160,5**	160,5	0,0%	160,7	0,1%	160,9	0,2%	161,1	0,4%

C2pi

0	**2486,9**								
30	**2306,7**	2311,7	0,2%	2316,7	0,4%	2324,7	0,8%	2340,5	1,5%
60	**1834,2**	1838,8	0,3%	1842,5	0,5%	1849,3	0,8%	1860,1	1,4%
90	**1420,3**	1423,7	0,2%	1426,4	0,4%	1430,1	0,7%	1439,5	1,4%
120	**1080,7**	1082,6	0,2%	1084,5	0,4%	1086,9	0,6%	1092,6	1,1%

D1pi

0	**119,9**								
30	**104,9**	105,5	0,6%	105,5	0,6%	105,5	0,6%	105,5	0,6%
60	**60,2**	60,2	0,0%	60,2	0,0%	60,2	0,0%	60,2	0,0%
90	**31,4**	31,4	0,0%	31,4	0,0%	31,4	0,0%	31,4	0,0%
120	**16,6**	16,6	0,0%	16,6	0,0%	16,6	0,0%	16,6	0,0%

D1pii

	119,9								
30	**116,8**	111,7	-4,4%	111,7	-4,4%	115,8	-0,9%	119,9	2,7%
60	**114,5**	103,9	-9,3%	107,4	-6,2%	108,4	-5,3%	119,9	4,7%
90	**112,1**	97,3	-13,2%	102,8	-8,3%	107,3	-4,3%	119,9	7,0%
120	**110,7**	83,4	-24,7%	96,7	-12,6%	105,2	-5,0%	119,9	8,3%

D2pi

0	**607,8**								
30	**577,5**	577,8	0,1%	577,8	0,1%	577,8	0,1%	577,8	0,1%
60	**454,9**	455,6	0,2%	455,6	0,2%	455,6	0,2%	455,6	0,2%
90	**338,5**	338,5	0,0%	338,5	0,0%	338,5	0,0%	338,5	0,0%
120	**241,6**	241,6	0,0%	241,6	0,0%	241,6	0,0%	241,6	0,0%

D2pii

0	**607,8**								
30	**599,6**	590,3	-1,6%	590,3	-1,6%	598,4	-0,2%	607,8	1,4%
60	**593,1**	576,3	-2,8%	576,3	-2,8%	590,1	-0,5%	607,8	2,5%
90	**587,1**	560	-4,6%	569,9	-2,9%	575,4	-2,0%	607,8	3,5%
120	**581,6**	547,1	-5,9%	557,6	-4,1%	568,1	-2,3%	607,8	4,5%

E1ri

0	**70,6**								
30	**70,2**	70,6	0,6%	70,6	0,6%	70,6	0,6%	70,6	0,6%
60	**63,8**	65,2	2,2%	65,2	2,2%	65,2	2,2%	65,2	2,2%
90	**45,9**	46,9	2,2%	46,9	2,2%	46,9	2,2%	46,9	2,2%
120	**32,2**	32,7	1,6%	32,7	1,6%	32,7	1,6%	32,7	1,6%

E1rii

0	**70,6**								
30	**60,8**	52,4	-13,8%	56,9	-6,4%	61,4	1,0%	70,6	16,1%
60	**55,7**	39,5	-29,1%	44,8	-19,6%	52,4	-5,9%	70,6	26,8%
90	**51,2**	29,5	-42,4%	34,1	-33,4%	44,8	-12,5%	70,6	37,9%
120	**47,2**	16,2	-65,7%	25,1	-46,8%	34,1	-27,8%	70,6	49,6%

E1pi

0	**39,8**								
30	**37,6**	37,7	0,3%	37,7	0,3%	37,7	0,3%	37,7	0,3%
60	**27,4**	27,5	0,4%	27,5	0,4%	27,5	0,4%	27,5	0,4%
90	**18,5**	18,6	0,5%	18,6	0,5%	18,6	0,5%	18,6	0,5%
120	**12**	12	0,0%	12	0,0%	12	0,0%	12	0,0%

E1pii

0	**39,8**								
30	**36,5**	30,6	-16,2%	33	-9,6%	35,2	-3,6%	39,8	9,0%
60	**34**	24	-29,4%	26,8	-21,2%	30,6	-10,0%	39,8	17,1%
90	**31,5**	18,6	-41,0%	20,6	-34,6%	26,6	-15,6%	39,8	26,3%
120	**28,9**	10,7	-63,0%	15,3	-47,1%	20	-30,8%	39,8	37,7%

E2ri

0	**233,4**								
30	**233,4**	233,4	0,0%	233,4	0,0%	233,4	0,0%	233,4	0,0%
60	**214**	214	0,0%	214	0,0%	214	0,0%	214	0,0%
90	**149,3**	149,3	0,0%	149,3	0,0%	149,3	0,0%	149,3	0,0%
120	**102,6**	102,6	0,0%	102,6	0,0%	102,6	0,0%	102,6	0,0%

E2rii

0	**233,4**								
30	**223,7**	215,2	-3,8%	219,8	-1,7%	224,3	0,3%	233,4	4,3%
60	**218,6**	201,4	-7,9%	208	-4,8%	215,2	-1,6%	233,4	6,8%
90	**214,2**	192,4	-10,2%	197	-8,0%	208	-2,9%	233,4	9,0%
120	**210,1**	183,3	-12,8%	192,4	-8,4%	201,4	-4,1%	233,4	11,1%

E2pi

0	**231,5**								
30	**218,6**	218,6	0,0%	218,6	0,0%	218,6	0,0%	218,6	0,0%
60	**157,9**	157,9	0,0%	157,9	0,0%	157,9	0,0%	157,9	0,0%
90	**106,1**	106,1	0,0%	106,1	0,0%	106,1	0,0%	106,1	0,0%
120	**68,6**	68,6	0,0%	68,6	0,0%	68,6	0,0%	68,6	0,0%

E2pii

0	**231,5**								
30	**224,5**	216,7	-3,5%	220,5	-1,8%	224,2	-0,1%	231,5	3,1%
60	**220**	204,6	-7,0%	210	-4,5%	216,3	-1,7%	231,5	5,2%
90	**215,1**	195	-9,3%	198,8	-7,6%	208,9	-2,9%	231,5	7,6%
120	**210,4**	184,9	-12,1%	193,4	-8,1%	201,9	-4,0%	231,5	10,0%

F1pi

0	**14,5**								
30	**13,4**	13,5	0,7%	13,5	0,7%	13,5	0,7%	13,5	0,7%
60	**8,3**	8,3	0,0%	8,3	0,0%	8,3	0,0%	8,3	0,0%
90	**4,6**	4,6	0,0%	4,6	0,0%	4,6	0,0%	4,6	0,0%
120	**1,9**	1,9	0,0%	1,9	0,0%	1,9	0,0%	1,9	0,0%

F1pii

0	**14,5**								
30	**13,1**	10,9	-16,8%	11,7	-10,7%	13	-0,8%	14,4	9,9%
60	**11,5**	6,8	-40,9%	7,9	-31,3%	10,1	-12,2%	14,5	26,1%
90	**9,5**	2,6	-72,6%	4,1	-56,8%	6,9	-27,4%	13,8	45,3%
120	**7,5**	-0,9	-112,0%	0,3	-96,0%	4	-46,7%	12,3	64,0%

F2pi

0	**31**								
30	**29,1**	29,1	0,0%	29,1	0,0%	29,1	0,0%	29,1	0,0%
60	**20,2**	20,2	0,0%	20,2	0,0%	20,2	0,0%	20,2	0,0%
90	**12,5**	12,5	0,0%	12,5	0,0%	12,5	0,0%	12,5	0,0%
120	**6,9**	6,9	0,0%	6,9	0,0%	6,9	0,0%	6,9	0,0%

F2pii

0	**31**								
30	**30,2**	28,9	-4,3%	29,4	-2,6%	29,9	-1,0%	31	2,6%
60	**29,6**	27	-8,8%	27,7	-6,4%	28,5	-3,7%	31	4,7%
90	**28,9**	25,3	-12,5%	26	-10,0%	27,5	-4,8%	31	7,3%
120	**28,3**	23,4	-17,3%	24,4	-13,8%	26,2	-7,4%	31	9,5%

F3pi

0	**93,3**								
30	**88**	88	0,0%	88	0,0%	88	0,0%	88	0,0%
60	**62,3**	62,3	0,0%	62,3	0,0%	62,3	0,0%	62,3	0,0%
90	**40,3**	40,3	0,0%	40,3	0,0%	40,3	0,0%	40,3	0,0%
120	**24,7**	24,7	0,0%	24,7	0,0%	24,7	0,0%	24,7	0,0%

F3pii

0	**93,3**								
30	**90,7**	88,4	-2,5%	89,6	-1,2%	90,9	0,2%	93,3	2,9%
60	**89**	82,5	-7,3%	84,6	-4,9%	87,2	-2,0%	93,3	4,8%
90	**87,1**	75,9	-12,9%	79,9	-8,3%	84,9	-2,5%	93,3	7,1%
120	**85,2**	68,7	-19,4%	74,1	-13,0%	80,7	-5,3%	93,3	9,5%

C TIME TO FAILURE FOR COLUMNS

Column with cross section 150x150 mm and length 1 m.

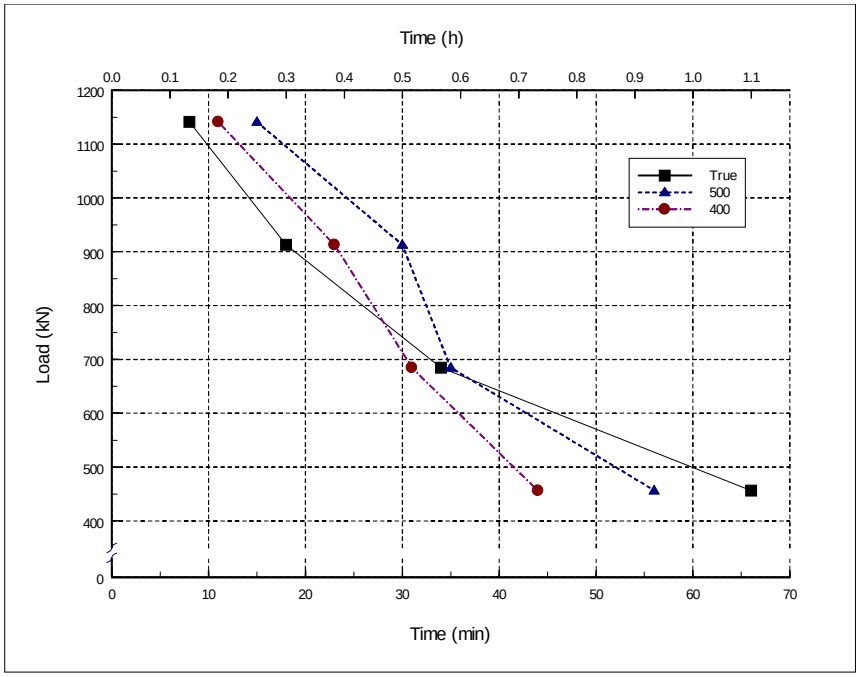

Column with cross section 150x150 mm and length 2 m.

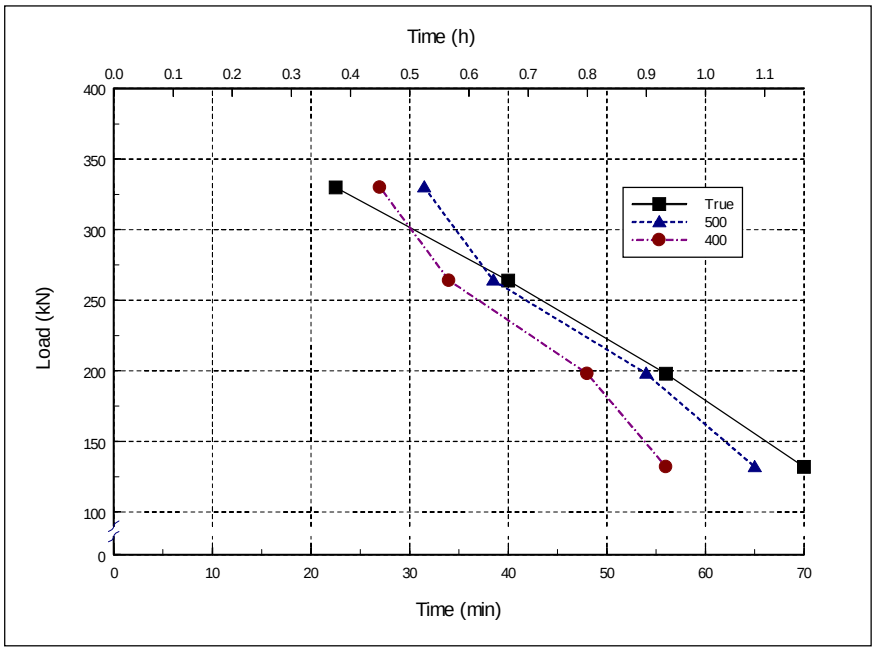

Column with cross section 300x300 mm and length 2 m.

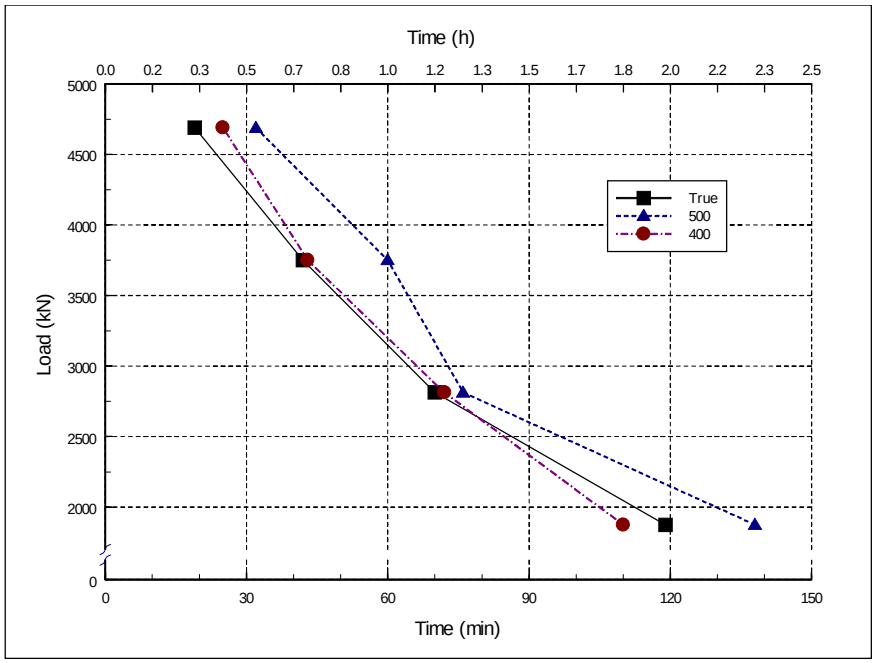

Column with cross section 300x300 mm and length 6 m.

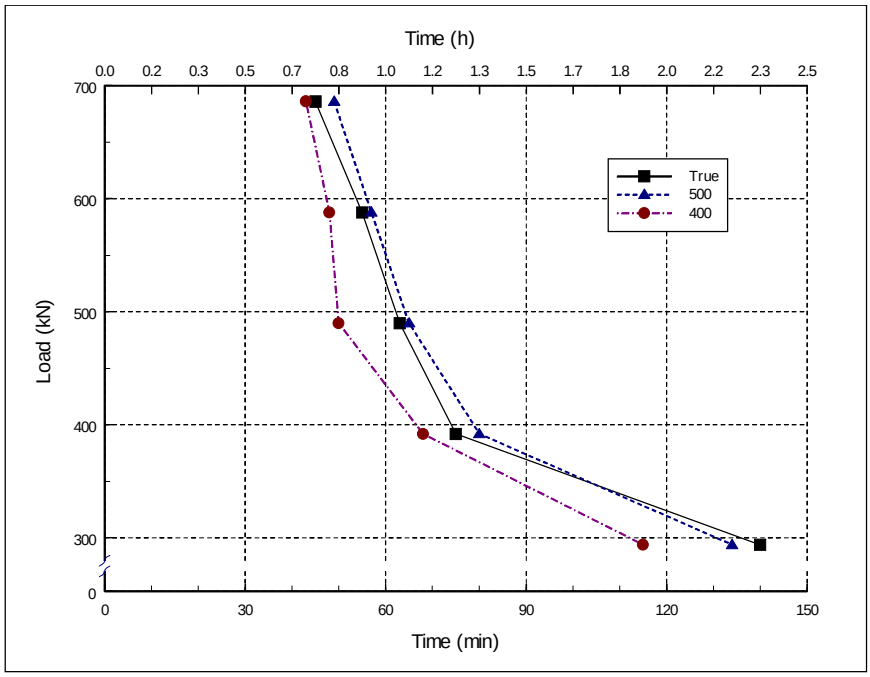

Column with cross section 400x400 mm and length 8 m.

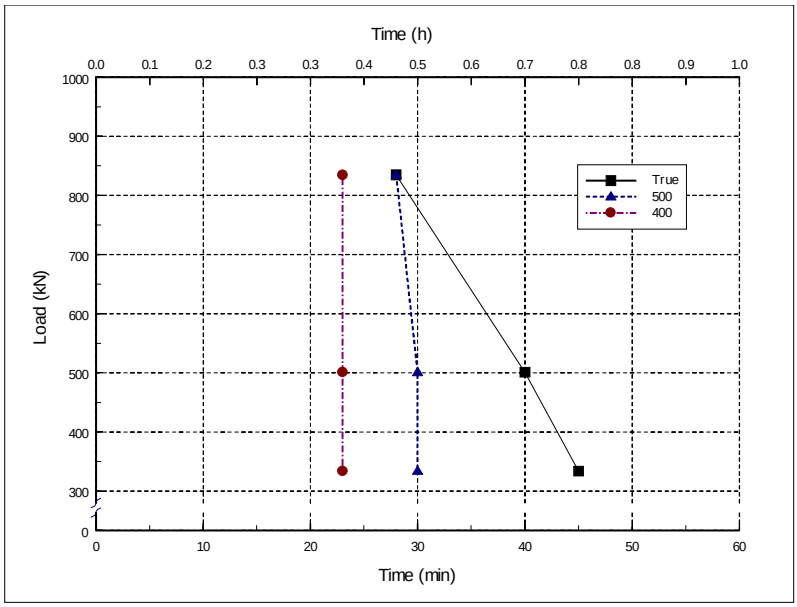

D COMPUTER PROGRAMS

The basic computer programs used in the simulation are; TCD SUPER-TEMPCALC, CBEAM and CONFIRE. In order to make these compatible and convert output data from one program to input data to another, use has been made of two of conversion programs, namely CFCONV and CONREAD. MATLAB and Microsoft EXCEL have been used for a visualisation of final output from CONFIRE.

SUPER-TEMPCALC

SUPER-TEMPCALC is a fire-adapted two-dimensional finite element program developed by FSD for use on personal and mainframe computers. It is a further development of TEMPCALC, originally developed in 1985.

The program solves the two-dimensional, transient, heat transfer differential Equation (D.1) incorporating thermal properties which vary with temperature.

$$\frac{\partial}{\partial x}\left(k_x \frac{\partial T}{\partial x}\right)+\frac{\partial}{\partial y}\left(k_y \frac{\partial T}{\partial y}\right)+Q=\rho c\frac{\partial T}{\partial t} \qquad \text{(D.1)}$$

where

T	is temperature [°C]
k_x, k_y	is thermal conductivity [W/m°C]
c	is specific thermal capacity [J/kg °C]
ρ	is density [kg/m^3]
Q	is internal heat generation [W/m^3]

The program allows the use of rectangular or triangular finite elements, in cylindrical or rectangular co-ordinates. Heat transferred by convection and radiation at the boundaries can be modelled as a function of time. Structures comprising several materials can be analysed and the heat absorbed by any existing void in the structure is also taken into account.

A materials properties database is integrated with the main program. Also integrated with the program are pre- and post-processors which allow fast and user-friendly input/output procedures. The pre-processor generates the finite element division and retrieves the relevant information from the database for use in the calculation. Finally, the post-processor presents the results graphically on screen or on plotter in a variety of forms, including time-temperature curves, isotherms, and temperature gradients.

Anderberg /1991/ gives a more detailed description the SUPER-TEMPCALC software.

CBEAM

CBEAM is a finite element program for calculation of load bearing capacity in fire exposed reinforced or pre-stressed concrete slabs and beams.

The geometrical input data consists of cross-sectional data for the concrete as well as the relative strength reduction of concrete as a function of temperature. Steel topology and strength reduction as a function of temperature must also be given as input.

Relevant temperature field data for the studied members are generated by SUPER-TEMPCALC, which thus is integrated with the program.

The finite element mesh from SUPER-TEMPCALC is employed in an iterative procedure which takes into account the true temperatures in the concrete sub-elements and its corresponding contribution to the total moment capacity.

The governing equations in CBEAM are presented below. Equation (D.2) comprises an equilibrium condition which determines the height of the compression zone and consequently the lever arms needed for calculation of the moment capacity in Equation (D.3).

$$\sum_i (f_{st,i}(T) \cdot A_{s,i}) - \sum_j (f_{cc,j}(T) \cdot A_{c,i}) = 0 \qquad \text{(D.2)}$$

$$M_{kap} = \sum_i \left(f_{cc,i}(T) \cdot A_{c,i} \cdot y_i \right) \qquad \text{(D.3)}$$

where,

M_{kap}	is moment capacity for a given cross-sectional temperature gradient
$f_{cc,i}(T_i)$	is compression strength of concrete element i at temperature T_i
T_i	is temperature of element i
$A_{c,i}$	is area of element i within the compression zone
y_i	is lever arm of resultant force in concrete compression element i
$f_{st,i}(T)$	is tension strength of reinforcement bar i with temperature T_{si}
T_{si}	is temperature of reinforcement bar i
$A_{s,i}$	is area of reinforcement bar i

Relative strength of concrete and reinforcing steel are input to the program as are reinforcement locations and initial values of steel and concrete strength.

CBEAM is further described by Oredsson /1995/.

CONFIRE

CONFIRE is a finite element non-linear fire-adapted computer program for calculation of the structural response and behaviour in plane reinforced concrete framework structures, subjected to fire exposure.

The program requires input data of several kinds; cross-sectional measures, mechanical data for concrete and reinforcement, load and eccentricities, structural data including topology, boundary conditions and supports and information about the incremental iteration process and time increments.

The non-linear geometrical effects (large displacements) are taken into account by up-dating the nodal co-ordinates of the structure during deformation.

The mechanical properties for concrete and reinforcing steel are up-dated for every change of temperature. Various structural boundary conditions may be employed, thus allowing for extended applicability and resemblance with actual conditions.

Nodal temperatures in the concrete cross-sections, for each time step throughout the fire scenario, may be retrieved from the output of SUPER-TEMPCALC. A relevant external loading situation may be achieved by applying concentrated forces, moments and distributed loads.

The output consists of a range of cross-sectional data involving stresses, strains, axial loading, moments, displacements, all of which are available for every time step of the calculation. The calculation proceeds until the studied structure fails to maintain structural stability under the adopted loading situation, thus indicating the length of the fire resistance time.

CONFIRE was developed by Dr. Nils Erik Forsén, Multiconsult AS, Norway.
For further reference see Forsén /1982/.

Conversion Programs

As mentioned before, two of conversion programs were used in the column analysis. These are CFCONV and CONREAD. CFCONV converts the SUPER-TEMPCALC temperature output file into an input file to CONFIRE. The temperature reported from the SUPER-TEMPCALC calculation represents every node of the element mesh. This format does however not comply with the request of input data to CONFIRE, and thus a conversion is necessary. CFCONV calculates average temperatures from the node points and arranges them in a way that agrees with the input format to CONFIRE. CONREAD is a utility which reads and converts the CONFIRE output file into MATLAB format from which graphical analysis easily can be done.